U.S. DEPARTMENT OF COMMERCE
National Technical Information Service

PB-267 764

The Fate of Nitrogen Oxides in the Atmosphere

Battelle Columbus Labs, Ohio

Prepared for

Coordinating Research Council, Inc, New York

Aug 76

PB 267 784

August 1976

Second Year Report

THE FATE OF NITROGEN OXIDES IN THE ATMOSPHERE

Battelle
Columbus Laboratories

A report of research conducted for the
Coordinating Research Council Inc.

REPRODUCED BY
NATIONAL TECHNICAL
INFORMATION SERVICE
U.S. DEPARTMENT OF COMMERCE
SPRINGFIELD, VA. 22161

BIBLIOGRAPHIC DATA SHEET	1. Report No. CRC-APRAC CAPA-9-71	3.	5. Recipient's Accession No.
4. Title and Subtitle The Fate of Nitrogen Oxides in the Atmosphere - Second Year Report			5. Report Date August 1976 6.
7. Author(s) C. W. Spicer, J. L. Gemma, P. M. Schumacher, G. F. Ward			8. Performing Organization Rept. No.
9. Performing Organization Name and Address Battelle-Columbus Laboratories 505 King Avenue Columbus, Ohio 43201			10. Project/Task/Work Unit No. 11. Contract/Grant No.
12. Sponsoring Organization Name and Address Environmental Protection Agency, Research Triangle Park, N.C. 27711 and The Coordinating Research Council, Inc. 30 Rockefeller Plaza, New York, N.Y. 10020			13. Type of Report & Period Covered Second Year 14.

15. Supplementary Notes

16. Abstracts: The report describes the second year of a continuing study to determine the distribution and fate of nitrogen oxides in the atmosphere. Analytical methods developed in the first year were refined and validated and results from the first year study were reexamined with the aid of additional data collected simultaneously by other research groups. An instrumental technique for nitric acid was refined, tested for interference, and verified against a long-path infra-red technique under simulated smog conditions. The interference by PAN and nitric acid with the chemiluminescent determination of NO_2 was studied with a view toward reducing or minimizing the interference. Nitric acid interference was eliminated by the use of a nylon prefilter on the chemiluminescent instrument. The interaction of gaseous nitric acid with alkaline glass-fiber filters was shown to yield artifact particulate nitrate.

17. Key Words and Document Analysis. 17a. Descriptors

Air Pollution
Nitrogen
Atmospheric
Air Quality
Ozone
$NO-NO_2-NO_x$
Ammonia
Peroxyacetyl Nitrate
Nitric Acid
Aerosol

17b. Identifiers/Open-Ended Terms

17c. COSATI Field Group: 13B; 07B; 07C; 07D; 04B; 11G

18. Availability Statement	19. Security Class (This Report)	21. No. of Pages
Releasable to the general public.	UNCLASSIFIED	122
	20. Security Class (This Page) UNCLASSIFIED	22. Price PC A06, A01

SECOND YEAR REPORT

THE FATE OF NITROGEN OXIDES IN THE ATMOSPHERE

TO

COORDINATING RESEARCH COUNCIL, INC.
(CAPA-9-71)

AUGUST, 1976

by

Chester W. Spicer, James L. Gemma,
Philip M. Schumacher, and Gerald F. Ward

BATTELLE
Columbus Laboratories
505 King Avenue
Columbus, Ohio 43201

Battelle is not engaged in research for advertising, sales promotion, or publicity purposes, and this report may not be reproduced in full or in part for such purposes.

ACKNOWLEDGMENTS

The authors wish to acknowledge the assistance of Dr. Philip Stickel in providing the air mass trajectory analyses and General Motors Corporation for providing carbon monoxide data from West Covina.

We would also like to acknowledge the guidance of the members of the CAPA-9-71 Project Committee:

Dr. William Glasson, Chairman
Dr. Emmett Burk
Dr. Robert Hammerle
Dr. Jack Pierrard
Dr. Joseph Bufalini (EPA Liason)
Mr. Timothy Belian (Project Manager for CRC)

TABLE OF CONTENTS

	Page
ACKNOWLEDGMENTS	i
LIST OF TABLES	iii
LIST OF FIGURES	iv
INTRODUCTION	1
Refinement of Methodology - Objectives	2
Data Analysis - Objectives	2
SUMMARY OF THE PROGRAM	3
REFINEMENT OF METHODOLOGY	6
Nitric Acid Analysis	6
Calibration	6
Interferences	7
Smog Chamber Comparison of the Coulometric Instrument and Long-Path Infrared Fourier Transform Spectrometer (LPIR-FTS)	9
Chemiluminescence Interference	16
Thermal Adjustment	19
Filtration Techniques	21
Alternative Converters	23
Interaction of Gaseous Nitric Acid With Filters	26
A.M./P.M. Aerosol Patterns	30
Results of the ESCA Analysis	32
DATA ANALYSIS	35
Interpretation of West Covina Results	35
Relationship of NO_x Reaction Products to Total Oxidized Nitrogen	37
Determination of Appropriate CO/NO_x Emissions Ratio	41
Variation of NO_x-Loss by Day and Time of Day For Several Los Angeles Locations	44
Nitrogen Oxides Loss and Nitrogen Balance at West Covina	49
Computer Simulations	55
Physical Scavenging of the Nitrogen Oxides	59
Trajectory and Emissions Analysis	60
Investigation of NO_x Removal in New York City	68
Analysis of Selected LARPP Operations for NO_x-Loss	73

TABLE OF CONTENTS
(Continued)

	Page
Operation 25	75
Operation 33	82
Operation 5	93
Operation 8	93
Operation 10	93
Operation 16	93
Operation 27	103
REFERENCES	112

LIST OF TABLES

Table 1.	Interference Testing of Coulometric Technique	7
Table 2.	Comparison of EPA and Battelle Smog-Chamber Experiments	12
Table 3.	Irradiation of C_3H_6/NO_2 Mixture in EPA Chamber (All Concentrations in PPM)	14
Table 4.	Irradiation of $C_3H_6/NO_2/SO_2$ Mixture in EPA Chamber (All Concentrations in PPM)	16
Table 5.	The Equilibrium Ratio, NO_2/NO, for $NO_2 \rightleftharpoons NO + 1/2\ O_2$	19
Table 6.	Conversion of HNO_3 by Carbon Converter	21
Table 7.	PAN-Filter Interaction Study Results	22
Table 8.	Effect of Ferrous Sulfate on NO_x (50% Relative Humidity) All Concentrations in PPM	23
Table 9.	Nitric Acid Removal by $FeSO_4$	24
Table 10.	Effect of Various Materials on PAN Removal (Concentrations in PPM)	25
Table 11.	Monthly Average Particulate Nitrate Concentrations, $\mu g/m^3$	26
Table 12.	Artifact Nitrate Formed on Quartz and Glass Filters From Gaseous Nitric Acid (47 mm Filters)	29
Table 13.	Results of A.M./P.M. Aerosol Studies	31
Table 14.	Results of Reduced Nitrogen Analysis of Daily Particulate Samples ($\mu g/m^3$)	33
Table 15.	Los Angeles Emissions Inventory Summaries	42

LIST OF TABLES (Continued)

Page

Table 16. Starting Conditions for the Computer Simulation of Los Angeles Smog Formation. 56
Table 17. Calculated Emissions Ratios. 65
Table 18. Comparison of Calculated NO_x-Loss With the Sum of PAN and Nitric Acid 67

LIST OF FIGURES

Figure 1. Response of Coulometric and Chemiluminescent Instruments to HNO_3. 8
Figure 2. Comparative Nitric Acid Analysis 11
Figure 3. Photooxidation of 3.65 ppm C_3H_6, 1.23 ppm NO_2. 13
Figure 4. Photooxidation of 3.7 ppm C_3H_6, 0.64 ppm NO_2, 0.28 ppm SO_2 15
Figure 5. Reduction of HNO_3 By a Stainless Steel Converter 20
Figure 6. Composite Profiles of F_N in St. Louis and West Covina. 38
Figure 7. Daily Trends in Measured Variables - St. Louis 39
Figure 8. Daily Trends in Measured Variables - West Covina 40
Figure 9. Locations of Primary Sources and Monitoring Stations in the Los Angeles Basin. 43
Figure 10. Normalized CO/NO_x Ratios for Five Los Angeles Basin Sites. 46
Figure 11. Comparison of Composite NO_x Loss at Four Sites. 47
Figure 12. Composite Profiles for West Covina 50
Figure 13. Composited NO_x Loss and PAN + HNO_3 Profiles for West Covina. 53
Figure 14. Trends in Measured Variables at West Covina 54
Figure 15. Urban Simulation 57
Figure 16. CO and NO_x Emissions Grids 62
Figure 17. Trajectory of Air Mass Arriving at West Covina at 14:00 on September 11, 1973 63
Figure 18. New York City Composite NO_x Loss 70

LIST OF FIGURES
(Continued)

		Page
Figure 19.	Trends in New York Measurements	72
Figure 20.	Trajectories Tracked During LARPP Operations	76
Figure 21.	Constant Altitude Plot for LARPP Operation 25 (~264 Meters)	77
Figure 22.	Plot of CO/NO_x (Profile Average) for LARPP Operation 25	79
Figure 23.	Plot of CO/NO_x by Altitude for LARPP Operation 25	80
Figure 24.	Plot of C_2H_2/NO_x (Profile Average) for LARPP Operation 25	81
Figure 25.	Plot of C_2H_4/C_2H_2 (Profile Average) for LARPP Operation 25	82
Figure 26.	CO/NO_x Ratio (Operation 33)	85
Figure 27.	CH_4/NO_x Ratio (Operation 33)	86
Figure 28.	C_2H_2/NO_x Ratio (Operation 33)	87
Figure 29.	CO/NO_x Ratios by Altitude for LARPP Operation 33	88
Figure 30.	CH_4/NO_x Ratios by Altitude for LARPP Operation 33	89
Figure 31.	C_2H_2/NO_x Ratios by Altitude for LARPP Operation 33	90
Figure 32.	CO/C_2H_2 Ratio for LARPP Operation 33	92
Figure 33.	CO/NO_x Ratio (Operation 5)	94
Figure 34.	C_2H_2/NO_x Ratio (Operation 5)	95
Figure 35.	CH_4/NO_x Ratio (Operation 5)	96
Figure 36.	CO/NO_x Ratio (Operation 8)	97
Figure 37.	C_2H_2/NO_x Ratio (Operation 8)	98
Figure 38.	CH_4/NO_x Ratio (Operation 8)	99
Figure 39.	CO/NO_x Ratio (Operation 10)	100
Figure 40.	C_2H_2/NO_x Ratio (Operation 10)	101
Figure 41.	CH_4/NO_x Ratio (Operation 10)	102
Figure 42.	CO/NO_x Ratio (Operation 16)	104
Figure 43.	C_2H_2/NO_x Ratio (Operation 16)	105
Figure 44.	CH_4/NO_x Ratio (Operation 16)	106

LIST OF FIGURES
(Continued)

Page

Figure 45. CO/NO_x Ratio for LARPP Operation 16. 107
Figure 46. CO/C_2H_2 Ratio Versus Time for Several Operations 108
Figure 47. CO/C_2H_2 Ratio Versus C_2H_2 for Several Operations 110

SECOND YEAR REPORT

THE FATE OF NITROGEN OXIDES IN THE ATMOSPHERE

by

Chester W. Spicer, James L. Gemma,
Philip M. Schumacher, and Gerald F. Ward

INTRODUCTION

The role of nitrogen oxides in the formation of photochemical smog has been extensively investigated in recent years. Although nitrogen oxides are known to be involved in a number of reactions leading to well-known smog manifestations, the distribution and ultimate disposition of the nitrogen oxides has been unclear. The objective of the CAPA-9-71 program is to determine the distribution and fate of nitrogen oxides in urban atmospheres. This report describes the second year of the program. The first-year study was initiated in 1973 and involved three distinct phases. First, analytical methods were developed to measure nitrogen oxides and their presumed reaction products. Extensive field sampling programs were then conducted for 5 weeks in St. Louis, Missouri, and 5 weeks in West Covina, California. The Battelle Mobile Air Quality Laboratory was used for air monitoring and particulate collection. NO, NO_2, NO_x, O_3, PAN, NH_3, HNO_3, solar intensity, wind speed and direction, temperature and relative humidity were monitored for 23 hours each day. In addition, total particulate loading, NH_4^+, NO_2^-, NO_3^-, and CHN were determined each day from high volume samples collected on high-purity quartz filters. The final phase of the first-year program involved the analysis and interpretation of the field study results. A thorough description of the first-year program is available[1].

The objective of the second-year study reported here is to further refine and validate the analytical methods developed in the first year and to expand the interpretation of the first year's results based on data collected simultaneously in West Covina by other research groups.

This year's study has involved a number of tasks which, for the purposes of this report, have been divided into two groups entitled Refinement of Methodology and Data Analysis. The Methodology section is presented first since some of the conclusions reached there bear directly on assumptions made in the Data Analysis section. The title of each task and a brief objective are given below.

Refinement of Methodology - Objectives

Nitric Acid Analysis - Refinement and evaluation of techniques for monitoring nitric acid.

Chemiluminescence Interference - Screen potential methods for eliminating interferences to NO_x chemiluminescence determination.

Filter Interactions - Investigate interactions between gaseous nitric acid and commonly used filter materials.

A.M./P.M. Aerosol Analyses - Study filter samples collected in St. Louis and West Covina on an a.m./p.m. basis.

Data Analysis - Objectives

Interpretation of West Covina Results - Reexamine the results of the West Covina field study with the aid of data collected at the same site by other organizations.

Trajectory and Emissions Analysis - Utilize trajectory analyses and spatially resolved emissions estimates to increase the accuracy of the calculation of NO_x deficit.

LARPP Data Analysis - Analyze selected operations of the Los Angeles Reactive Pollutant Program for NO_x-loss and compare results with West Covina data.

NO_x Removal in New York City - Investigate nitrogen oxides losses and loss patterns for New York City.

SUMMARY OF THE PROGRAM

During this year's program, a number of tasks were undertaken with the ultimate aim of (1) refining and verifying the analytical procedures employed in the first year of the program and (2) reexamining the West Covina results from the first-year study with the aid of additional data which recently became available. By far the greatest effort went into two tasks: nitric acid analysis and West Covina data interpretation. A number of observations and conclusions from the various tasks stand out and are summarized below.

- The coulometric nitric acid procedure has been refined, interference-tested, and verified against a long-path infrared technique under simulated smog conditions. The assembly and operation of the instrument have been simplified, and improved calibration procedures have been investigated.

- The interference by PAN and nitric acid with the chemiluminescent determination of NO_2 has been studied with a view toward reducing or minimizing the interference. Nitric acid interference can be eliminated by the use of a nylon prefilter on the chemiluminescent instrument. No completely satisfactory method of removing PAN interference has been found. However, since PAN interference is quantitative, PAN can be monitored separately and its concentration subtracted from the chemiluminescent NO_2 output.

- The interaction of gaseous nitric acid with alkaline glass-fiber filters has been shown to yield artifact particulate nitrate. Under certain conditions the level of artifact nitrate can seriously interfere with the determination of the true particulate nitrate concentration. High-purity quartz-fiber filters have been shown to minimize artifact formation. Our results suggest that the ratio $\frac{\text{gaseous nitrate}}{\text{particulate nitrate}}$ in polluted atmospheres is probably much higher than previously suspected.

- Making certain assumptions, we observed an overall average 0.018 ppm NO_x deficit in air arriving at our monitoring site in West Covina. Of this 0.018 ppm deficit, 0.012 ppm can be accounted for as PAN, 0.003 ppm as HNO_3, and about 0.001 ppm as particulate nitrate.

- The average ratio (F_N) of NO_x reaction products to total gaseous oxidized nitrogen in all forms ($\frac{PAN + HNO_3}{NO + NO_2 + PAN + HNO_3} = F_N$) was about 0.11 in both St. Louis and West Covina. The ratio $\frac{NO_x\text{-Predicted}}{NO_x\text{-Lost}}$, which should be an upper bound to F_N and similar to F_N if the major NO_x reaction products have been accounted for, was found to average 0.12 in West Covina, in close agreement with F_N.

- A simplified computer model of the reactions presumed to occur in polluted Los Angeles air masses has been employed to predict the behavior of a number of smog reaction products including O_3, aldehydes, PAN, HNO_3, and H_2O_2. The predicted maximum concentrations and temporal variations are in good agreement with the results of this and other ambient monitoring studies.

- The estimated patterns of NO_x-loss in New York City were found to be similar to those for West Covina.

During the first 5 years of this program much progress has been made in developing and improving analytical methods for measurement of the nitrogen oxides and their reaction products, and much has been learned about these species. The atmospheric distribution of the reaction products has been studied, the relationships of the products to chemical and meteorological variables have been investigated, and the accountability of NO_x in terms of these products has been estimated. However, many questions remain unanswered; the NO_x accountability needs additional verification, the formation mechanisms of some of the products remain obscure, the residence time and ultimate fate of some of the products is unknown, and the effect of seasonal changes on the fate of the nitrogen oxides is unclear. With increasingly frequent reports of detrimental health effects associated with NO_x reaction products, the possibility of a future need to control these products must be considered. However, at the present time it is unlikely that enough atmospheric data exist to devise safe and efficient strategies for control. Future efforts along these lines are needed and recommended.

REFINEMENT OF METHODOLOGY

This section of the report describes our efforts to refine and validate the monitoring techniques for HNO_3, NO_x, and particulate nitrate and presents some additional aerosol data from the West Covina field study.

Nitric Acid Analysis

The purpose of this task has been to refine our coulometric technique for nitric acid monitoring and to further verify its applicability to atmospheric anaysis. A description of the coulometric method has been presented elsewhere[2]. As part of this task, the coulometric instrument has been modified to permit extended operation and to improve its response characteristics, calibration procedures have been investigated and extensive interference evaluations conducted, and finally, the coulometric instrument has been compared with a long-path Fourier Transform Infrared Spectrometer during smog-chamber experiments.

Field and laboratory experience with the coulometric instrumentation has suggested two specific areas where the performance of the instrument could be improved. First, the solenoid valves used in the original design of the instrument were bulky and tended to heat up during continuous operation. Secondly, the large volume of the nylon wool/pyrex trap used to scrub HNO_3 affected the response time of the instrument, and the packing of the trap for optimum efficiency was a time-consuming and essentially empirical task. Improvements in these problem areas have been made by modifications to the instrument.

The first modification involved replacing the solenoid valves with smaller, low-temperature (.4 watt), Routon* seated solenoid valves. These valves have less dead-volume, are more inert, and should have a considerably longer operating life than the original valves.

The second refinement to the instrument involved replacing the nylon wool/Pyrex trap with a Teflon filter-holder containing a nylon filter.

*A Teflon composite.

This change results in improved response characteristics by lowering the system volume and minimizing the effect of surface adsorption. This modification also greatly simplifies the assembly and operation of the coulometric nitric acid monitor, which will be a major benefit to researchers interested in employing the coulometric monitor. The investigations of performance and interferences described later in this section have been carried out using this modified instrument. In extensive side-by-side smog chamber comparisons, both the original and modified instruments yielded the same nitric acid concentrations, but the response-time characteristics of the modified unit were much improved.

Another modification which has been made to the instrument has involved increasing the capacity of the reagent and waste vessels for longer unattended operation of the unit.

Calibration

The theoretical response of the microcoulometric detector to strong acids has been discussed in other publications[2,3]. To further verify this response factor we have employed a certified standard HCl (7 ppm) in nitrogen mixture. Dilution of this mixture to the sub-ppm range permits direct calibration of the detector for strong acid. The results of such experiments confirm the theoretical coulometric response factor. For example, dilution of the HCl standard to 0.85 ppm in "zero" nitrogen yields a response by the coulometric detector of 0.85 ppm acid. Similar response checks by Gantner[4] using HCl and SO_2 have also confirmed the theoretical response of the detector cell.

Calibration of the instrument with sub-ppm concentrations of nitric acid has been accomplished by injecting small quantities of nitric acid into a large dilution vessel (smog chamber) and monitoring the resulting concentrations with both the coulometric instrument and a chemiluminescent instrument. The response of commercial chemiluminescent instruments to nitric acid is discussed in another section of this report. However, under suitable conditions and over short time periods the response is quantitative. The chemiluminescent instrument was calibrated with a NBS "primary standard"

NO_2 permeation tube. The concentrations of nitric acid reported by the chemiluminescent and coulometric instruments were very similar, as shown in Figure 1. This is admittedly a secondary calibration method, yet it also tends to confirm the theoretical coulometric response to strong acids and, more importantly, nitric acid.

Interferences

During the initial development of the coulometric procedure for nitric acid, we investigated the effects of a number of possible interferences[1]. In the current program some additional species have been tested, and the original potential interferences reinvestigated. Table 1 lists the species studied. In most cases the concentrations shown in the table are the highest investigated. The exception is NO_2, for which two experiments at 1.3 ppm gave conflicting results. Experiments at 1.0 ppm NO_2 have never shown any interference; this is the value listed in Table 1.

TABLE 1. INTERFERENCE TESTING OF COULOMETRIC TECHNIQUE

Specie	Comment
Ozone	No interference up to 0.6 ppm
Nitrogen Dioxide	No interference up to 1 ppm
Sulfur Dioxide	No interference up to 1.1 ppm
Sulfuric Acid	No interference up to 100 $\mu g/m^3$
Hydrochloric Acid	No interference up to 0.4 ppm
Formaldehyde	No interference up to 0.5 ppm
Peroxyacetyl Nitrate	No interference up to 0.2 ppm
Formic Acid	Variable interference between 0-10%
Nitrous Acid	No interference up to 0.4 ppm

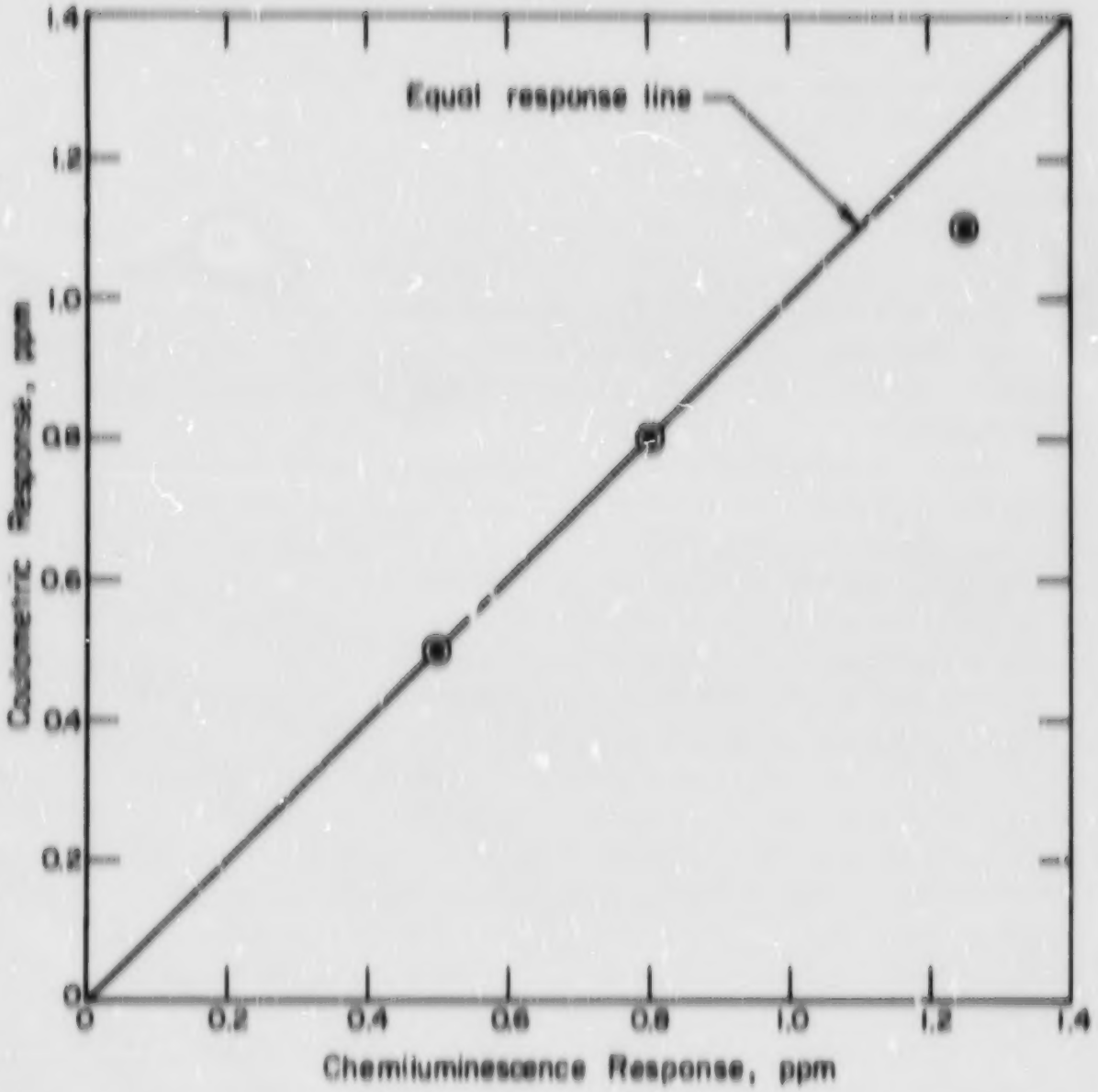

FIGURE 1. RESPONSE OF COULOMETRIC AND CHEMILUMINESCENT INSTRUMENTS TO HNO_3

In many experiments, formic acid shows no interference with gaseous nitric acid determination. However, we occasionally observe a formic acid interference of up to 10% of the formic acid concentration. The highest ambient formic acid concentrations have been observed in Los Angeles by Hanst, et al.[5], during a severe smog episode. Formic acid levels up to 70 ppb were reported during a period when ozone exceeded 0.65 ppm. Under this worst-case condition, formic acid could show as much as a 7 ppb nitric acid interference. Since our measurements in the Los Angeles basin indicate that nitric acid concentrations would approach at least 50 ppb under such severe smog conditions, formic acid response would constitute only a 10-15% interference at maximum. Smog-chamber experiments to be discussed shortly suggest that even this is an overestimate and that the interference due to formic acid is negligible.

In efforts to remove the possibility of formic acid interference we have attempted to use prefilters to selectively scrub formic acid from the sample air stream. The successful scrubber would have to remove formic acid but quantitatively pass nitric acid. A brief investigation of Teflon, cellulose acetate, and polycarbonate filters was unsuccessful. Attempts at minimizing the interference by sensitizing the nylon filter used in the coulometric instrument to formic acid, so that it would still scrub nitric acid but pass formic acid, were also successful.

Because of the relatively small impact of formic acid on nitric acid monitoring, and because of additional data presented in the next section which indicate minimal interference, no further effort was expended on attempts to eliminate formic acid response.

Smog Chamber Comparison of the Coulometric Instrument and Long-Path Infrared Fourier Transform Spectrometer (LPIR-FTS)

Validation of the coulometric nitric acid monitor would not be complete without a comparison of the technique, under actual smog formation conditions, to a good physical measurement of nitric acid concentration. The EPA laboratories in Research Triangle Park, N.C., are equipped for such

experiments, and graciously volunteered to participate in this program*. The EPA facility used in this study is a 36-foot-long Pyrex smog chamber surrounded by fluorescent ultraviolet lamps and equipped with a multiple-pass FTS infrared instrument. The smog chamber is filled and evacuated through a standard vacuum line. For these experiments, where air was continuously withdrawn from the chamber for the coulometric monitor, the chamber was maintained at atmospheric pressure by allowing room air to replace the air used for sampling. Since there is no provision for mixing within the chamber, this process, as well as the process of injecting gases into the chamber, could result in some inhomogeneity within the chamber. Since the LPIR instrument integrates its concentration measurements over the entire length of the chamber while the coulometric unit samples at a fixed point, concentration gradients within the chamber could be a source of error and must be considered in interpreting the results.

Three experiments were carried out to intercompare the coulometric and infrared methods of nitric acid monitoring. These experiments consisted of

(1) Dilution of nitric acid in air
(2) Irradiation of C_3H_6/NO_x mixture
(3) Irradiation of $C_3H_6/NO_x/SO_2$ mixture.

The purpose of the first experiment was to investigate any differences between the two monitoring techniques under simplified conditions. The objective of the second and third experiments was to compare the two monitoring techniques under actual (and severe) smog formation conditions, where high concentrations of potential interferences should be present.

The results of the initial experiment, in which HNO_3 was injected into the smog chamber and continuously diluted with room air, are shown in Figure 2. The line drawn through the circles represents the LPIR measurements, the squares represent the coulometric measurements. Except for one data point, agreement between the two techniques was excellent. It should be noted that the calibrations of the infrared and coulometric instruments

*The aid of Drs. Bruce Gay and Joseph Bufalini of the EPA is gratefully acknowledged.

FIGURE 2. CHROMATOGRAPHIC ACID ANALYSIS

used in deriving these curves were totally independent. The calibration of the coulometric instrument was discussed earlier. The nitric acid absorption coefficients used in calculating the infrared results have been presented elsewhere[6]. Considering the differences in the monitoring methods and the calibration techniques, and the potential inaccuracies introduced by any concentration gradient within the cell, the agreement between the two methods is remarkable.

The results of the propylene/NO_x irradiation are plotted in Figure 3. The initial conditions of the experiment were 3.65 ppm C_3H_6 and 1.23 ppm NO_2 in air. The irradiation intensity of the fluorescent blacklamps yields a k_d value of 0.33 min^{-1}. No interference due to NO_2 was observed with the coulometric monitor, even through 1.23 ppm of NO_2 was present initially. Reasonably good agreement was observed between the coulometric and infrared methods, even in the presence of extremely high levels of ozone, peroxyacetyl nitrate and formic acid. The concentrations of these possible interferences are well above the levels observed in the atmosphere. The initial conditions of this experiment were selected to approximate the conditions of a similar experiment carried out in the larger Battelle smog chamber[7]. In spite of the differences in chamber size, surface to volume ratio and surface composition, the behavior of PAN and HNO_3 in the two experiments was quite similar, as seen in Table 2.

TABLE 2. COMPARISON OF EPA AND BATTELLE SMOG-CHAMBER EXPERIMENTS

	EPA Chamber		Battelle Chamber	
Specie	Initial Conditions	After 175 min. Irradiation	Initial Conditions	After 180 min. Irradiation
C_3H_6	3.65 ppm	—	3.20 ppm	—
NO_2	1.23 ppm	—	1.02 ppm	—
PAN	0.00 ppm	0.60 ppm	0.00 ppm	0.74 ppm
HNO_3	0.00 ppm	0.10 ppm	0.00 ppm	0.17 ppm
PAN/HNO_3	—	6.0 ppm	—	4.4 ppm

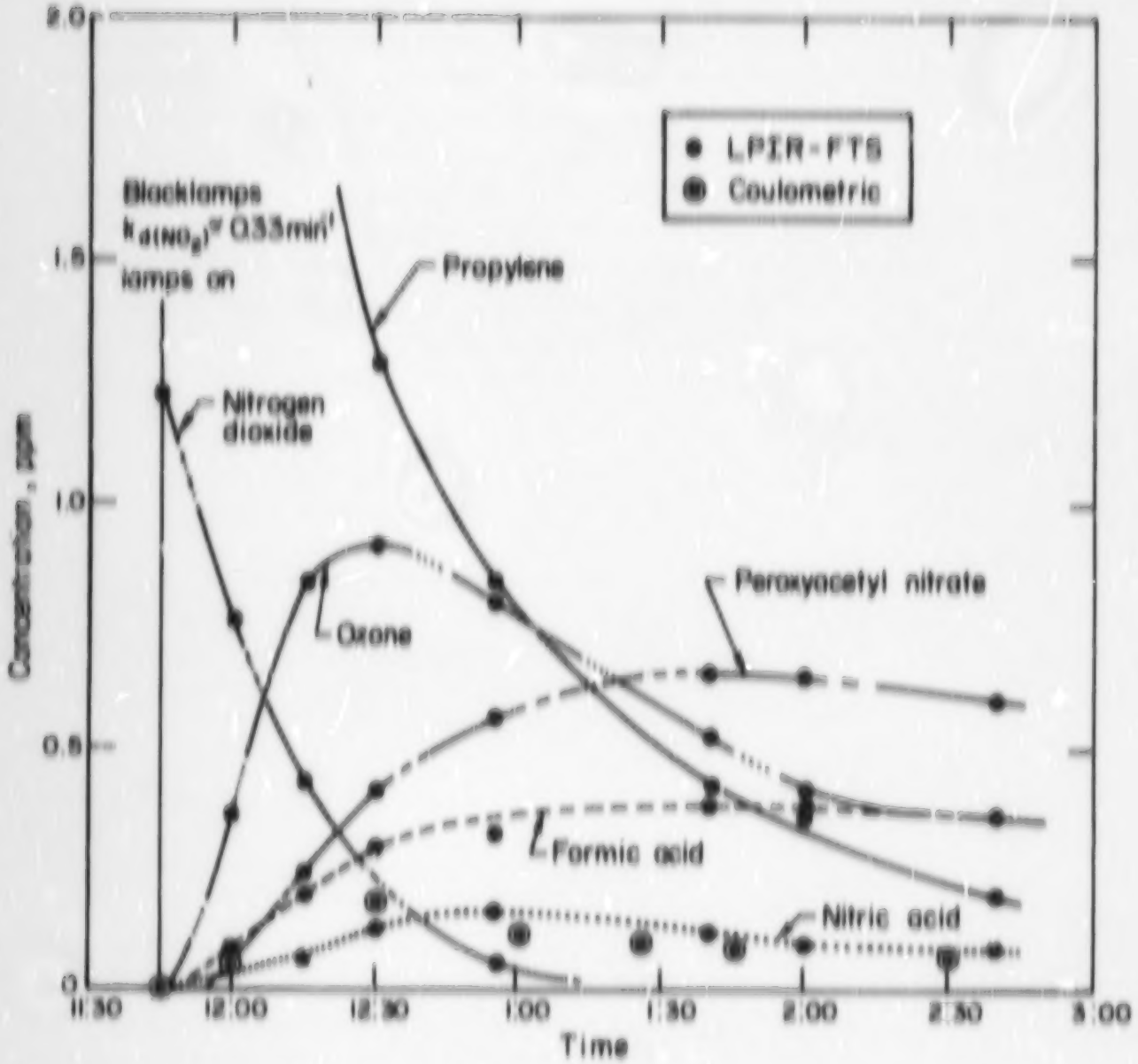

FIGURE 3. PHOTOOXIDATION OF 3.65 ppm C_3H_6, 1.23 ppm NO_2

In the original Battelle experiment a close nitrogen balance was observed throughout the irradiation. In the EPA chamber there was an initial rapid (15 min.) decrease in accountable nitrogen as NO_2 decreased without a corresponding increase in PAN or HNO_3. After the first 15 minutes of the experiment however, the nitrogen accountability was excellent, as shown in Table 3. Some nitric oxide formation is expected early in the experiment due to the photolysis of NO_2. However, our kinetic model predicts that once a photostationary state is attained, this concentration of NO would be much too low to explain the initial discrepancy. Loss of nitric acid to the glass walls of the reactor is another possible explanation for the missing NO_x.

TABLE 3. IRRADIATION OF C_3H_6/NO_2 MIXTURE IN EPA CHAMBER (ALL CONCENTRATIONS IN PPM)

Time	NO_2	PAN	HNO_3	Total Accountable Nitrogen
11:45	1.23	—	—	1.23
12:00	.74	.05	.03	.82
12:15	.43	.24	.07	.74
12:30	.24	.41	.12	.77
12:50	.04	.56	.16	.76
1:40	—	.65	.12	.77
2:00	—	.65	.10	.75
2:40	—	.60	.10	.70

The results of the third comparison experiment are plotted in Figure 4. Sulfur dioxide was included in this run to study the effects of SO_2 reaction products (e.g., H_2SO_4) on the coulometric monitor. Again, the coulometric instrument was unaffected by high levels of NO_2 and SO_2 at the start of the experiment, and O_3, PAN, formic acid, and (presumably) H_2SO_4 during the irradiation. Good agreement between the two monitors was again observed. The nitrogen accountability during this experiment is reported in Table 4. Again, after an initial rapid decline in accountable nitrogen,

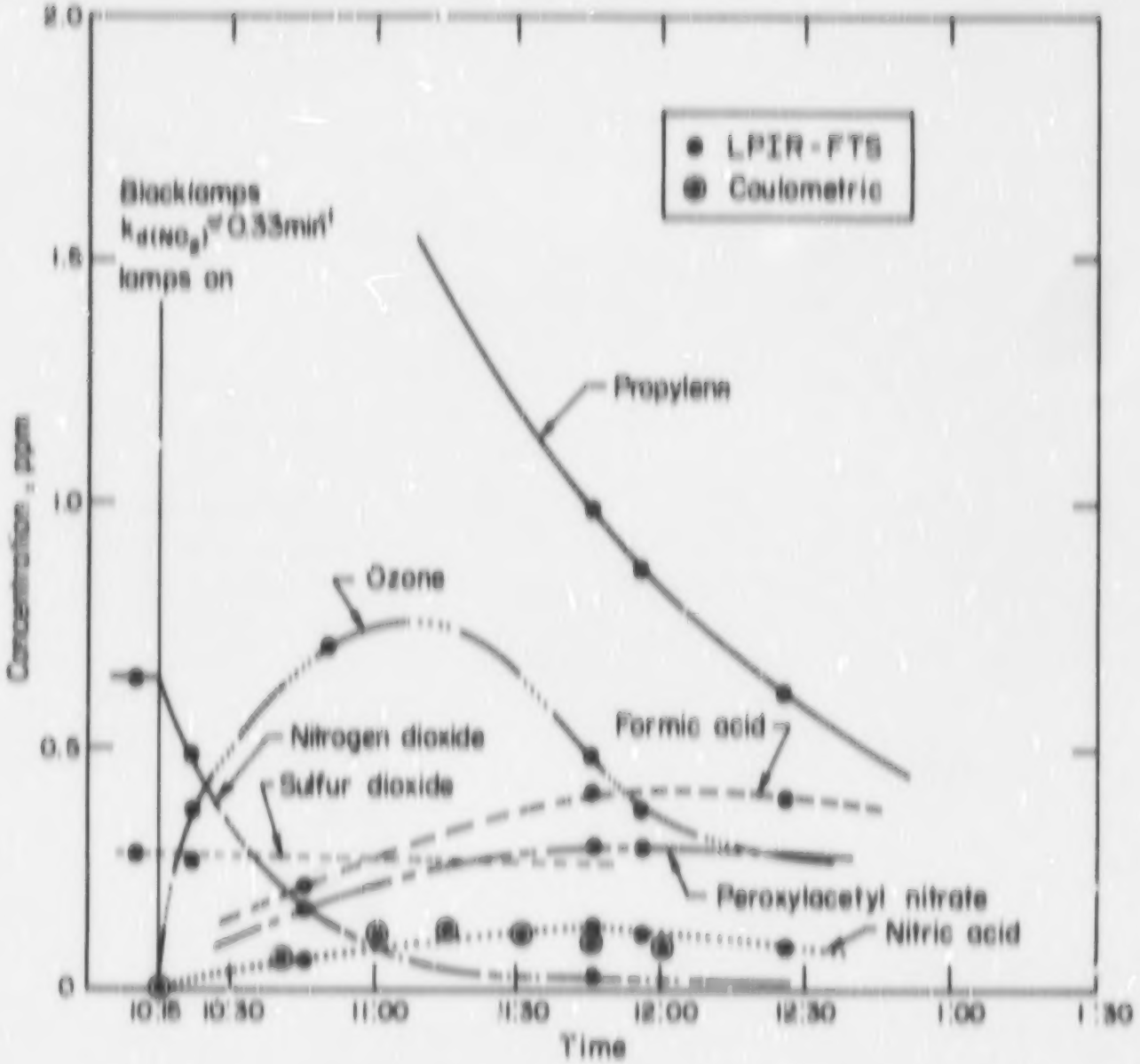

FIGURE 4. PHOTOOXIDATION OF 3.7 ppm C_3H_6, 0.64 ppm NO_x, 0.28 ppm SO_2

a fairly constant nitrogen balance was maintained throughout the remainder of the experiment.

TABLE 4. IRRADIATION OF $C_3H_6/NO_x/SO_x$ MIXTURE IN EPA CHAMBER (ALL CONCENTRATIONS IN PPM)

Time	NO_2	PAN	HNO_3	Total Accountable Nitrogen
10:15	.64	—	—	.64
10:45	.16	.16	.06	.38
11:46	.02	.29	.13	.44
12:25	—	.26	.08	.36

In summary, there are several factors which could potentially influence the comparison between the two nitric acid measurement techniques during the three experiments just described. The very different analytical methods employed, the difference in calibration procedures, and possible concentration gradients within the LPIR smog chamber are all potential causes of disagreement between the two methods. Considering these possible sources of inaccuracy, the agreement between the two methods was quite good. The results of these intercomparisons should serve to confirm the utility of the coulometric technique for nitric acid monitoring, even under the rather adverse conditions found in smog chambers.

Chemiluminescence Interference

Since the early 1970's, chemiluminescence procedures have been widely employed to monitor NO and NO_2 in ambient air. At first the measurement was claimed to be interference free. Indeed, to the best of our knowledge, there are no interferences to the measurement of NO by chemiluminescence. The determination of NO_2 by this technique requires that the NO_2 be reduced to NO prior to measurement. Catalytic converters of various compositions and operating at different temperatures have been employed for this reduction. It is this conversion step which introduces interferences

into the NO_2 measurement, since any compound which is converted to NO by the catalyst will be displayed as NO_2.

High-temperature (~700 C) stainless steel converters were first employed for the reduction of NO_2 to NO. However, it soon became apparent that this type of converter oxidizes NH_3 and amines to NO and therefore interferes with the NO_2 determination. This fact has been advantageously employed to monitor ammonia in the atmosphere[1,8]. To eliminate the ammonia interference, instrument manufacturers switched to lower temperature converters formulated from molybdenum, gold, and carbon.

Even those lower temperature converters are not free from interference, however. In 1974, Winer, et al.[9], reported essentially quantitative interference by peroxyacetyl nitrate (PAN) and several other organic nitrates and nitrites to instruments with carbon and molybdenum converters. They found nonquantitative response to nitroethane and nitric acid. At about the same time, we were observing and attempting to quantify nitric acid response in the chemiluminescent determination of NO_2[1]. We found that the nitric acid response was variable, but was often close to quantitative. There was some evidence at higher nitric acid concentrations that the catalyst was subject to fatigue or poisoning over longer time periods.

For many monitoring applications these interferences may not be too serious, as long as the user is aware that the instrument response in the catalytic mode approximates total oxidized gaseous nitrogen (excluding N_2O) rather than just NO and NO_2. However, for two applications, smog-chamber measurements and the determination of atmospheric trace nitrogen distribution, these interferences are critical. We have discussed this problem with smog-chamber measurements elsewhere[7].

The impact of these interferences on the determination of NO_x can be large during afternoon periods of peak photochemical smog. In some cases, the interferences comprise more than 50% of the "total NO_x" signal. If PAN is measured simultaneously with the chemiluminescence measurements, its concentration can be subtracted from the NO_2 output, since PAN is known to interfere quantitatively. This is one way to minimize the impact of the interference. However, because the extent of HNO_3 response may vary, the use of a subtraction procedure is much less certain to correct for nitric acid interference.

Since many monitoring facilities are not equipped to measure either PAN or HNO_3, and since the appropriateness of subtracting HNO_3 to correct chemiluminescent NO_2 measurements is uncertain anyway, it would be very useful if the interferences could be eliminated or at least minimized during the measurement process. The objective of this task is to briefly investigate some potential methods for removing these interferences.

During this investigation of chemiluminescent interferences, we continued to observe nearly quantitative but occasionally variable response by HNO_3. Data presented earlier in this report (Figure 1) are typical of the nearly quantitative response frequently obtained from the chemiluminuscent instrument using a carbon converter at 240 C. However, variability of response is still observed under some conditions, especially at longer exposure times. It seems that the prior history of the converter, the exposure time, the relative humidity and the condition of the sampling lines all influence the apparent response of the instrument to nitric acid. The experimental determination of this response factor is fraught with difficulties, including the adsorption/desorption behavior of gaseous HNO_3, the thermal decomposition of HNO_3, and the preparation and dilution of pure gaseous nitric acid. A number of experiments conducted for the purpose of determining the response factor have still not uncovered all of the factors which affect the HNO_3 response. Under most conditions we have investigated, when we were reasonably certain that we has prepared pure dilute gaseous nitric acid, the response was quantitative. However, some of our experiments displayed erratic behavior, with nonquantitative response, and Gantner[4] has reported no chemiluminescent response to nitric acid at all.

Determination of the response factor would no longer be so important if a means to eliminate the chemiluminescence interference of HNO_3 (and also PAN) could be devised. We have investigated three different techniques to eliminate or minimize the interferences. The first involves control of the converter temperature, the second the use of filtration techniques, and third, the use of alternative catalytic converters.

Thermal Adjustment

One means of reducing interference to the NO_2 measurement might be to "adjust" the catalytic converter to a temperature at which NO_2 is still efficiently reduced but interfering species such as HNO_3 and PAN are no longer decomposed to NO. This technique is unlikely to work for PAN, since PAN decomposes at temperatures too low for the conversion of NO_2 to NO (<100 C). However, such a procedure might eliminate the variable nitric acid interference, which is more important from our viewpoint since correction for HNO_3 by subtraction is uncertain due to the variable response.

Two types of converters were studied: stainless steel and carbon. The stainless steel converter acts as a true catalyst. The equilibrium ratio NO_2/NO decreases with increasing temperature and decreasing oxygen pressure as shown in Table 5[10]. It is clear from this table that temperatures in excess of 500 C are necessary to efficiently reduce NO_2 to NO using a stainless steel converter at the O_2 pressures used in many converters (≈100 Torr). Nitric acid response as a function of temperature is shown for a stainless steel converter in Figure 5. The data indicate that reduction of temperature to about 400 C is necessary to eliminate the nitric acid interference. It is obvious from Table 5 that such a low temperature adversely affects the efficiency of NO_2 to NO conversion and is therefore unacceptable.

TABLE 5. THE EQUILIBRIUM RATIO, NO_2/NO, FOR $NO_2 \rightleftarrows NO + 1/2\ O_2$[10]

Temperature, °C	Oxygen Pressure 1 Torr	10 Torr	100 Torr
27	4.92×10^{4}	1.56×10^{5}	4.92×10^{5}
127	1.55×10^{2}	4.90×10^{2}	1.55×10^{3}
227	4.72	1.49×10	4.72×10
327	4.57×10^{-1}	1.44	4.57
427	8.75×10^{-2}	2.77×10^{-1}	8.75×10^{-1}
527	2.43×10^{-2}	7.69×10^{-2}	2.43×10^{-1}
627	9.16×10^{-3}	2.90×10^{-2}	9.16×10^{-2}
727	4.19×10^{-3}	1.32×10^{-2}	4.19×10^{-2}

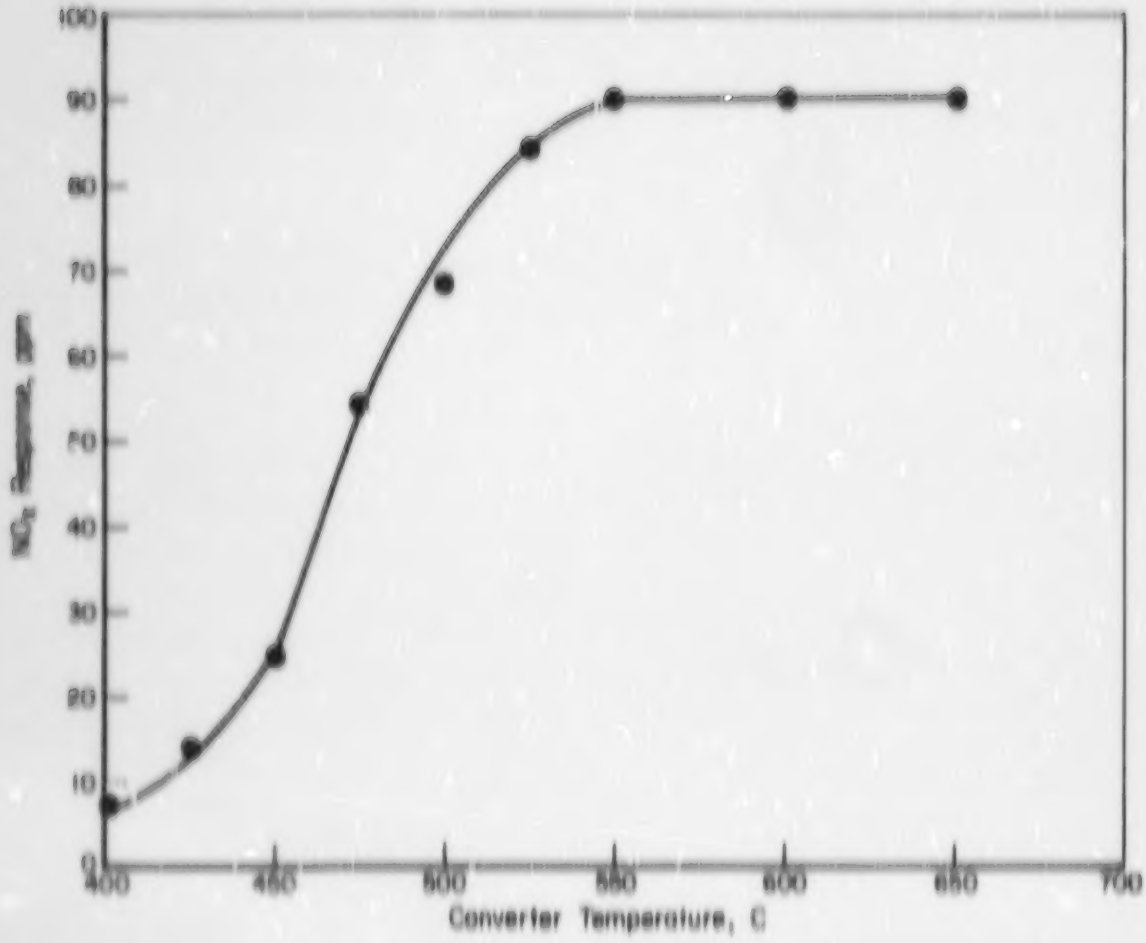

FIGURE 6. REDUCTION OF HNO_3 BY A STAINLESS STEEL CONVERTER

The use of carbon converters lowers the temperature at which efficient NO_2 reduction occurs, because the carbon participates in the reaction via $NO_2 + C \rightarrow CO + NO$. The carbon converter used in routine monitoring operates at about 260 C and is >98% efficient at reducing NO_2 at that temperature. The results of our experiments to thermally "adjust" this converter to minimize HNO_3 response are shown in Table 6. Even at temperatures as low as 140 C the carbon converter still effectively decomposed HNO_3 to NO. Since the efficiency of NO_2 reduction falls off at this temperature, adjustment of the carbon converter to eliminate HNO_3 interference does not appear feasible.

TABLE 6. CONVERSION OF HNO_3 BY CARBON CONVERTER

Temperature, °C	Response of Chemiluminescence Instrument to 0.18 ppm HNO_3, ppm
285	0.180
260	0.180
230	0.180
192	0.180
153	0.180
140	0.180

Filtration Techniques

Filtration was also investigated as a means for removing HNO_3 and/or PAN interference. We knew from previous experience that nylon filters remove HNO_3 without scrubbing NO_2 or NO, but it was also necessary to determine whether the HNO_3 was truly removed by nylon or merely decomposed to NO_2 and NO. If decomposition occurs, the nylon filter would be useless in removing HNO_3 interference with the chemiluminescent technique. A number of experiments at different humidities in our laboratory have shown that nylon does remove >95% of the gaseous nitric acid without conversion to NO or NO_2. Thus nylon filters can be used to eliminate nitric acid interference with chemiluminescent NO_2 measurements.

Additional experiments were run to determine whether PAN could also be selectively removed from ambient air by nylon or some other filter material. We recently conducted PAN adsorption experiments for another program (EPA Contract No. 68-02-2213) using quartz fiber, glass fiber, nylon, polycarbonate, and cellulose acetate filter materials. The results of these experiments are shown in Table 7. It is clear from the table that neither nylon nor any of the other filter materials has a large enough capacity for PAN removal to make it attractive as a PAN scrubber for chemiluminescence instruments.

TABLE 7. PAN-FILTER INTERACTION STUDY RESULTS

Filter Material	PAN Adsorbed, µg
Quartz - Microquartz	0.003
Quartz - Pallflex 7500 QAST	0.006
Quartz - Pallflex E 70-0275W	0.009
Glass - Gelman AA	0.15
Glass - Gelman A	0.010
Glass - Gelman E	0.012
Glass - Gelman AE	0.18
Glass - Gelman Spectro	0.020
Nylon - Duralon	0.008
Cellulose Acetate	0.062
Polycarbonate	0.007
Teflon	0.005

The experiments on interference removal by filtration show that nitric acid can be effectively removed by nylon filters, whereas no filters have been identified which selectively scrub PAN. Incidentally, it has not escaped our notice that the selective removal of HNO_3 prior to measurement by chemiluminescent instruments could serve as the basis for an analytical method for gaseous HNO_3. We have been investigating this possibility for some time and hope to report on it in the near future.

Alternative Converters

A number of researchers have suggested that ferrous sulfate ($FeSO_4$) could be employed as a catalytic converter in chemiluminescent instruments. Steadman[1] at Michigan and Miller, et al.[3], at Battelle have reported quantitative conversion of NO_2 to NO at room temperature. If $FeSO_4$ quantitatively reduces NO_2 without converting HNO_3 or PAN, it would be the ideal converter. We have studied the efficiency of NO_2 to NO conversion by $FeSO_4 \cdot 7H_2O$ (the anhydrous $FeSO_4$ is ineffective) under a variety of conditions. Unfortunately, the reduction does not appear to be quantitative under all circumstances. However, ferrous sulfate could still serve the purpose if it removes HNO_3 and PAN but quantitatively passes NO and NO_2. If this were the case, a $FeSO_4 \cdot 7H_2O$ trap could be added to chemiluminescent instruments just ahead of the thermal converter. In the NO-mode, the instrument would read only NO (no trap or converter in line). In the NO_x mode, the air passes through the $FeSO_4$ trap where some NO_2 is reduced to NO and, more importantly, HNO_3 and PAN might be scrubbed. The air then flows to the thermal converter where the NO_2 reduction is completed, and on to the detector cell for determination of total NO_x ($NO + NO_2$) as NO. All of our experiments have shown that ferrous sulfate does quantitatively pass NO/NO_2 mixtures, even though the reduction is not complete. The results of these experiments are shown in Table 8. Experiments were therefore initiated to determine whether the material would scrub nitric acid and PAN.

TABLE 8. EFFECT OF FERROUS SULFATE ON NO_x (50% RELATIVE HUMIDITY) ALL CONCENTRATIONS IN PPM

Initial Conditions			After Passage Through $FeSO_4$			Percent Conversion	Percent NO_x
NO	NO_2	NO_x	NO	NO_2	NO_x	to NO	Passed
0.00	1.18	1.18	0.88	0.28	1.16	75	98
0.01	1.02	1.03	0.78	0.27	1.05	75	102
0.01	0.95	0.96	0.72	0.20	0.92	75	96
0.01	0.21	0.22	0.17	0.05	0.22	76	100
0.00	0.36	0.36	—	—	0.35	—	100

We were fairly confident that PAN would be destroyed by interaction with the large surface area within the ferrous sulfate trap, since PAN is relatively unstable. Therefore, we began our investigations by determining the efficiency of ferrous sulfate in scrubbing nitric acid. Table 9 shows the results of several experiments at different nitric acid concentrations. The efficiency of removal was high in all cases. Since these results were obtained with a NO_x chemiluminescence instrument, it is clear that the nitric acid is removed so that neither HNO_3 nor its possible NO_x decomposition products pass through the trap. In another experiment, a mixture of 0.22 ppm NO, 0.21 ppm NO_2, and 0.61 ppm HNO_3 was passed through a ferrous sulfate trap. The trap decreased the total NO_x ($NO + NO_2 + HNO_3$) reading by 0.62 ppm, implying strongly that the HNO_3 was removed selectively.

TABLE 9. NITRIC ACID REMOVAL BY $FeSO_4$

HNO_3 Initial, ppm	HNO_3 Final, ppm	Percent Removal
2.70	0.3	89
.464	0.035	92
.160	0.000	100
.155	0.005	97
.100	0.005	95
.112	0.004	97
.073	0.000	100
1.00	0.000	100
.150	0.000	100

With the assurance that ferrous sulfate efficiently removes nitric acid while quantitatively passing NO_x, we next conducted experiments to determine the efficiency of PAN removal. The results of a number of experiments showing the removal of PAN by different scrubber materials are given in Table 10. We were quite surprised to observe that $FeSO_4 \cdot 7H_2O$ passes a considerable fraction of the PAN undisturbed. The fact that only a variable fraction of PAN is removed by the ferrous sulfate trap greatly

TABLE 10. EFFECT OF VARIOUS MATERIALS ON PAN REMOVAL (CONCENTRATIONS IN PPM)

Trap Material	Relative Humidity, %	PAN, Initial	PAN, Final	Percent Removal
$FeSO_4 \cdot 7H_2O$	<5	0.060	0.045	25
$FeSO_4 \cdot 7H_2O$	<5	0.123	0.080	35
$FeSO_4 \cdot 7H_2O$	65	0.125	0.125	0
$FeSO_4 \cdot 7H_2O$ + Cu(power)	65	0.130	0.036	72
K_2CO_3	65	0.130	0.000	100
K_2CO_3	45	0.170	0.000	100

reduces the attractiveness of ferrous sulfate traps as a solution to chemiluminescence interferences. It has no advantage over nylon filters, since both remove HNO_3 and pass NO_x, and it has the disadvantage that it may remove an unknown fraction of the PAN interference. EPA[12] has also conducted a study of the effect of ferrous sulfate on PAN. They find that much of the PAN is decomposed to NO, so that PAN still interfers with the chemiluminescent technique.

Another material which was examined, potassium carbonate, completely eliminated PAN from the sample stream. However, a limited number of experiments indicated that the PAN was decomposed by K_2CO_3 to NO_x, and thus still interfered with the chemiluminescence NO_x measurement.

On the basis of the experiments described above, we recommend using nylon prefilters to eliminate HNO_3 interference to chemiluminescence monitors. We have discovered no means of removing PAN interference; however, since PAN responds quantitatively, its concentration can be mathematically subtracted from the chemiluminescence NO_x output. By employing a nylon prefilter and PAN subtraction, the NO_2 output from commercial chemiluminescence monitors should approximate the ambient NO_2 concentration fairly closely.

Interaction of Gaseous Nitric Acid With Filters

One of the most surprising results of our 1973 St. Louis and West Covina field studies was the low observed concentration of particulate nitrate. The nitrate concentration in West Covina averaged 1.7 $\mu g/m^3$ during late August and September, compared to annual average nitrate concentrations 2-3 times higher [13] at many stations in the Los Angeles basin. There are some reports of annual average concentrations in excess of 15 $\mu g/m^3$ [14] in Los Angeles. However, LAAPCD data for September, 1973, indicate that low nitrate levels were prevalent throughout the basin during our study period. The monthly average nitrate concentrations for downtown Los Angeles and Azusa during 1973 are shown in Table 11 [15]. Even though the annual averages were 6.8 and 6.5 $\mu g/m^3$ for those two locations, the September concentrations were only 1.4 and 2.0 $\mu g/m^3$. These values are very much in line with our results, so that concern over our apparently low values was largely unwarranted.

TABLE 11. MONTHLY AVERAGE PARTICULATE NITRATE CONCENTRATIONS[15], $\mu g/m^3$

Month	Downtown Los Angeles	Azusa
January	15.4	14.0
February	14.2	9.9
March	13.1	7.7
April	8.4	14.3
May	5.7	5.9
June	4.4	5.6
July	2.4	2.9
August	1.6	3.4
September	1.4	2.0
October	5.0	11.9
November	5.5	4.3
December	4.0	3.4
Annual Average	6.8	6.5

In searching for possible explanations of what were thought to be low nitrate values, we observed a phenomenon which may seriously influence the accuracy of particulate nitrate collections. Specifically, we observed artifact particulate nitrate collection on glass-fiber filters caused by the interaction of the alkaline glass surface with gaseous nitric acid. In preliminary experiments, neutral quartz filters such as those used in the 1973 field program did not appear to be significantly affected by nitric acid. The objective of this task was to determine whether gaseous nitric acid significantly affects particulate nitrate collections. Simultaneously with this study, Battelle conducted a program for the Environmental Protection Agency (Contract No. 68-02-2213) on the broader topic of particulate nitrate sampling and analysis methodology, in which the interactions of numerous gases with filter media were investigated. Artifact nitrate formation by several nitrogen-containing gases was investigated during the EPA program[16].

The interaction of nitric acid with glass and quartz filter materials is the specific subject of this task. We investigated those interactions using a 500-cu-ft Teflon chamber enclosed in a large darkened box. Clean compressed air was used to fill the Teflon chamber. The chamber was filled and evacuated twice before each experiment. After the final filling, gaseous nitric acid was injected into the chamber by slowly passing dry air through a HNO_3/H_2SO_4 mixture and filtering to remove any aerosol prior to flowing to the chamber. Additional air was rapidly added to the chamber to facilitate mixing. The concentration was monitored with a NO_x chemiluminescence monitor with high-temperature stainless steel catalytic converter. For several experiments, the chamber was checked with an electrical aerosol analyzer (Thermal Systems, Inc.) after nitric acid injection to be certain no nitrate aerosol was present.

Approximately 1 cubic meter of the chamber mixture was sampled in parallel through several 47 mm filters. The nitric acid concentration was adjusted to obtain approximately the same mass of acid through each filter as would pass through a standard high-volume sampler ($\sim$2000 m^3) during a moderately smoggy day in Los Angeles.

After sampling, the filters were analyzed for nitrate and total nitrogen. Nitrate was determined by the brucine colorimetric procedure and total nitrogen by a combustion/thermal conductivity method.

The results of the investigation into nitric acid interactions are shown in Table 12.

The exposed filter surface in a high volume sampler is about 70 in.^{2} and a 24-hour sample volume is ~2000 m^3 of air. Based on these values we can calculate an equivalent interference due to artifact nitrate by multiplying the values in Table 12 by 70/2000 or 0.035. The resulting values approximate the interference to particulate nitrate collection caused by gaseous nitric acid in a moderately smoggy atmosphere (the nitric acid concentrations in Table 12 simulate the mass of nitric acid passing through a high volume filter when ambient levels average between 0.2-9 ppb).

In every experiment, artifact nitrate collection on the quartz filters is much less than on any of the glass filters. In fact, artifact collection is negligible in most of the quartz collections. In the humidified experiment, no nitrate figure is available for the quartz filter; however, the lack of any increase in the total nitrogen on this filter indicates no significant artifact nitrate collection. There appear to be only slight increases in the quantity of artifact nitrate collected by the glass filters as the nitric acid concentration increased from 0.35 to 17.5 ppm. This is an indication that the surface active sites which are collecting nitric acid probably become saturated at rather low levels of the acid. Under these conditions, where the collection of artifact nitrate is limited by the surface area rather than the concentration of pollutant gas, larger filters will collect proportionately larger amounts of bogus nitrate. Filters collected over short periods (up to the point where the filter becomes "saturated") will show the greatest interference, since sampling past the point of saturation serves to dilute the impact of the interference. Thus, glass-fiber filters collected over short time intervals during periods of high nitric acid concentration (midafternoons) are expected to exhibit the maximum interference due to gaseous nitric acid collection.

If the distribution of nitrate between the gaseous and particulate phases is important in terms of physiological manifestations, as seems likely,

TABLE 12. ARTIFACT NITRATE FORMED ON QUARTZ AND GLASS FILTERS FROM GASEOUS NITRIC ACID (47 mm FILTERS)

Filter Type[a]	Relative Humidity, %	Nitric Acid, ppm	Artifact Nitrate,[b] µg/in.^{2} filter	Artifact Total N,[c] µg/in.^{2} filter
Quartz A	5	1.4	<7	<13
Glass A	5	1.4	126	40
Glass E	5	1.4	133	53
Glass E	5	1.4	127	60
Quartz A	5	1.5	<7	<7
Glass A	5	1.5	120	33
Glass A	5	1.5	153	27
Glass E	5	1.5	127	40
Quartz A	5	8.0	<7	<7
Glass A	5	8.0	167	40
Glass E	5	8.0	247	67
Quartz A	5	3.0	<7	<7
Glass A	5	3.0	160	33
Glass E	5	3.0	160	53
Quartz A	30	3.3	.	<7
Glass A	30	3.3	213	67
Glass E	30	3.3	307	60
Quartz A	5	0.35	<3	7
Quartz P	5	0.35	61	20
Glass AE	5	0.35	153	27
Quartz A	5	17.5	10	30
Quartz P	5	17.5	16	17
Glass S	5	17.5	229	166

(a) Quartz A is experimental fiber produced by Arthur D. Little; Quartz P is Pallflex QAST; Glass A, E, and AE are Gelman A, E, and AE; Glass J is Gelman Spectrograde.

(b) All NO_3^- blanks <3 µg/in.^{2} of filter.

(c) All Total N blanks <13 µg/in.^{2} of filter; Quartz A, Quartz P, and Glass S are usually <7 µg/in.^{2} of filter.

then a careful separation of the gaseous and particulate nitrate components is necessary. Evidence from field studies in which quartz filters were used indicates that the ratio $\frac{\text{gaseous inorganic } NO_3^-}{\text{particulate inorganic } NO_3^-}$ is probably much higher than is generally recognized. At West Covina we observed an average ratio of about 10. The ratio is likely to be very site dependent, decreasing at longer distances downwind of the emissions source.

A.M./P.M. Aerosol Patterns

During the 1973 field studies in St. Louis and West Covina, several sets of high volume filters were collected on roughly an a.m./p.m. basis to investigate the daily pattern of nitrogen aerosol formation. The samples were collected on high-purity quartz filters during days of predicted high pollution. These special samples were collected on 1 day in St. Louis and 2 days in West Covina. On each of these days, one filter was sampled between midnight and noon and a second filter between noon and 11 p.m. A third filter sampled continuously between midnight and 11 p.m. The continuous sample was analyzed at the conclusion of the 1973 field programs; the a.m./p.m. filters were sealed and stored in a freezer. Since these filters were stored for nearly 2 years before analysis, there is a possibility that the integrity of the sample was affected. Any such effect should show up in the data and would be of interest in its own right.

The results of the aerosol analyses of the samples described above are shown in Table 13. The NH_4^+, NO_3^-, and $SO_4^=$ results are shown in both mass and concentration units. Daily average ozone, NO, and mass loading are also tabulated for comparison. The sum of the individual compound's masses on the a.m. and p.m. filters should approximately equal the mass of each specie on the continuous filter, since the flow rates were nearly the same for all samples. An exception is August 29, where the times of the a.m. and p.m. collections do not equal the time of the continuous collection.

The aerosol concentrations in Table 13 show that ammonium and sulfate are more prevalent in the p.m., especially in St. Louis. The ammonium and sulfate data are highly correlated and show an average molar ratio close to 1.0. The correlation and molar ratio taken together suggest

TABLE 13. RESULTS OF A.M./P.M. AEROSOL STUDIES

	Filter Analyses						Daily Averages		
	NH_4^+	NO_3^-	$SO_4^=$	C	H	N	Mass Loading, $\mu g/m^3$	O_3, ppm	NO_2, ppm
August 10, 1973 (St. Louis)			mg per Filter ($\mu g/m^3$)				66.4	0.041	0.041
Sampling Times									
00:00 - 12:00	0.2(0.3)	0.4(0.5)	3.2(3.9)	7.8	-	0.5			
12:00 - 23:00	1.5(2.2)	0.1(0.1)	8.9(12.4)	9.0	-	1.6			
00:00 - 23:00(a)	2.0(1.3)	0.5(0.3)	-	22.6	3.6	2.4			
August 29, 1973 (West Covina)							98.9	0.062	0.171
Sampling Times									
00:00 - 12:00	1.8(2.0)	0.4(0.4)	11.3(12.7)	14.5	4.3	2.5			
12:00 - 21:30	2.0(3.7)	0.2(0.4)	10.2(18.8)	14.9	4.7	2.5			
00:00 - 23:30(a)	4.8(3.2)	2.2(1.5)	-	35.4	6.1	6.6			
September 7, 1973 (West Covina)							135.8	0.047	0.239
Sampling Times									
00:00 - 10:00	3.5(4.8)	0.4(0.5)	15.4(21.1)	19.9	6.0	3.9			
10:00 - 23:00	5.6(6.4)	0.3(0.3)	23.4(26.9)	18.3	6.8	5.8			
00:00 - 23:00(a)	10.5(7.2)	2.0(1.3)	-	41.8	9.3	14.8			

(a) Values for a 23-hour filter sample collected simultaneously with the a.m./p.m. filters.

that ammonium and sulfate are associated chemically, possibly in a form such as $(NH_4)HSO_4$. Similar findings have been reported for midwestern cities[17,18]. The sums of the a.m. and p.m. masses of NH_4^+, C,H, and N agree reasonably well with the masses on the continuously collected filter, considering differences in sampling periods and the fact that the a.m./p.m. filters were stored for 2 years before analysis.

Judging from the concentration data, particulate nitrate seems to have formed during the morning on August 10 in St. Louis. The concentrations were more evenly distributed at the West Covina site, both a.m. and p.m. concentrations being about equal. However, the nitrate masses on the West Covina a.m. and p.m. filters are not in agreement with the continuous filters. This discrepancy suggests a decay of the nitrate during the 2-year storage period. If nitrate has been lost during storage then the a.m./p.m. nitrate comparisons are invalid. It is puzzling however, that nitrate would be lost from the West Covina filters but not the St. Louis filters; both sets of samples were stored in the same manner and for the same length of time. Also, recent experiments at Battelle-Columbus on the effect of storage of filters of known nitrate composition have indicated no significant decay over periods of several months. Our uncertainty regarding the effect of the 2-year storage period on the nitrate values causes difficulty in interpreting the a.m./p.m. nitrate results. The St. Louis results, which seem most reliable, suggest strong nitrate formation before midday. This agrees with Hidy and Burton's findings[19] in the Los Angeles basin. However, much additional work is needed to define the rates, mechanisms and conditions conducive to particulate nitrate formation in urban air. In future studies we plan to obtain much better time resolution of the particulate nitrate samples in order to answer these questions.

Results of the ESCA Analysis

Following the 1973 West Covina study we were able to account for an average of about 75 percent of the total aerosol nitrogen collected on high volume filters in terms of ammonium, nitrite, and nitrate[1]. The identify of the remaining 25% particulate nitrogen was unresolved. Reduced

nitrogen species (amine and pyridine-type compounds) have been observed in urban aerosol collections by Novakov and coworkers[20] and could account for the remaining particulate nitrogen. To investigate this possibility, several silver membrane filters suitable for ESCA (electron spectroscopy chemical analysis) were collected in West Covina, sealed, and sent to Dr. Novakov* at Lawrence Berkeley Laboratory for ESCA analysis. The results of the ESCA analyses are summarized in Table 14.

TABLE 14. RESULTS OF REDUCED NITROGEN ANALYSIS OF DAILY PARTICULATE SAMPLES ($\mu g/m^3$)

Date	Total Reduced Nitrogen(a) ESCA	Total Reduced Nitrogen(a) Battelle(b)	Total Nitrogen
8/29/73	7.1	1.6	4.4
8/31/73	5.3	0.8	5.2
9/8/73	2.9	1.0	5.5
9/9/73	2.3	1.4	3.7
9/12/73	4.8	2.6	6.3

(a) Excluding ammonium.
(b) Total aerosol nitrogen minus NH_4^+ and NO_3^-.

The ESCA technique determines total reduced nitrogen other than ammonium in the particulate collection. For comparison we have also tabulated the total particulate nitrogen minus NH_4^+ and NO_3^- as determined from high volume filter samples collected simultaneously with the silver filters. If reduced nitrogen compounds (other than NH_4^+) were responsible for the 25% unaccountable nitrogen, the first two columns in Table 14 should agree, or at least show similar trends. However, the ESCA reduced nitrogen concentrations are in every case considerably greater than our "unexplained" nitrogen concentrations, and in some cases even greater than our total (reduced and oxidized) nitrogen determinations. The trend in the ESCA results does not follow the trends in either the total nitrogen or "unexplained" nitrogen data. Since different sampling media were employed for the ESCA collections, there is a possibility

*Our thanks to Dr. T. Novakov, Lawrence Berkeley Laboratory, for performing these analyses.

that gas/aerosol/filter interactions on one or the other of the filter materials has caused these discrepancies. The sample handling and analytical procedures are also quite different and may contribute to the uncertainty. In any case, the interpretation of the ESCA results is so uncertain that it sheds no light on the discrepancy in the particulate nitrogen balance.

DATA ANALYSIS

This section of the report describes several tasks which were undertaken to increase the accuracy and/or scope of the first year's data interpretation.

Interpretation of West Covina Results

At the conclusion of the 1973 West Covina field study, a report was issued based on the data available to us at that time. Subsequently we have obtained additional data and conducted further analyses to expand and refine the interpretation of the West Covina results. The results of the additional analyses are presented in this section of the report.

In the intial analysis of the West Covina data the diurnal trends in NO_x concentration were examined for clues as to the processes removing NO_x from the air. It was obvious that the major factors affecting the NO_x concentration are not the removal processes but rather the intensity of emissions sources and meteorological conditions. These gross determinants of NO_x concentration overwhelm the changes due to removal processes, and mask the relationships being sought. In order to draw conclusions regarding the extent of NO_x removal from the air and the accountability of NO_x in terms of measured reaction products, it was necessary to detemine the quantity of NO_x removed from air masses to minimize the masking effect of emission rates and dispersion. To calculate the amount of NO_x lost from the air (quantity hereafter termed NO_x-loss) we made use of carbon monoxide as a relatively inert tracer to account for dispersion effects. The NO_x-loss was derived using the equation

$$NO_x\text{-loss} = \frac{(CO)_{measured}}{(CO/NO_x)_{emission\ inventory}} - (NO_x)_{measured} \qquad (1)$$

where $(CO/NO_x)_{emission\ inventory}$ is the ratio based on emission inventory estimates and $(CO)_{measured}$ and $(NO_x)_{measured}$ are the actual concentrations of CO and NO_x at any time. The first term on the right-hand side of the equation can be thought of as a predicted NO_x concentration based on the

estimated emissions ratio of CO and NO_x and the measured CO concentration. The assumption was made that over short time periods (several hours) CO is inert and can be used as a tracer for NO_x concentration. Subtracting the actual measured NO_x concentration from the predicted concentration yields the term "NO_x-loss".

This equation will only yield accurate answers if the CO and NO_x concentrations are measured accurately and if the starting CO/NO_x ratio of the air parcel is known exactly. This ratio is undoubtedly the greatest source of error in making the NO_x-loss calculation. In calculating NO_x-loss from Equation 1 it is first assumed that air parcels monitored at West Covina start out relatively clean (only background levels of CO and NO_x) and pick up a major charge of pollutants in the vicinity of downtown Los Angeles. The CO/NO_x ratio of this initial charge of pollutants is termed the "emissions inventory" ratio. As the air moves toward West Covina, chemical and physical processes are at work to transform or remove NO_x. If we know the initial ratio of CO/NO_x picked up over Los Angeles and if no additional CO or NO_x were added to the air as it moves to West Covina, the calculation of NO_x-loss by Equation 1 would be precise. However, the situation is not that ideal. The initial CO/NO_x ratio must be estimated from emission inventories and, since a number of sources which emit different ratios are involved, uniform mixing of the emissions from these sources must be assumed. The contribution of some sources may vary in intensity during the day (e.g., exhaust contribution from rush-hour traffic), further complicating matters. Finally, additional input of CO and NO_x to the air as it moves toward West Covina does occur. All of these factors can affect the calculation of NO_x-loss. In this and other sections of this report we discuss the accuracy of the variables involved in the NO_x-loss calculation and the applicability of the assumptions just described. Before discussing the NO_x-loss calculations, however, it is instructive to examine the relationship between NO_x and the measured NO_x reaction products.

Relationship of NO_x Reaction Products to Total Oxidized Nitrogen

The nitrogen oxides reaction products measured during our 1973 field studies included PAN, nitric acid, particulate nitrate, and particulate nitrite. The particulate nitrite levels were negligible and the particulate nitrate concentrations were quite low in comparison to PAN and nitric acid (particulate nitrate averaged less than 5% of the sum of PAN and HNO_3 at West Covina).

During midafternoon hours, the sum of the PAN and nitric acid concentrations frequently contributed a significant fraction of the measured gaseous oxides of nitrogen* in both St. Louis and West Covina. The ratio, F_N, ($F_N = \frac{PAN + HNO_3}{NO + NO_2 + PAN + HNO_3}$) ranged from 0 to 76% in St. Louis and 2 to 54% in West Covina during midafternoons. The overall average of this ratio was remarkably similar in the two cities, averaging 10.9% in St. Louis and 10.8% in West Covina. It is interesting that this ratio was the same in the two cities, even though average NO_x in West Covina was three times that found in St. Louis. Plots of this ratio composited over the entire 5-week sampling periods in each city are shown in Figure 6. It is clear from the figure that the contribution of NO_x reaction products to total oxidized gaseous nitrogen rises to a peak of 20-25% during midafternoon in both St. Louis and West Covina. The similarity of the profiles is noteworthy.

Trends in this ratio ($F_N = \frac{PAN + HNO_3}{NO + NO_2 + PAN + HNO_3}$), particulate mass, peak ozone, and average particulate nitrate are shown in Figures 7 and 8 for St. Louis and West Covina, respectively. There appears to be some correspondence in the trends of F_N and other measured variables, but the relationships are not strong. In St. Louis, both mass loading and peak O_3 frequently showed the same trends as F_N. Since both O_3 and mass loading serve as indicators of photochemical smog activity, it is not surprising

*N_2O is not thought to be involved in photochemical smog reactions in the lower atmosphere and is excluded from this discussion.

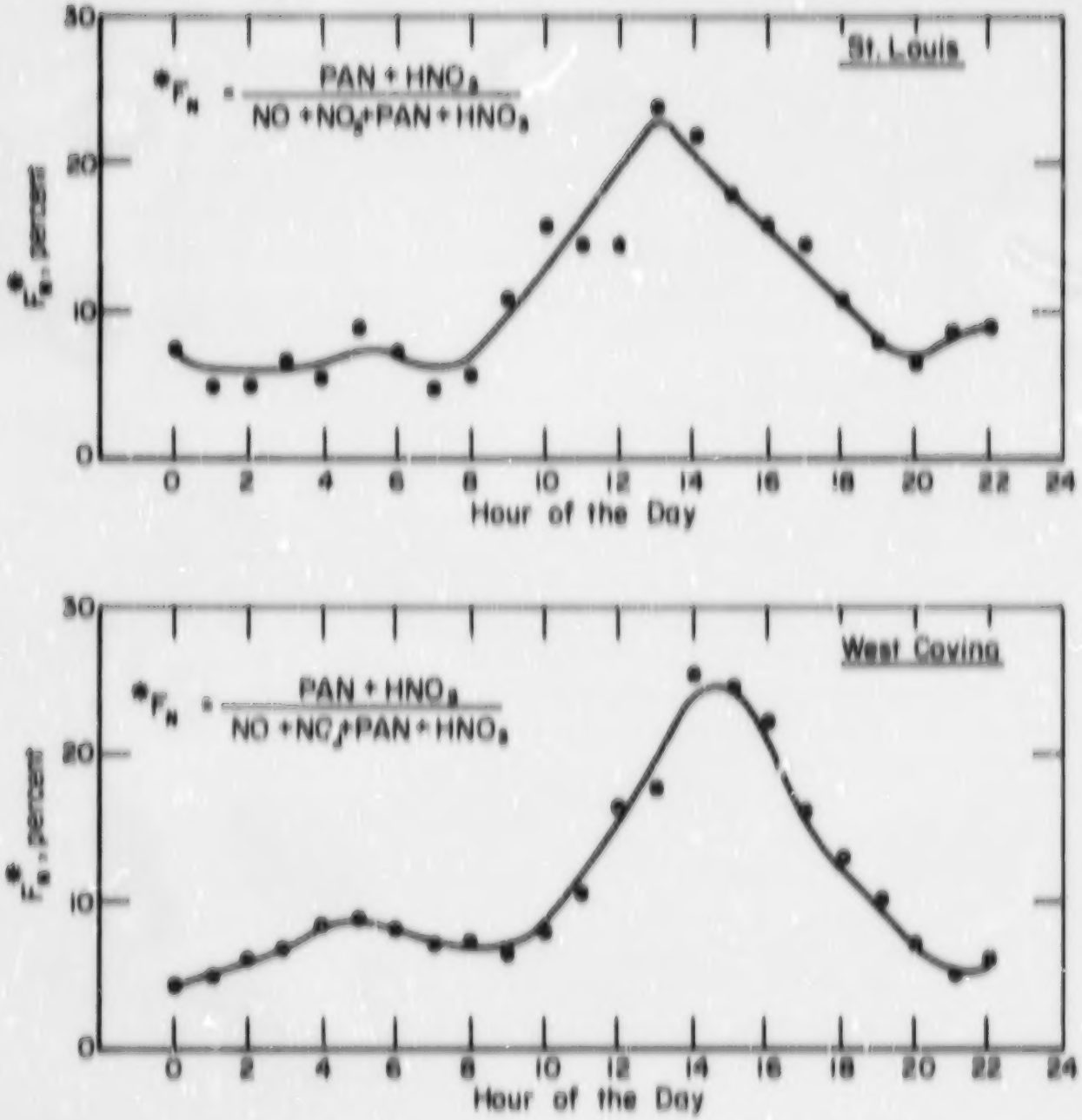
St. Louis
$*F_N = \frac{PAN + HNO_3}{NO + NO_2 + PAN + HNO_3}$
$*F_N$, percent
30
20
10
0
0 2 4 6 8 10 12 14 16 18 20 22 24
Hour of the Day
West Covina
$*F_N = \frac{PAN + HNO_3}{NO + NO_2 + PAN + HNO_3}$
$*F_N$, percent
30
20
10
0
0 2 4 6 8 10 12 14 16 18 20 22 24
Hour of the Day

FIGURE 6. COMPOSITE PROFILES OF F_N* IN ST. LOUIS AND WEST COVINA

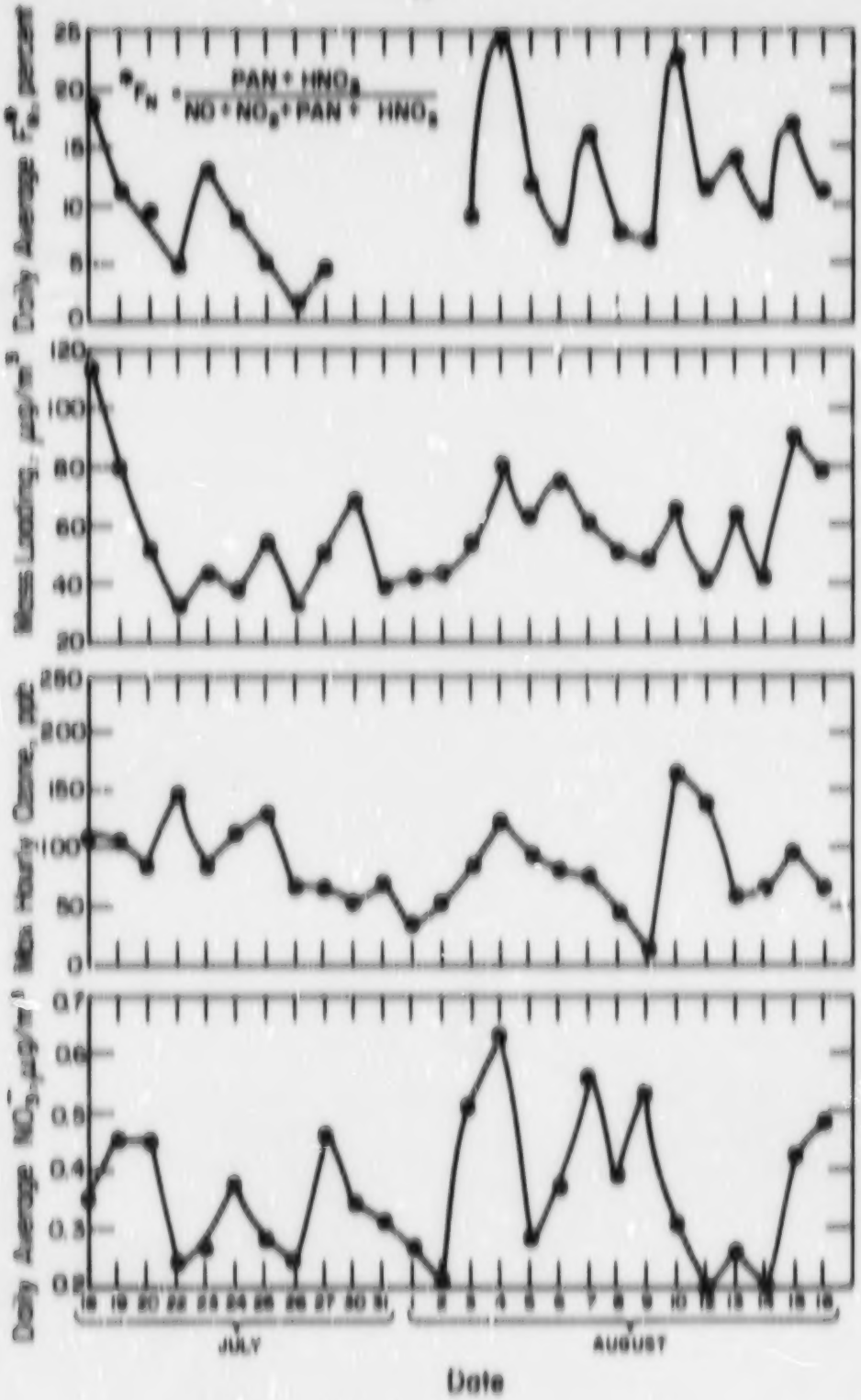

FIGURE 7. DAILY TRENDS IN MEASURED VARIABLES — ST. LOUIS

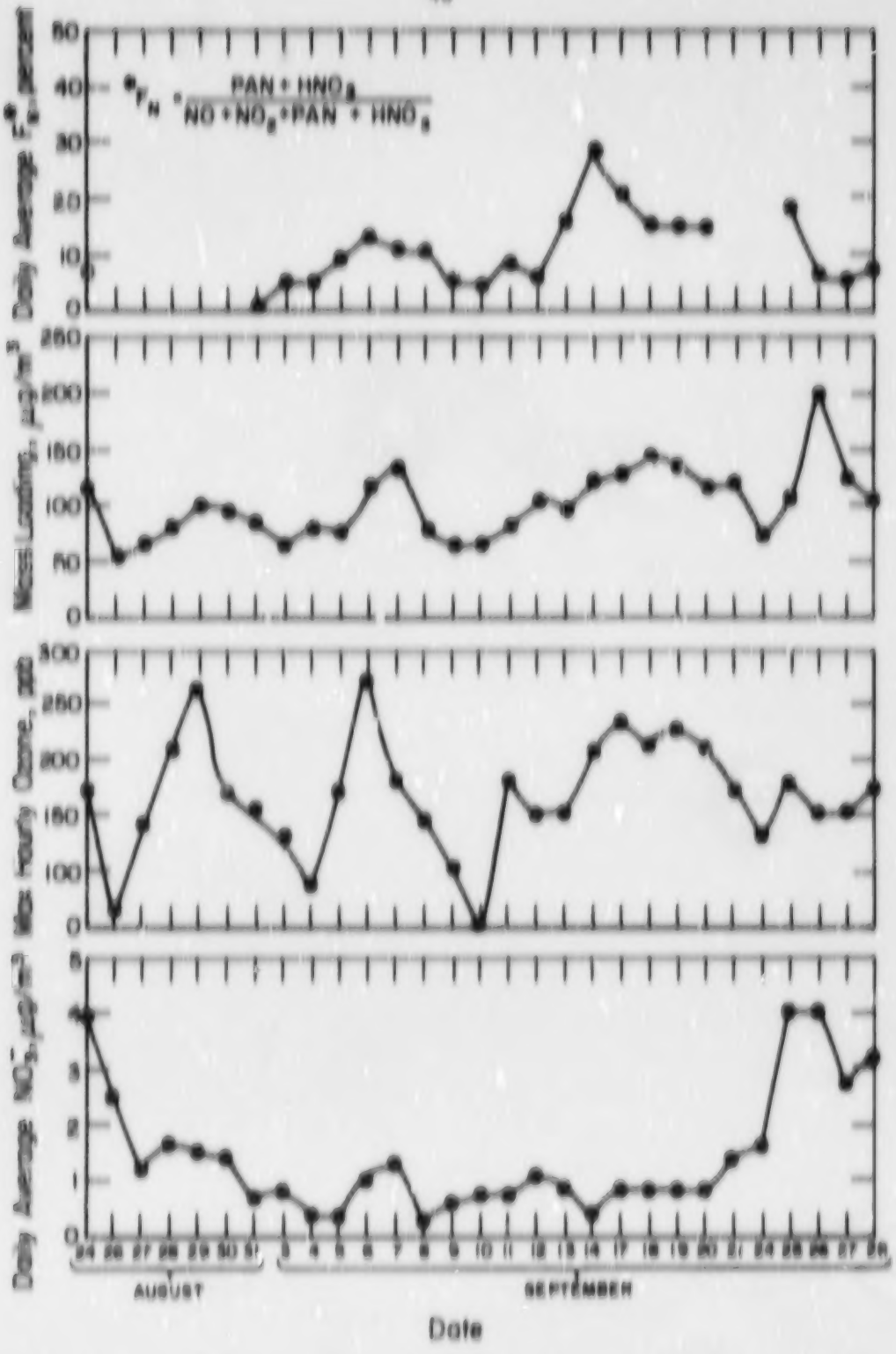

FIGURE 8. DAILY TRENDS IN MEASURED VARIABLES — WEST COVINA

that the ratio of NO_x reaction products to total oxidized nitrogen tracks them. The same relationships seem to hold in West Covina, although they are perhaps not as clear. The high levels of mass loading and particulate nitrate which were observed in West Covina on September 25 and 26 occurred during a period of Santa Ana winds (hot dry desert winds) and should probably be excluded from this comparison.

Further discussion of the ratio of NO_x reaction products to total oxidized nitrogen will be reserved for later in this section.

Determination of Appropriate CO/NO_x Emissions Ratio

As mentioned earlier, one of the critical parameters used to calculate NO_x-loss by Equation (1) is the emissions ratio for CO/NO_x. In our initial analysis of the West Covina data, as presented in the first year report[1], the total Los Angeles basin emissions inventory values for CO and NO_x were used for the emission ratio estimate. The sources of CO and NO_x are not entirely the same (98% of CO and 72% of NO_x are due to motor vehicles)[21] and the sources are not uniformly distributed throughout the basin, however, so the trajectory of an air mass will play a role in determining the ratio of CO and NO_x emitted into the air mass. We have assumed that the random error introduced into the NO_x-loss calculation by the use of basin-wide emissions estimates will be minimized when the data are averaged over long periods of time, since the differences in emissions ratios associated with different air mass trajectories will be minimized by the averaging process (i.e., the ratios are averaged over many different trajectories and should therefore tend toward the basin average ratio). Later in this report we will investigate the possibility of using trajectory-specific emissions ratios to calculate NO_x-loss over short time periods. In the remainder of this section we will use a single, average, emissions ratio in calculating NO_x-loss. The use of an average emissions ratio will introduce an error into the calculation when the emissions from any one source

show a strong diurnal variation (e.g., auto exhaust). However, this type of error, while not eliminated, is minimized by averaging over the entire day (i.e., over periods when the source contribution to the (CO/NO_x) emissions inventory ratio is high and also over periods when it is low). The choice of the appropriate emissions ratio is discussed below.

Emissions inventories for the Los Angeles area are available from a number of different sources. Several of these are summarized in Table 15.

TABLE 15. LOS ANGELES EMISSIONS INVENTORY SUMMARIES

Source of Data	Year	CO/NO_x Ratio For: Motor Vehicles	All Area Sources	All Sources
LAAPCD[21]	1971	19.8	19.4	14.2
LAAPCD[22]	1973	15.0	—	10.8
LAAPCD[23]	1974	14.9	—	10.5
SAI[24]	1971 (L.A. County)	23.9	—	14.9
SAI[24]	1971 (L.A. & Orange County)	23.9	—	15.3
EPA[25]	1972	18.0	16.8	8.7

The appropriate ratio to use for our site at West Covina should lie between the motor vehicle and "all sources" ratios, but selection of an exact value is difficult. The West Covina site was purposely far removed from major point sources of NO_x, as shown in Figure 9, so that any NO_y-rich emissions would be well diluted before they reached our site. Because of this the emissions ratio characteristic of air masses arriving at West Covina should approximate the vehicular more closely than the "all sources" ratio. As shown in Table 15, the vehicular ratio reported by LAAPCD in 1973 was about 15.

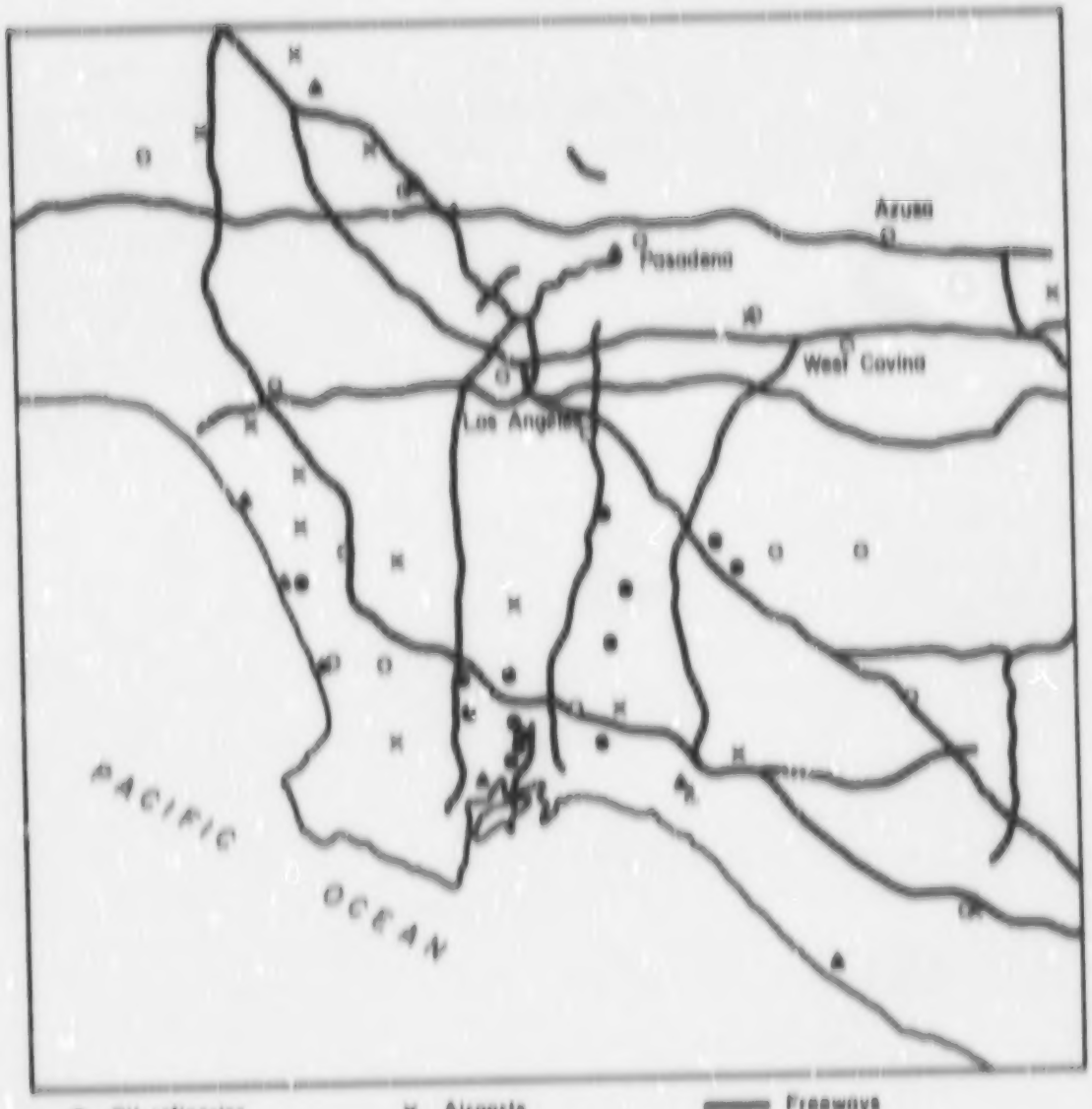

FIGURE 9. LOCATIONS OF PRIMARY SOURCES AND MONITORING STATIONS IN THE LOS ANGELES BASIN

We can use our measured CO and NO_x results to indicate the approximate value of the average CO/NO_x emissions ratio for air at West Covina. As shown in Equation (1), any removal of NO_x from the air will increase the measured ratio slightly, so that the measured ratio can only serve as an upper limit to the emissions ratio. Nevertheless, it can help to pinpoint the approximate value of the emissions ratio. A linear regression has been run on the CO and NO_x data, using gas chromatographic CO results and correcting the NO_x for chemiluminescence interferences (as discussed earlier). The correlation coefficient is quite high, at 0.85. Such a high degree of correlation indicates a similar source for CO and NO_x. The intercept of the regression line is 0.1 ppm CO, which is consistent with currently accepted values of geochemical background CO concentrations (0.1-0.2 ppm in the northern hemisphere)[26-28]. The CO/NO_x ratio as given by the slope of the regression line is 15.3. This is consistent with the 1973 vehicular emissions ratio and strengthens the case for selecting the vehicular ratio of 15.0 as most appropriate to the West Covina site.

In the remainder of this section, a CO/NO_x emissions ratio value of 15.0 will be used in NO_x-loss calculations. Other ratios will also be employed occasionally to help define the variation in calculated NO_x-loss due to the choice of emissions ratio.

Variation in NO_x-Loss by Day and Time of Day For Several Los Angeles Locations

We will shortly discuss CO/NO_x ratios and NO_x losses at our West Covina site in some detail. Before doing so, however, it is interesting to compare measured CO/NO_x ratios at several locations within the Los Angeles basin during the time period of the West Covina field study. The measured CO/NO_x ratios are related to NO_x-loss through Equation (1). However, the absolute value of the NO_x-loss calculated for sites other than West Covina is questionable due to the major inaccuracies introduced into the calculation by inaccurate CO data collected at these other sites by a non-dispersive infrared (NDIR) procedure. The problems with these CO data and their effect on NO_x-loss calculations were discussed in our earlier report[1].

Figure 10 shows a comparison of the trends in daily average CO/NO_x ratios in downtown Los Angeles*, Pasadena*, West Covina, Azusa*, and Pomona*. All but the West Covina plots are based on NDIR CO measurements. This figure is not meant to be related to NO_x-loss in a quantitative manner due to the CO measurement difficulties; rather, it is presented to show the trends for the various sites. The results have been normalized by dividing the CO/NO_x ratios from each site by the lowest daily average ratio at that site.

In general, correspondence in trends at the different sites is not strong. Several of the sites show an increase in the ratio on September 13 and 14, and again on September 24, but an examination of the chemical and meteorological data for these 3 days at West Covina shows no unusual variations. The daily variation in CO/NO_x and NO_x-loss at West Covina will be discussed in detail later in this section.

The CO and NO_x data used to construct Figure 10 can also be used to show the diurnal trends in NO_x-loss at several Los Angeles basin locations. Such profiles are shown in Figure 11. It must be recalled that NDIR CO data were used to compute the composite profiles in this figure so that the absolute magnitude of the NO_x-loss will not be accurate. The West Covina results will be discussed separately since they are based on accurate gas chromatographic CO determination.

Each of the NO_x-loss profiles in Figure 11 shows an increase in the early morning (6-8 a.m.) which we ascribe to the increased emissions ratio of CO/NO_x during the morning rush hours[1]. If this assumption is valid, then these apparent morning increases in the amount of NO_x removed from the air are artificial**. Three of the sites, Pasadena, Pomona, and Azusa, show peaks in the NO_x-loss profile at approximately 2 p.m. The downtown Los Angeles profile shows a period of extended high loss from 8 a.m. to about 1 p.m. While the first few hours of this interval are probably due to the rush-hour traffic emissions, we suggest that the plateau between 10-12 a.m. is due to true NO_x removal from the air. We believe that this late morning peak is propagated downwind and appears in Pasadena.

*Data obtained from the Los Angeles Air Pollution Control District.

**Periods of artifically high NO_x-loss should be largely compensated by periods of lower calculated NO_x-loss at other times of the day when the exhaust contribution to the (CO/NO_x) emissions ratio is low.

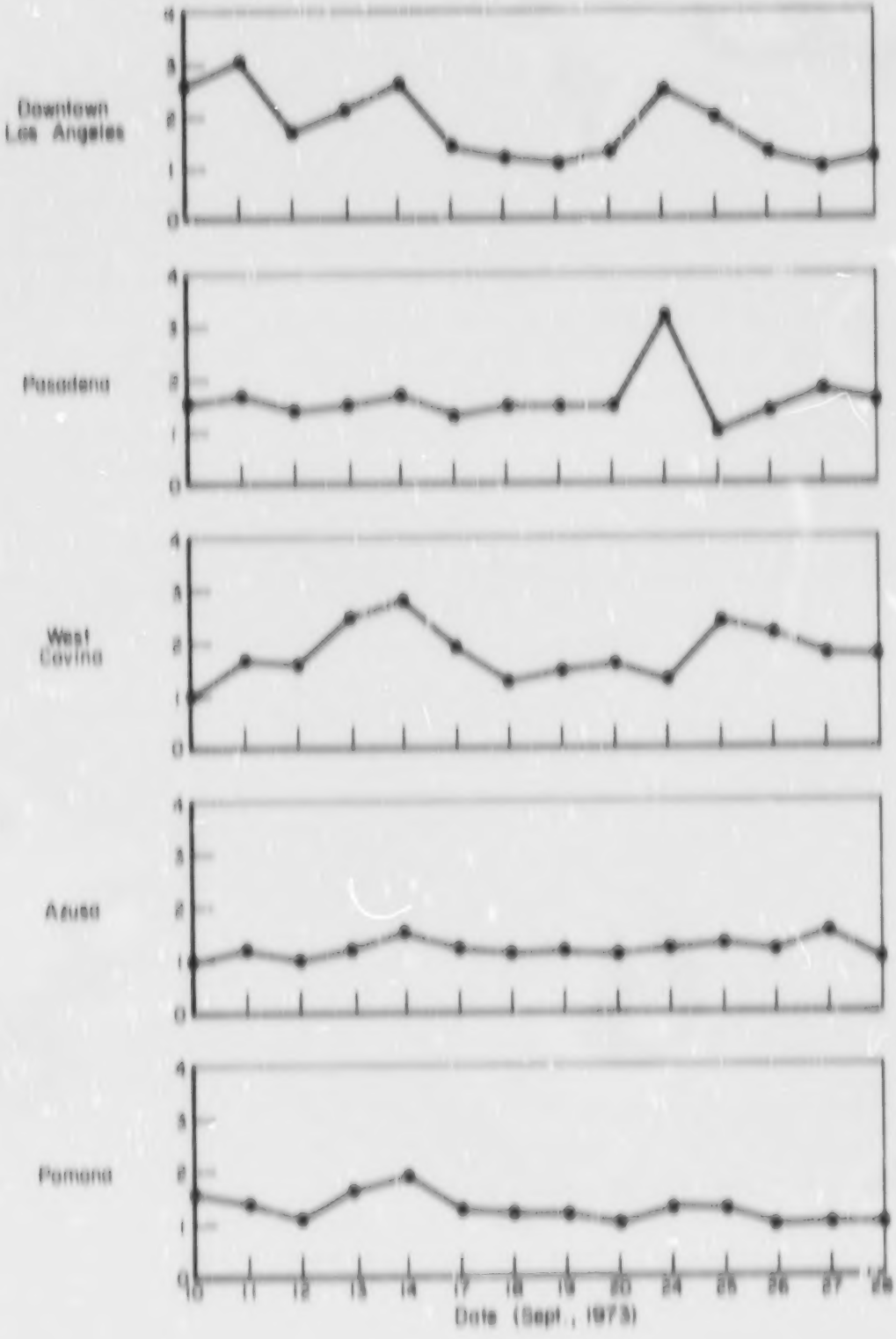

FIGURE 10. NORMALIZED CO/NO_x RATIOS FOR FIVE LOS ANGELES BASIN SITES

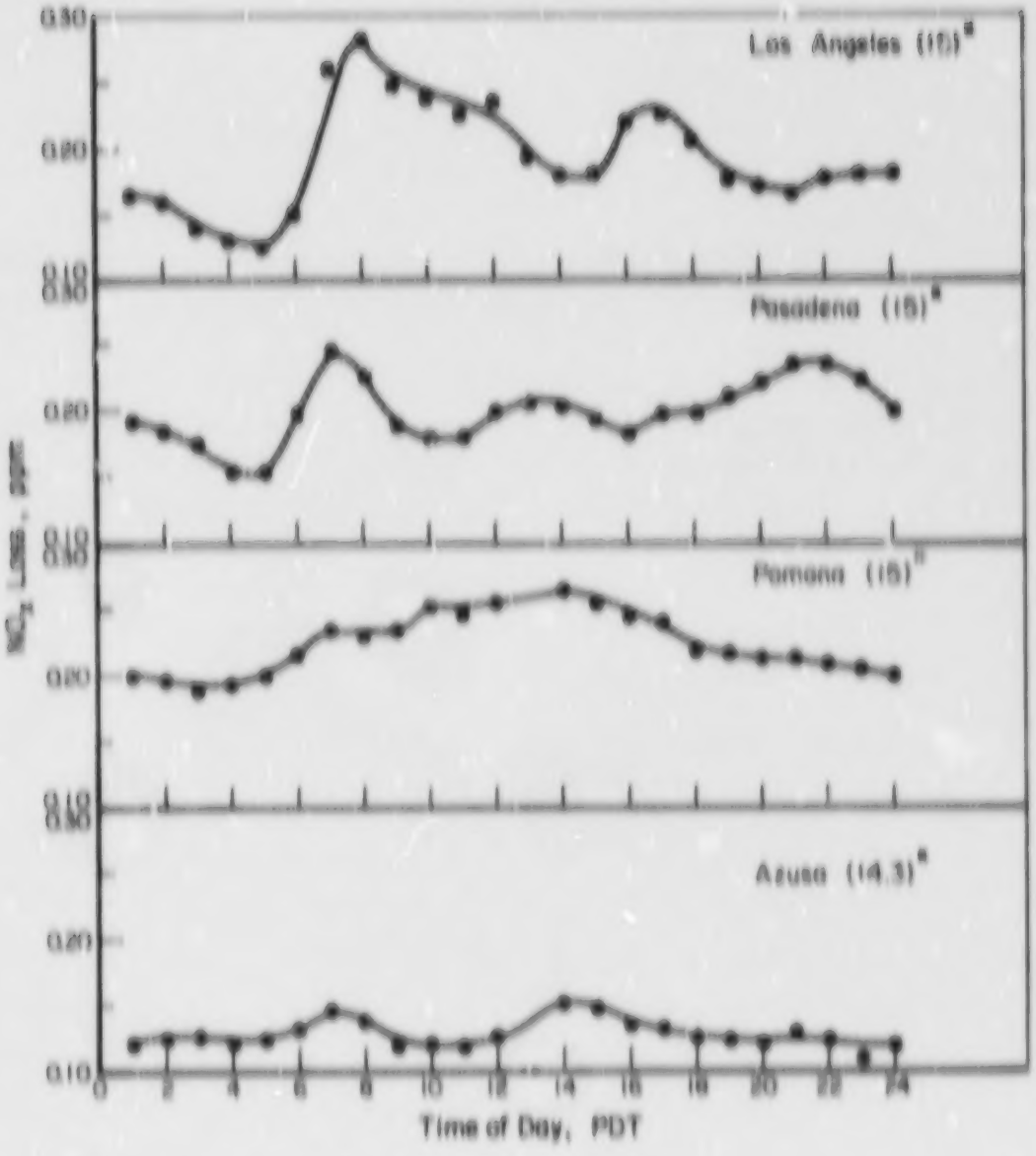

* Emissions Inventory Ratio Used in Calculations.

FIGURE 11. COMPARISON OF COMPOSITE NO_x LOSS AT FOUR SITES

Pomona, and Azusa slightly later in the day. Such behavior is analogous to the transport of ozone which has been observed in Los Angeles[29] and a number of other locations[30,31]. The NO_x-loss peak which occurs in the downtown area at about 5 p.m. may be due to increased vehicular emissions during this rush-hour period, and may therefore be an artifact of our procedure for calculating NO_x-loss.

If one accepts the assumption that the late morning and early afternoon peaks in NO_x-loss are due to actual NO_x removal from the air, then one can determine an average afternoon NO_x-loss for each site by determining the magnitude of the peak above the natural baseline of the curves. This rationale has been discussed in our earlier report[1]. Such a procedure yields the following estimates for the maximum hourly afternoon NO_x deficit (averaged over the entire study period since the curves are composites of all the study period data):

Location	NO_x Deficit
Downtown Los Angeles	0.060 ppm
Pasadena	0.025 ppm
Pomona	0.055 ppm
Azusa	0.035 ppm

The profile of the composite NO_x reaction product concentrations (PAN + HNO_3) for West Covina, which will be presented shortly, shows an afternoon peak of 0.033ppm. This reaction product sum is similar to the NO_x deficits reported above, especially when one considers the differences in location and the errors likely to be present in the NO_x-loss calculations. The similarity of these values suggests that the peak afternoon deficit in measured NO_x is largely due to the conversion of the NO_x to reaction products via the photochemically initiated smog reactions. This view is consistent with our observation that these same reaction products account for virtually all of the reacted NO_x in smog-chamber simulations of urban atmospheres[7]. In addition, these are about the same levels of NO_x deficit and reaction products predicted by photochemical models of urban atmospheres[32]. More will be said about the comparison with photochemical models in the discussion of West Covina results.

Nitrogen Oxides Loss and Nitrogen Balance at West Covina

One of the major difficulties in interpreting the results of the West Covina field study for the first-year report was the lack of sensitive and accurate CO data. Since that first-year report was published, we have obtained[a] hourly gas chromatographic CO data which were collected simultaneously with our data during much of our study (9/10/73-9/28/73) at the same site in West Covina. These data have been transferred to magnetic tape and integrated with the West Covina data files.

Composite profiles of CO, NO_x, and adjusted NO_x (corrected for chemiluminescent interferences) are pictured in Figure 12. These data were collected at the West Covina site between September 10-28, 1973. The morning traffic peaks and nighttime buildup beneath the inversion are shown by these profiles. During the afternoon when atmospheric mixing is usually good, the concentrations of both CO and NO_x are low.

Using the new CO values and our adjusted NO_x results, we can now determine the overall NO_x deficit during the West Covina study via Equation (1):

$$NO_x\text{-loss} = \frac{(CO)_{measured}}{(CO/NO_x)_{emission\ inventory}} - (NO_x)_{measured} \qquad (1)$$

The background concentration of CO is not included in emissions inventory estimates and should be substrated from the measured CO for the most accurate calculation of NO_x-loss. As mentioned earlier, the background CO concentration in the northern hemisphere is reported to average 0.1-0.2 ppm, so we have subtracted 0.15 ppm CO from all the measured CO values. Equation (1) was then used to calculate NO_x-loss for each hour of the field study. Two emissions inventory estimates of the CO/NO_x ratio were used, in order to gain a feeling for the sensitivity of the results to this quantity. Values of 15.0 and 14.3 were used for the ratio. Several indicators suggest the 15.0 ratio is the most appropriate, as discussed earlier. In any case, we believe that these two ratios probably bracket the actual average emissions ratio over the period of the field study.

---

[a]We thank General Motors Corporation for making these data available to us.

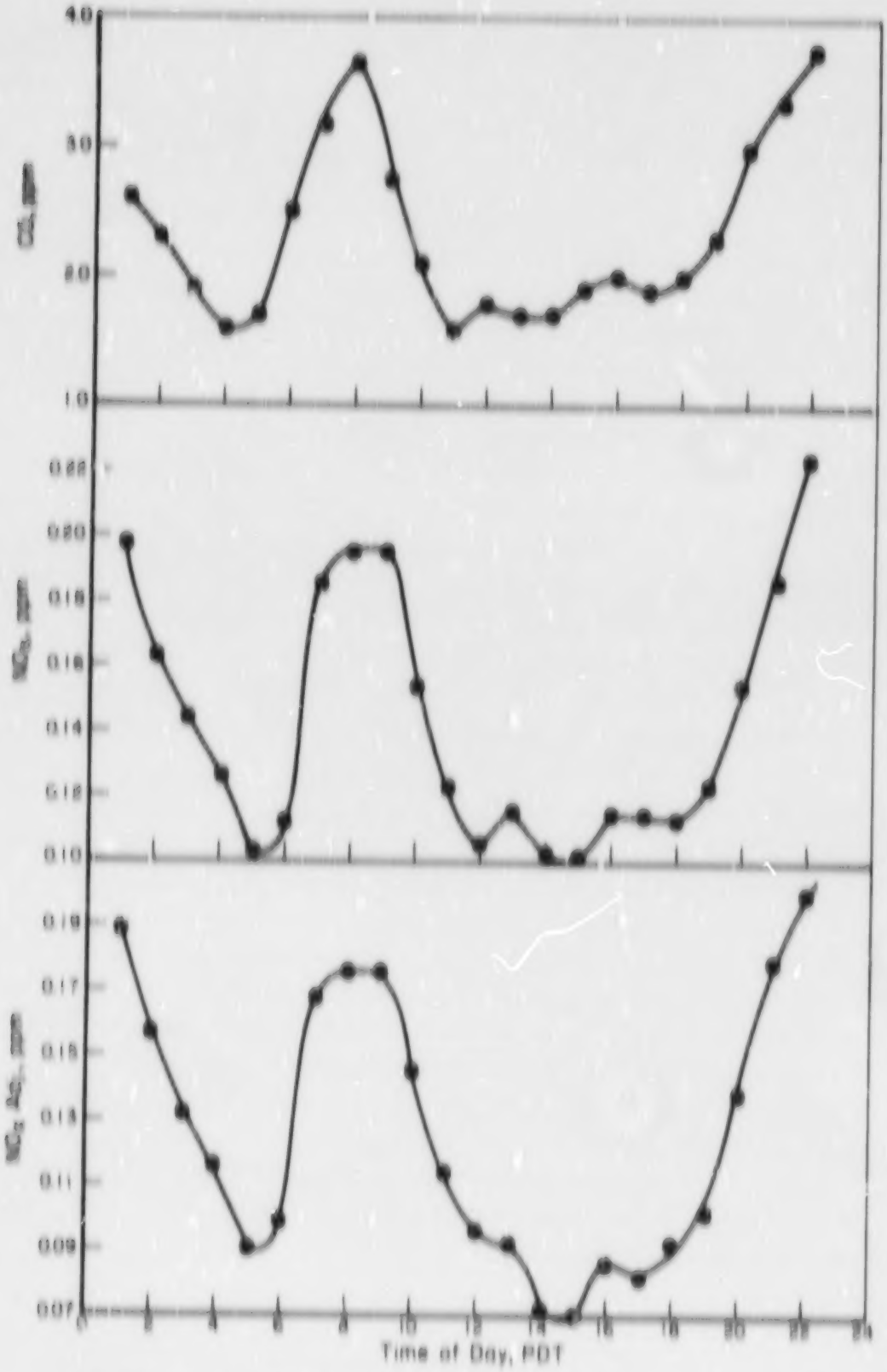

FIGURE 12. COMPOSITE PROFILES FOR WEST COVINA

Averaging the hourly NO_x-loss results for the entire study period yields the following:

NO_y-loss = 0.018 ppm (using 15.0 emissions ratio)

NO_x-loss = 0.025 ppm (using 14.3 emissions ratio).

Assuming that the ratio of 15.0 is correct, a nitrogen balance for the West Covina study period can be attempted. During this study period, the concentrations of the measured NO_x reaction products were

$$[PAN] = 0.012 \text{ ppm}$$
$$[HNO_3] = 0.003 \text{ ppm}$$
$$[NO_3^-] = \underline{0.001 \text{ ppm}}$$
$$0.016 \text{ ppm}.$$

Thus, 0.016 ppm out of the missing 0.018 ppm can be accounted for by the measured gaseous and particulate NO_x reaction products. On the average, PAN and nitric acid account for 67% and 17% of the NO_x deficit, respectively. These percentages are similar to those observed in smog-chamber experiments[7]. For example, in synthetic auto exhaust-NO_x irradiation, PAN was found to account for 67% and nitric acid 32% of the reacted nitrogen. If the 14.3 ratio is used to calculate NO_x-loss, then 0.016 ppm of a 0.025 ppm deficit are accountable as measured products. Gaseous deposition, to be discussed later, can probably account for part of the remaining deficit.

These findings, which suggest that PAN and nitric acid are the major initial products of NO_x reactions and can account for the vast majority of reacted NO_x are consistent with our smog chamber[7] and kinetic model[32] simulations of urban atmospheres, and are a most important result of this research program.

Earlier we reported that the overall ratio of measured NO_x reaction products to total gaseous nitrogen was

$$\frac{PAN + HNO_3}{NO + NO_2 + PAN + HNO_3} = 0.11.$$

If PAN and HNO_3 are indeed the major NO_x reaction products, then the ratio of NO_x-loss to the predicted concentration of NO_x should be similar to this $\frac{\text{product}}{\text{total oxidized nitrogen}}$ ratio. From Equation (1), the predicted concentration of NO_x is

$$NO_x\text{-Predicted} = \frac{(CO)_{measured}}{(CO/NO_x)_{emissions\ inventory}} = 0.151 \text{ ppm.}$$

Hence,

$$\frac{NO_x\text{-loss}}{NO_x\text{-Predicted}} = 0.12$$

which is indeed quite close to the 0.11 value found for the $\frac{product}{total\ nitrogen}$ ratio.

The individual hourly NO_x-loss values can be used not only to derive an overall average NO_x deficit, as just shown, but also to indicate the diurnal trends in removal of NO_x from the air. Averaging the NO_x-loss for each hour of the day over all the days of the study, yields the composite NO_x-loss profile shown in Figure 13. Because each hourly point in the figure is averaged over only a limited number of days (and therefore a limited number of air mass trajectories), some scatter in the data must be expected.

One feature of the plot which is striking is the natural baseline formed by the hourly points, which now fluctuates close to zero NO_x-loss. When compared with the 0.1 ppm baseline found in our first-year analysis or the 0.1-0.2 ppm baseline shown for other Los Angeles sites in Figure 11, it is clear that the gas chromatographic CO data have greatly improved the accuracy of our results. A discussion of the effect of errors in the CO concentration on this baseline was presented in our earlier report and will not be repeated here.

Included in Figure 13 is a plot of the sum of the composite PAN and HNO_3 concentrations for the same days as the NO_x-loss curve. The concentration of the NO_x products peaks at about 0.035 ppm between 14:00-16:00 hours. It is difficult to compare the two curves due to the scatter in the NO_x-loss data and the apparently steadily rising baseline of this curve after 11:00. However, with the exception of the early morning (6-9 a.m.) peaks, it appears that the increases in NO_x-loss occur at about the same time as the increases in NO_x reaction products.

In Figure 14 we compare the trend in daily average CO/NO_x ratio, which is related to NO_x-loss through Equation (i), to the measured daily trends in the concentrations of several measured species. The trends in

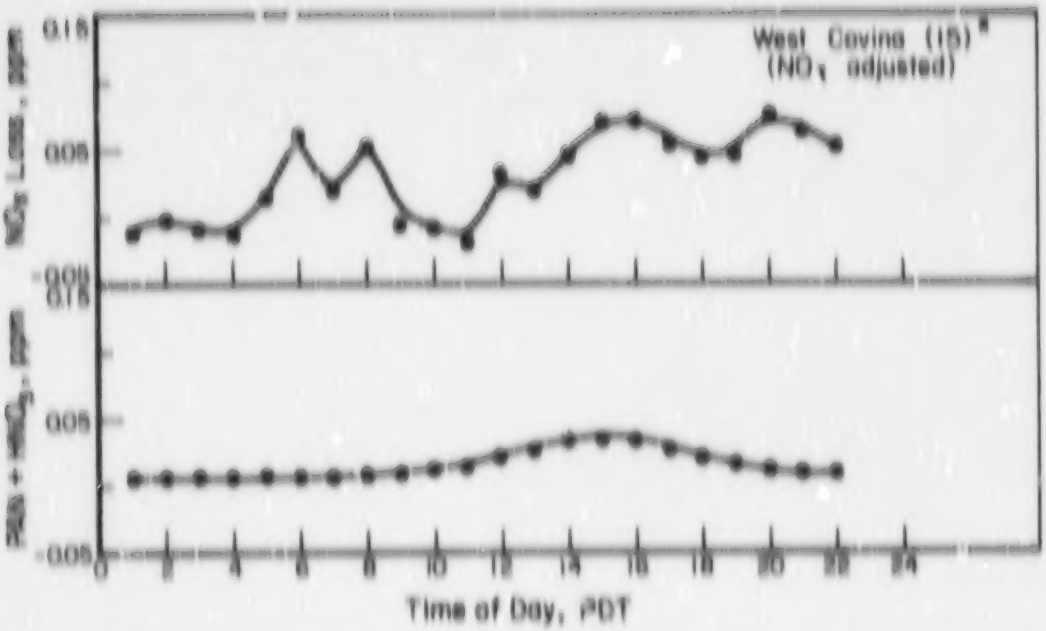

* Emissions Inventory Values Used in Calculation.

FIGURE 13. COMPOSITED NO_x LOSS AND PAN + HNO_3 PROFILES FOR WEST COVINA

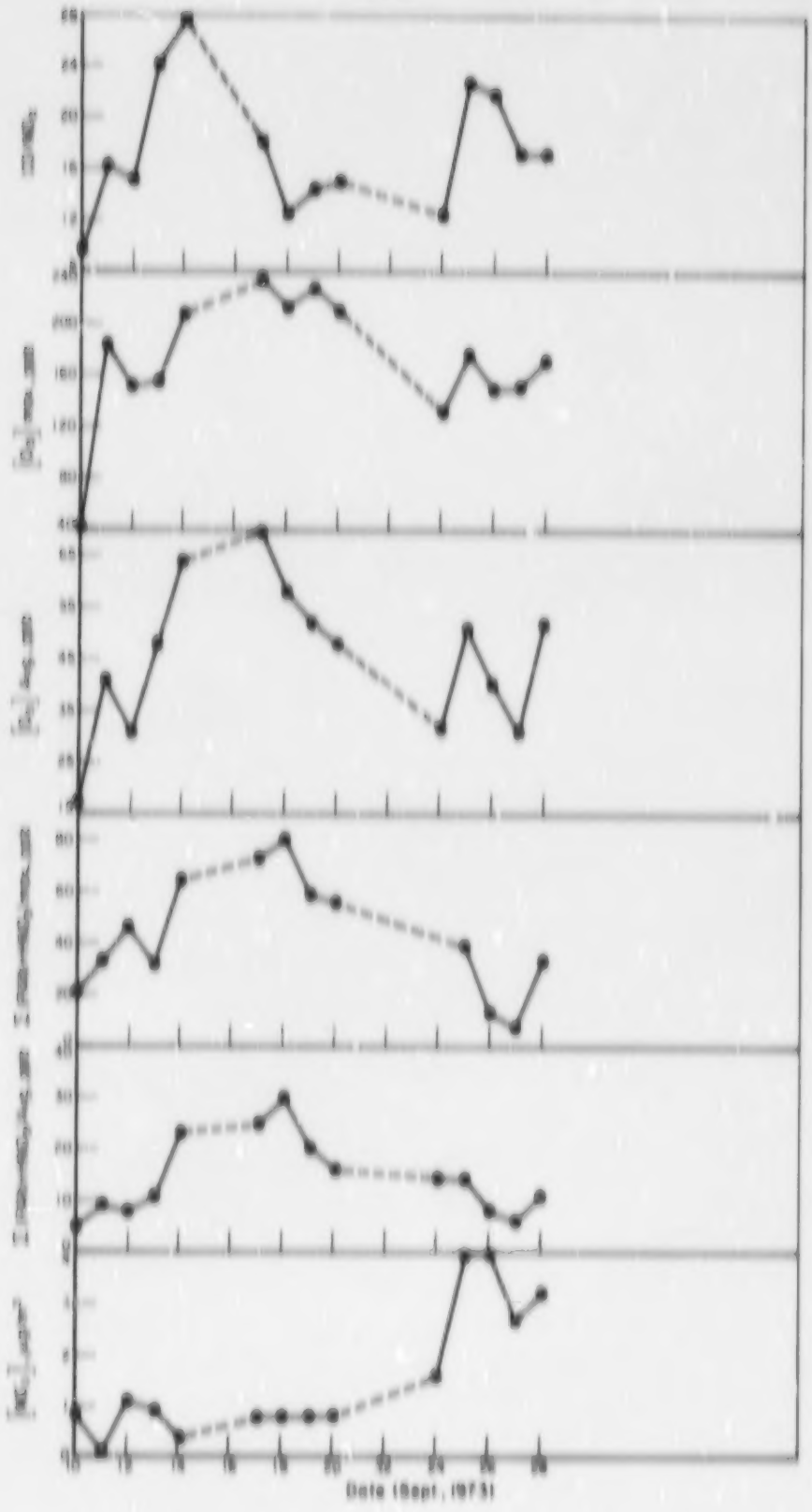

FIGURE 14. TRENDS IN MEASURED VARIABLES AT WEST COVINA

in the daily CO/NO_x averages are frequently similar to those displayed by the daily average ozone and the maximum and average sums of PAN and HNO_3. The particulate nitrate values show no strong pattern with the exception of a sharp increase on September 25 and 26 which corresponds with increases in CO/NO_x and O_3. Although this increase in particulate nitrate occurred during a period of changing meteorology (Santana winds), the cause of the high nitrate is unclear at this time.

The general agreement in the daily trends of CO/NO_x, O_3, and the sum of PAN and nitric acid are consistent with a photochemical mechanism of conversion of nitrogen oxides to PAN and nitric acid reaction products. Results of kinetic simulations of urban smog formation predict such trends and will be discussed briefly.

Computer Simulations

The atmospheric chemistry group at Battelle has recently added the capability to computer-simulate photochemical smog reactions via kinetic models. The computer programs for solving the coupled differential equations were obtained from Jefferies[33] and are similar to those employed by Hecht, et al.[34]. We have expanded the program to accommodate a greater number of reactions and species, and have added the capability to display and plot the model results and interact with the model in real time via a cathode ray tube output device. The wealth of smog-chamber and ambient monitoring data on file at Battelle-Columbus is allowing us to generate and validate kinetic mechanisms for use in the model; at the same time, the validated mechanisms are greatly enhancing our ability to understand and interpret our smog-chamber and field-study results.

Using a 38-step mechanism (hydrocarbons lumped as nonmethane hydrocarbons-NMHC) and literature values for the rate constants, we have attempted to simulate typical Los Angeles reaction conditions for comparison with our West Covina field study results. No attempt has been made to "fit" the data by adjusting rate constants. The initial conditions of the simulations are given in Table 16.

TABLE 16. STARTING CONDITIONS FOR THE COMPUTER SIMULATION OF LOS ANGELES SMOG FORMATION

Specie	Concentration, ppm
NO_2	0.050
NO	0.100
H_2O	20,000
CO	2.00
NMHC	0.50
SO_2	0.60

The pollutant profiles from this simulation are shown in Figure 15 A and B. Figure 15A shows NMHC decreasing gradually during the 10-hour irradiation, with aldehyde increasing to nearly 0.3 ppm. This aldehyde value is almost identical to the average daily maximum aldehyde concentration in Los Angeles reported by LAAPCD in Leighton[35]. The relatively unreactive carbon monoxide remains at essentially 2.0 ppm throughout the experiment. The concentrations of a number of additional trace species are plotted in Figure 15B. The NO and NO_2 profiles are typical of urban smog formation and are quite similar, both in concentration and temporal variation, to the NO and NO_2 profiles we observed in West Covina[1]. The ozone concentration reaches a maximum value of nearly 0.16 ppm about 8 hours into the irradiation. This is exactly the same maximum hourly O_3 (composited over the entire study period) that we observed 8 hours after the NO peak (7 a.m.) in West Covina. The SO_2 concentration decreases slowly as particulate sulfate is formed. The particulate sulfate levels (not shown) predicted by the model are somewhat greater than those observed during our study, but the initial concentration of SO_2 used in the simulation is probably too high for Los Angeles. The concentration of hydrogen peroxide has reached about 0.090 ppm and is still climbing after 10 hours of irradiation

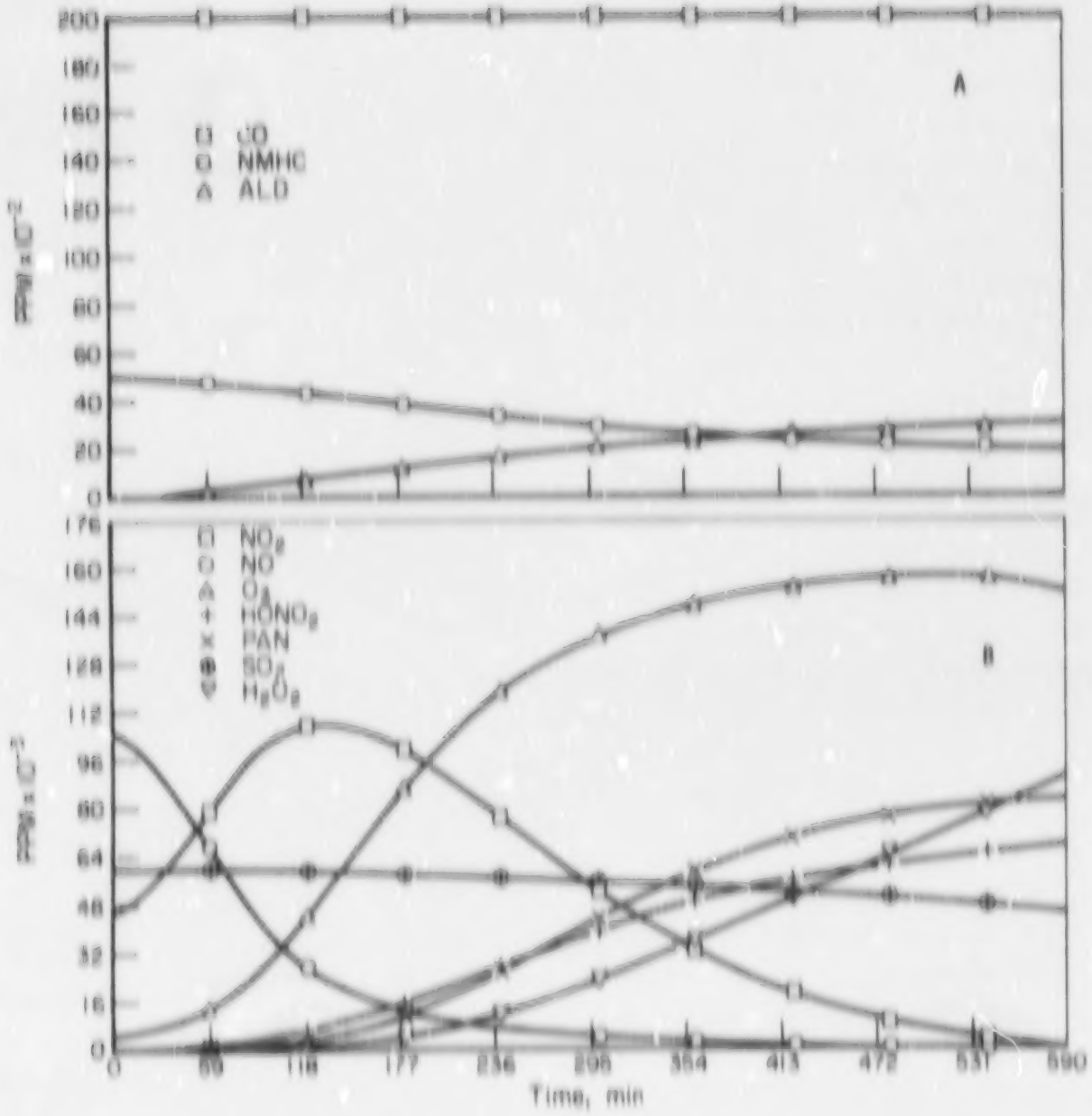

FIGURE 15. URBAN SIMULATION

(in the real atmosphere H_2O_2 production would cease at sundown). Bufalini, Gay, and Brubaker[36] have observed H_2O_2 concentrations in Riverside, California, under severe smog conditions (oxidant = 0.65 ppm) of 0.18 ppm. Under more moderate conditions (oxidant = 0.3 ppm) the H_2O_2 concentration was 0.06 ppm.

The PAN and nitric acid profiles track the O_3 profile, as we observed in West Covina, with maximum levels of about 0.080 ppm PAN and 0.065 ppm nitric acid. These concentrations are somewhat greater than those maximum hourly averages we actually observed in West Covina (0.046 ppm PAN, 0.040 ppm HNO_3). However, the fact that full sunlight intensity was assumed for the simulation would tend to increase the predicted concentrations of these species, and no scavenging steps were included in the model to lower their concentrations. The ratio of maximum PAN to maximum nitric acid is about 1.2, again very similar to the ratio we observed on many days in West Covina.

Other species which are of interest but are not shown in the figure are nitrous acid, N_2O_5, and alkyl nitrates. The maximum concentration of HONO is predicted to occur 4 hours into the experiment at about 0.012 ppm. The nitrous acid formed at this time is due largely to the NO_2 + HO_2 reaction, with some contribution from the HO + NO reaction. The maximum predicted concentration of N_2O_5 occurs at about the same time at 9×10^{-5} ppm. Alkyl nitrate reaches its peak concentration at the same time as PAN with levels of 2×10^{-5} ppm predicted by the model.

The agreement between the model and our West Covina data for the concentrations and temporal variations of the trace constituents of photochemical smog lend credence to the model. Future work will involve additional validation of the model, inclusion of scavenging reactions for NO_x reaction products (e.g., particulate NO_3^- formation), and studies of the dependence of the NO_x reaction products on initial conditions (e.g., levels of NMHC, NO, NO_2, H_2O, NO/NO_2, NMHC NO_x, etc.). We look to computer modeling as a tool for future investigations of the fate of nitrogen oxides under the changing atmospheric conditions likely to be brought about by future emission control strategies.

Physical Scavenging of the Nitrogen Oxides

Thus far in our treatment of the West Covina field data we have dealt primarily with chemical removal processes for the nitrogen oxides. However, the physical removal of NO_x from the air also deserves discussion. The most important physical removal processes for atmospheric pollutants are rain-out, wash-out, and dry deposition. Since we encountered no precipitation during our West Covina field study, the wash-out process can be ignored. The rain-out mechanism (i.e., the adsorption of trace gases on cloud elements) must be considered, since we experienced many foggy mornings during the first half of our West Covina field program. Rodhe and Grandell[37] have shown however, that the most important factor in determing the efficiency of the rain-out mechanism is the frequency of rains. They have further demonstrated that even in the case of very effective transfer of a pollutant into cloud drops, the average residence time of a pollutant in the atmosphere would be about 4 days in summer if rain-out were the only sink mechanism. Since no rain occurred during our study, this residence time would be expected to be considerably longer during our West Covina operations. Furthermore, it is unlikely that nitric oxide would be affected by the rain-out process. Thus the expected residence time for total NO_x would be even longer. Since we are concerned primarily with removal processes over time scales of a few hours, we should be able to effectively ignore the rain-out mechanism.

Bolin, et al.[38], have discussed the dry deposition process in terms of emission height, turbulence, surface roughness, and other factors. Using their model and the deposition velocity for NO_x derived from Tingley's data (V_d (NO_x) = 0.5 cm/sec), we determine that the residence time of NO_x in the atmosphere, assuming only rain-out and dry deposition as sink mechanisms, it is on the order of 50-60 hours. This residence time includes some rain-out, which we have already shown was unlikely during our West Covina study due to the lack of rain. Since most of the NO_x that we monitored at the West Covina site was probably emitted within the preceding 4-6 hours, deposition is not likely to have affected our nitrogen balance to any great extent.

In summary, physical removal mechanisms are unlikely to be important in our consideration of nitrogen oxides losses during the West Covina operation. One further point; even if dry deposition appeared to be an important short-term NO_x removal mechanism, this proces. would only affect the NO_x-loss calculations to the extent that the deposition velocities of NO_x and the tracer differed.

Trajectory and Emissions Analysis

In the treatment of the data thus far, the total Los Angeles basin emissions inventory values for CO and NO_x have been employed to calculate NO_x-loss. Such a calculation assumes that the initial ratio of CO/NO_x is the same throughout the entire basin, regardless of air mass trajectory. The sources of CO and NO_x are not uniformly distributed throughout the basin, however, so that the trajectory of the air mass will have an impact on the ratio of CO and NO_x emitted into the air mass. Thus far our calculations have assumed that the use of the basin emissions inventory ratio is warranted when many days of data are averaged, since the differences in emissions ratios associated with different air mass trajectories will be minimized by the averaging process (i.e., the ratios are averaged over a number of different trajectories). We would expect that for some short time interval such as an hour, the use of the basin-wide emissions ratio to calculate NO_x-loss could result in high or low (even negative) losses depending on whether the trajectory passed over power plants (CO/NO_x lower than the basin average) or highways (CO/NO_x greater than the basin average).

In order to assess the impact of air mass trajectory on the calculation of NO_x-loss, and also to gain some knowledge of the age of emissions in West Covina air masses, we have performed a detailed trajectory and emissions analysis of air masses reaching our West Covina site on 3 days in September, 1973. Estimates of CO and NO_x emissions into air masses reaching

our West Covina site will be back-calculated based on the air mass trajectory. The ratio of these inputs will then be used along with our measured CO and NO_x data to calculate NO_x loss over short time intervals.

Air mass trajectories were derived manually from the meteorological data at the West Covina site and similar data collected at Pomona, downtown Los Angeles, Azusa, and Pasadena. The input of CO and NO_x along the air mass path is computed from spatial estimates of CO and NO_x source strengths in the Los Angeles basin. A 2-mile by 2-mile grid concept, which has been used by other investigators[24], was employed in order to spatially characterize emissions in the Los Angeles basin. Carbon monoxide emissions were derived for each grid square using freeway and nonfreeway traffic count data and CO emissions factors[24]. The assumption that all the CO has a vehicular origin should not affect the accuracy of the calculation, since LAAPCD estimates[21] that more than 98% of the Los Angeles CO burden is from motor vehicles. Nitrogen oxides emissions were computed for each grid square by summing NO_x emissions within each square due to vehicle traffic (using freeway and nonfreeway traffic data and vehicular emissions factors), power plant emissions, refinery emissions, emissions from petroleum marketing, ships, railroads, incinerators, domestic sources and minerals, metals, and other industries. The data used in preparing the "all sources" emissions grids were taken from the report by Roberts, et al.[24]. The final CO and NO_x emissions grids are shown in Figure 16.

The trajectories of air masses arriving at our West Covina site were plotted for the 6 hours prior to their arrival and these trajectories superimposed on the emissions grids for CO and NO_x. This process was carried out for each hour between 13:00-19:00 on September 11, 13, and 18, 1973. An example of the results of these plots is shown in Figure 17. The grid squares used in computing the CO and NO_x emissions to the air mass for each trajectory are outlined in the figure. Selection of squares to be used in computing emissions was not based on any firm set of rules. We believe that the errors associated with the trajectory derivation greatly outweigh errors in the choice of emissions squares; so long as the CO and NO_x emissions from the same squares are used in computing the CO/NO_x ratio, errors resulting from the choice of squares should be negligible in most

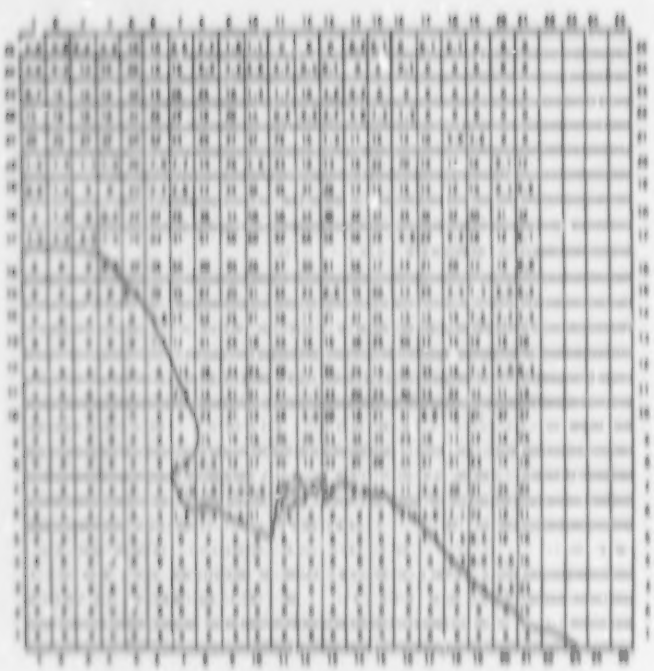

CO Emissions Grid (10^6 g/day)

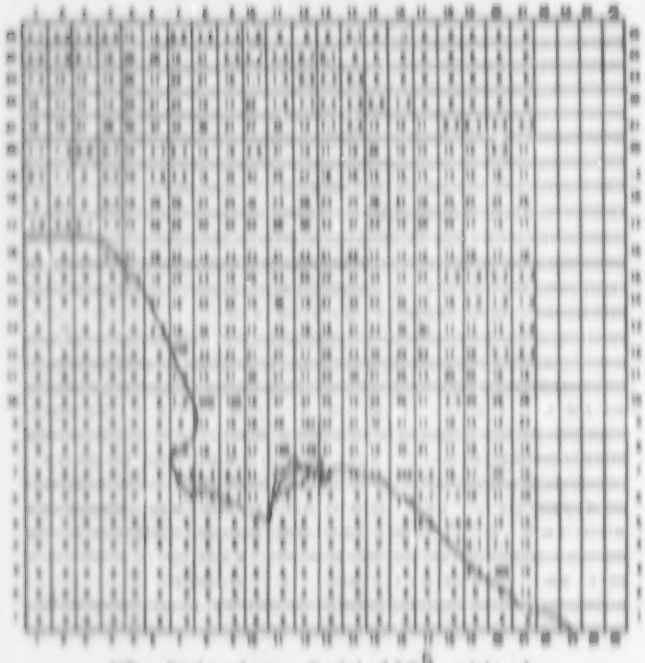

NO_x Emissions Grid (10^5 g/day)

FIGURE 16. CO AND NO_x EMISSIONS GRIDS

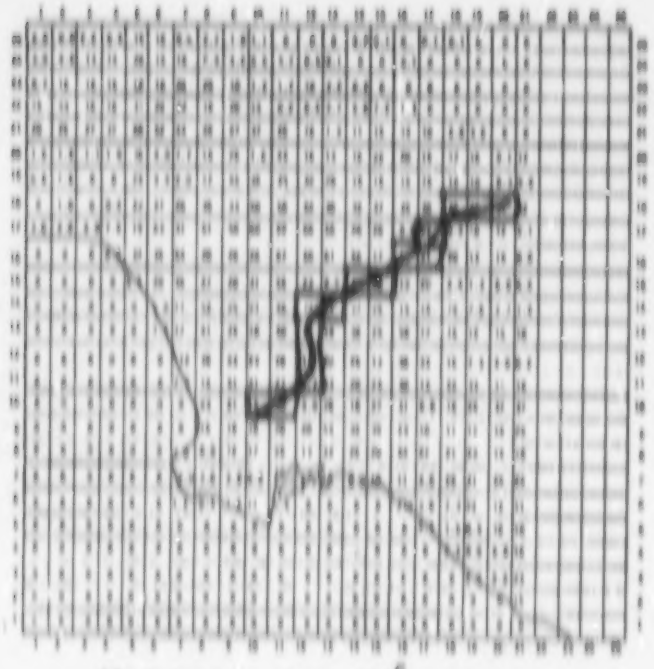

CO Emissions Grid (10^6 g/day)

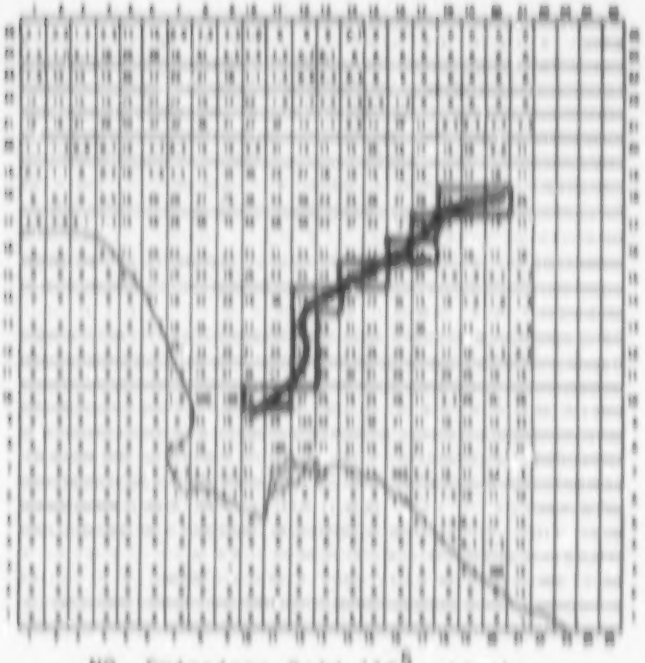

NO_x Emissions Grid (10^5 g/day)

FIGURE 17. TRAJECTORY OF AIR MASS ARRIVING AT WEST COVINA AT 14:00 ON SEPTEMBER 11, 1973

cases. No effort has been made to consider the time that the air mass resides in each emissions square. It has been assumed that each square contributes its full complement of emissions to the air mass. Again, since the ratio of emissions will be used, this assumption should not lead to major errors.

The emissions from each grid square along the air mass trajectory can now be summed and an hourly CO/NO_x emissions ratio for the West Covina site calculated. However, a simple summing of the emissions implies that the impact of nearby emissions on the CO/NO_x ratio is the same as that of emissions released early in the air mass history. This is of course not true since the earlier emissions are diluted along the trajectory. We must account for this dilution in order to better approximate the true pollutant ratio of the air arriving at West Covina. A rigorous approach to this problem is beyond the scope of this task; we will merely apply weighting factors to the emissions from different points along the trajectory in order to approximately compensate for dilution.

Under typical atmospheric conditions, each doubling distance downwind of a source results in a doubling of the half-width of the source plume's cross-section. Using Sutton's diffusion equation and assuming interaction with the ground to be negligible, the concentration of a pollutant at any point downwind of an emission source is inversely proportional to the downwind distance to the 2-n power where n is a turbulance index equal to about .2 under normal conditions. While this is a very crude approximation of the actual situation, it should allow us to weight our emissions factors to roughly account for dilution. We can now break the trajectories up into three segments of approximately equal length and apply weighted factors to the sum of the emissions from each segment; the factors being derived from the relationship just described. In the following discussion, weighting factors of 0.14, 0.33, and 0.54 are used for the emissions in the farthest, middle, and closest segments of the trajectory relative to our West Covina site.

A comparison between the weighted and unweighted emissions ratios for each trajectory is made in Table 17. It is clear from this tabulation that the weighting procedure only rarely has an important effect on the calculated CO/NO_x emissions ratio.

TABLE 17. CALCULATED EMISSIONS RATIOS

Date	Hour	CO/NO_x Calculated (Unweighted)	CO/NO_x Calculated (Weighted)	CO/NO_x Measured
9/11/73	13	16.4	16.1	19.2
	14	17.9	19.0	23.6
	15	16.0	17.8	18.2
	16	17.6	17.9	—
	17	17.6	17.6	—
	18	17.4	17.2	20.2
	19	7.8	12.3	16.8
9/13/73	13	17.5	18.3	16.4
	14	17.2	17.3	22.5
	15	16.8	16.5	37.8
	16	17.0	17.4	28.1
	17	7.5	10.2	25.4
	18	6.9	11.2	22.2
	19	13.1	15.0	24.7
9/18/73	13	18.8	18.4	9.4
	14	18.4	18.5	9.2
	15	16.2	16.4	—
	16	17.2	16.8	—
	17	7.2	10.7	8.4
	18	15.2	17.1	12.2
	19	15.3	17.2	15.4

We can now compare the two different procedures for calculating NO_x-loss based on (1) use of a constant "basin-wide" emissions ratio of 14.3 and (2) use of the weighted hourly emissions ratios derived from the individual air mass trajectories (from Table 17). The results of these two methods of computing NO_x-loss are shown in Table 18, along with the corresponding measured sum of the reaction products PAN and HNO_3. The NO_x-loss in both columns of the table was calculated using the hourly NO_x values adjusted for chemiluminescence interference ($NO + NO_2$ - PAN - HNO_3) and assuming the nonanthropogenic CO concentration is 0.15 ppm. The loss in the first column was calculated using the constant "basin-wide" CO/NO_x ratio of 14.3. The loss in the second column was derived using the weighted hourly CO/NO_x emission ratio estimates from Table 16.

The use of the trajectory-derived emissions estimates yields NO_x losses which show no consistent trend when compared to losses in column 1. Both positive and negative deviations result from a comparison of the two calculation methods. Even within any single day, the deviations change from positive to negative almost randomly. Comparison of the calculated losses from the first two columns of the table with the sum of PAN and nitric acid shows that neither method of calculating NO_x-loss agrees very well with the sum of these NO_x reaction products, and again, the differences can be either positive or negative. Perhaps the most disconcerting feature of these data is the fact that the gross trends in NO_x-loss and the sum of PAN and HNO_3 are not in agreement. For example, both calculational procedures suggest September 13 was a day of high NO_x-loss and September 16 a day of low loss. However, the levels of NO_x reaction products indicate just the opposite trend.

These comparisons suggest that the uncertainties involved in attempting to calculate NO_x removal from an air mass over such short times as 1 hour are too great; that the inaccuracies and unknowns overwhelm the determination of NO_x-loss, which is very sensitive to a number of inputs.

TABLE 18. COMPARISON OF CALCULATED NO_x-LOSS WITH THE SUM OF PAN AND NITRIC ACID

Date	Hour	NO_x-Loss[a] (ppb)	NO_x-Loss[b] (ppb)	PAN + HNO_3 (ppb)
9/11/73	13	—	—	27
	14	89	46	33
	15	83	27	32
	16	—	—	30
	17	—	—	13
	18	40	21	8
	19	13	30	6
9/13/73	13	14	-12	10
	14	48	27	19
	15	112	92	24
	16	110	77	30
	17	105	180	19
	18	58	95	11
	19	59	54	4
9/18/73	13	-21	-50	72
	14	—	—	79
	15	—	—	74
	16	—	—	63
	17	-51	- 5	57
	18	20	- 2	41
	19	40	18	34

(a) Calculated using a constant emissions ratio of 14.3.

(b) Calculated using the weighted hourly emission ratios from Table 16.

Investigation of NO_x Removal in New York City

In order to extend the results of our study to areas other than St. Louis and West Covina, we have investigated the trends in NO_x removal in New York City. The New York data were obtained by Battelle-Columbus as part of the CRC-APRAC CAPA-6 study[40], "Haze Formation: Its Nature and Origin". The data were collected by the Battelle-Columbus mobile laboratory situated on Roosevelt Island (formerly Welfare Island) during August 10-30, 1972. Nitrogen oxides were determined by chemiluminescence and CO by gas chromatography (after conversion to CH_4). One of the primary reasons these data were selected for study is because of the accurate and interference-free CO measurements. Additional details on the New York study and experimental methods are available elsewhere[40] and will not be presented here.

To gain an overall feeling for the extent of NO_x-loss in New York during this study period, we ran a regression of hourly average CO versus hourly average NO_x. The correlation between CO and NO_x was reasonably high, with a correlation coefficient of 0.78. The CO intercept of 0.1 ppm is consistent with background CO concentrations. The slope of the regression line was 15.1 ± 0.6. To compare the CO/NO_x ratio represented by this slope to the emissions ratio of CO to NO_x, we contacted a number of city, state, and federal agencies requesting emissions data for New York City in 1972. The emissions inventory summaries (1973) from the New York City Department of Air Resources yielded a motor vehicle CO/NO_x emissions ratio of 25.6 and an "all sources" ratio of 6.7. The average emissions ratio pertinent to the Roosevelt Island site is likely to be weighted toward the vehicular ratio due to proximity to the heavily trafficked midtown Manhattan area. The CO/NO_x ratios for the New York City AQCR for 1972 are reported[25] to be 12.2 for all sources and 14.9 for area sources. These values lie between the "all sources" and vehicular ratios reported for the city itself, and are very similar to the emissions ratios we used for St. Louis and Los Angeles in our previous data interpretation. Use of these ratios to compute an overall average NO_x-loss using Equation (1) yields:

NO_x-loss = 0.001 ± 0.003 ppm (based on area source ratio)
NO_x-loss = 0.016 ± 0.003 ppm (based on "all sources" ratio).

Thus the average loss is between 1 and 16 ppb, depending on the actual ratio of CO and NO_x emitted into the air masses sampled at the Roosevelt Island site.

The slope of the CO vs NO_x regression line can be used as an estimate of the average measured CO/NO_x, corrected for background CO, over the entire sampling period. The CO/NO_x emissions inventory ratio is also an average value; the emissions ratio very likely varies seasonally (due to space heating in winter and increased power demands in summer), daily (due to lesser vehicular components on weekends), hourly (due to traffic and electricity generating patterns) and with wind direction. Comparison of the average measured ratio (slope of regression line) with the average emissions ratio yields an estimate of average NO_x-loss over the study period.

Loss of NO_x can also be calculated on an hourly basis using the hourly average CO and NO_x values. In doing so, however, we face the problem of using specific short term CO and NO_x concentrations with a long term average emissions inventory ratio. During any given hour the actual ratio of CO to NO_x emitted into the air mass could be greater or less than the overall average ratio (i.e., 14.9 for area sources). Thus, both positive and negative hourly losses of NO_x might be observed, but the overall average should be valid. The overall average of the hourly NO_x-loss values is 0.008 ppm when the area sources emissions ratio is employed in the calculation. This loss value will be somewhat high due to the background CO which appears in the measured ratio but not in the emissions inventory ratio. Assuming a background CO concentration of 0.15 ppm, the overall average NO_x-loss becomes 0.002 ppm.

The hourly average NO_x-loss results have been composited and plotted in Figure 18 to show the average diurnal pattern of NO_x removal. The area source emissions inventory ratio of CO to NO_x was used in calculating the composited hourly NO_x losses. Negative losses have been plotted as zeros. The negative losses, which appear between 1-7 a.m., must be

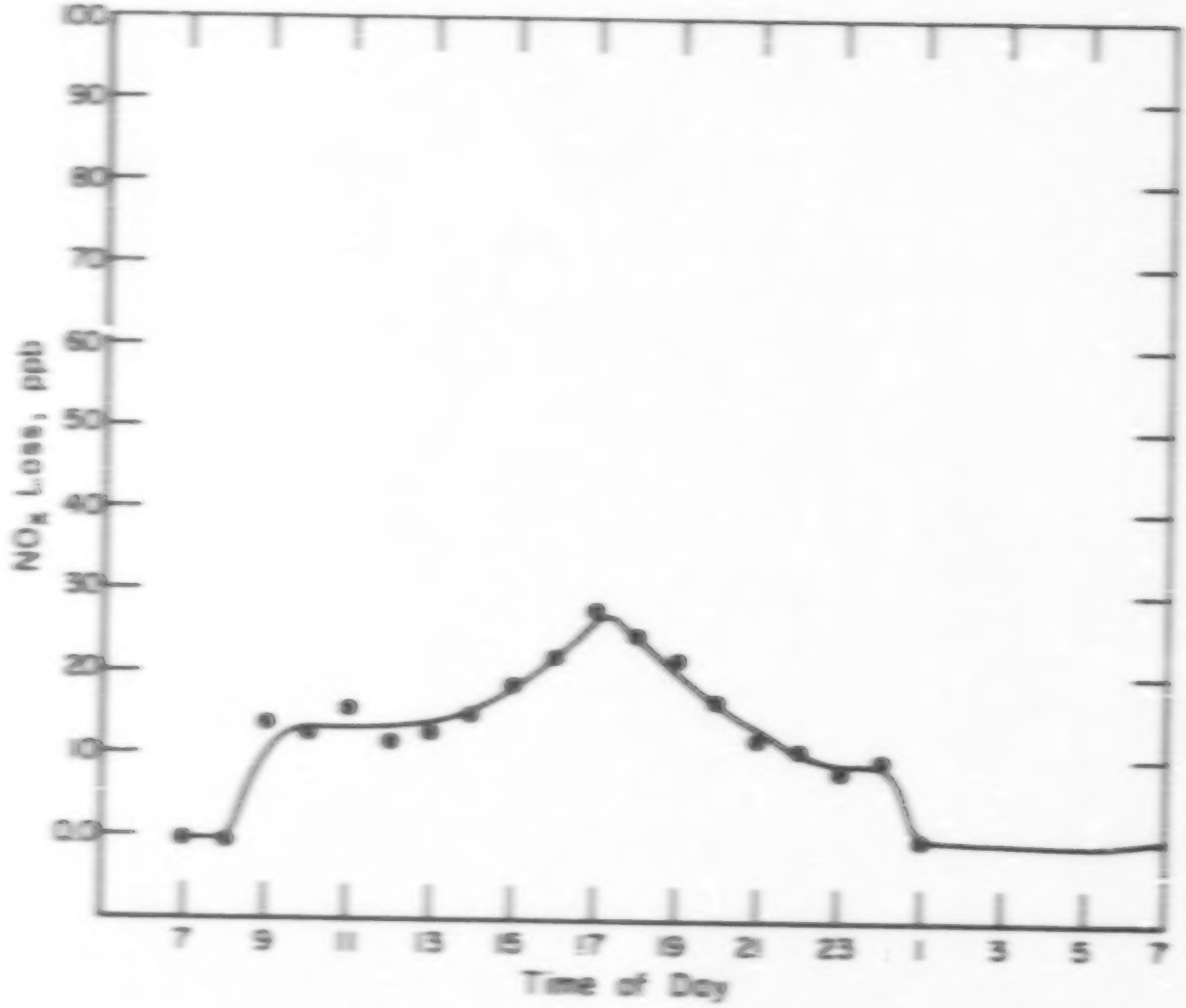

FIGURE 18. NEW YORK CITY COMPOSITE NO_x LOSS

caused by a lower emissions ratio of CO/NO_x due to the increased importance of stationary sources (NO_x rich) versus mobile sources (CO rich) late at night. Between 9 a.m. and midnight, the curve shown in Figure 18 exhibits a natural baseline at 10-12 ppb NO_x-loss. Nonanthropogenic CO present in the background air contributes 6 ppb to this apparent loss. The remaining 4-6 ppb loss may be an artifact of our choice of emissions ratio or it may represent an actual constant loss of NO_x in New York due to deposition and/or other processes.

The loss profile shows that during the middle to late afternoon, there is an additional loss of NO_x superimposed on the natural baseline. This additional loss, which reaches nearly 15 ppb above the baseline at 5 p.m., is very likely related to photochemical processes converting nitrogen oxides to reaction products. The midafternoon NO_x-loss is only about half of that observed in West Covina; interestingly the average midafternoon ozone levels observed in New York were only one-half the levels in West Covina. This is consistent with our observation in West Covina of very high correlation ($R = 0.7$-0.8) between O_3 and the major NO_x reaction products PAN and HNO_3, and provides circumstantial evidence that the processes removing NO_x from the air are similar in New York and West Covina.

Trends in daily average NO_x-loss are compared with the daily trends of a number of other variables in New York in Figure 19. Shown in the figure are the average NO_x-loss, maximum hourly ozone, average NO_2, and average particulate nitrate for each study day. The NO_x-loss was calculated using the area source emissions ratio. Negative values of NO_x-loss are plotted as such in order to emphasize the trends in the data. The trends in NO_x-loss track the trends in maximum ozone reasonably well. This is expected if chemical losses (PAN, HNO_3, NO_3^-) are occurring. The average NO_2 concentration is remarkably constant throughout most of the study making it difficult to discern any relationships between NO_2 and NO_x-loss.

Unfortunately there are not enough particulate nitrate data to definitely determine whether the trends correspond. However, between August 22 and 26 the particulate nitrate level rises rapidly, as does the NO_x-loss curve. Ozone also reached its highest values over this same time period. It is likely that these increases are all interrelated by the

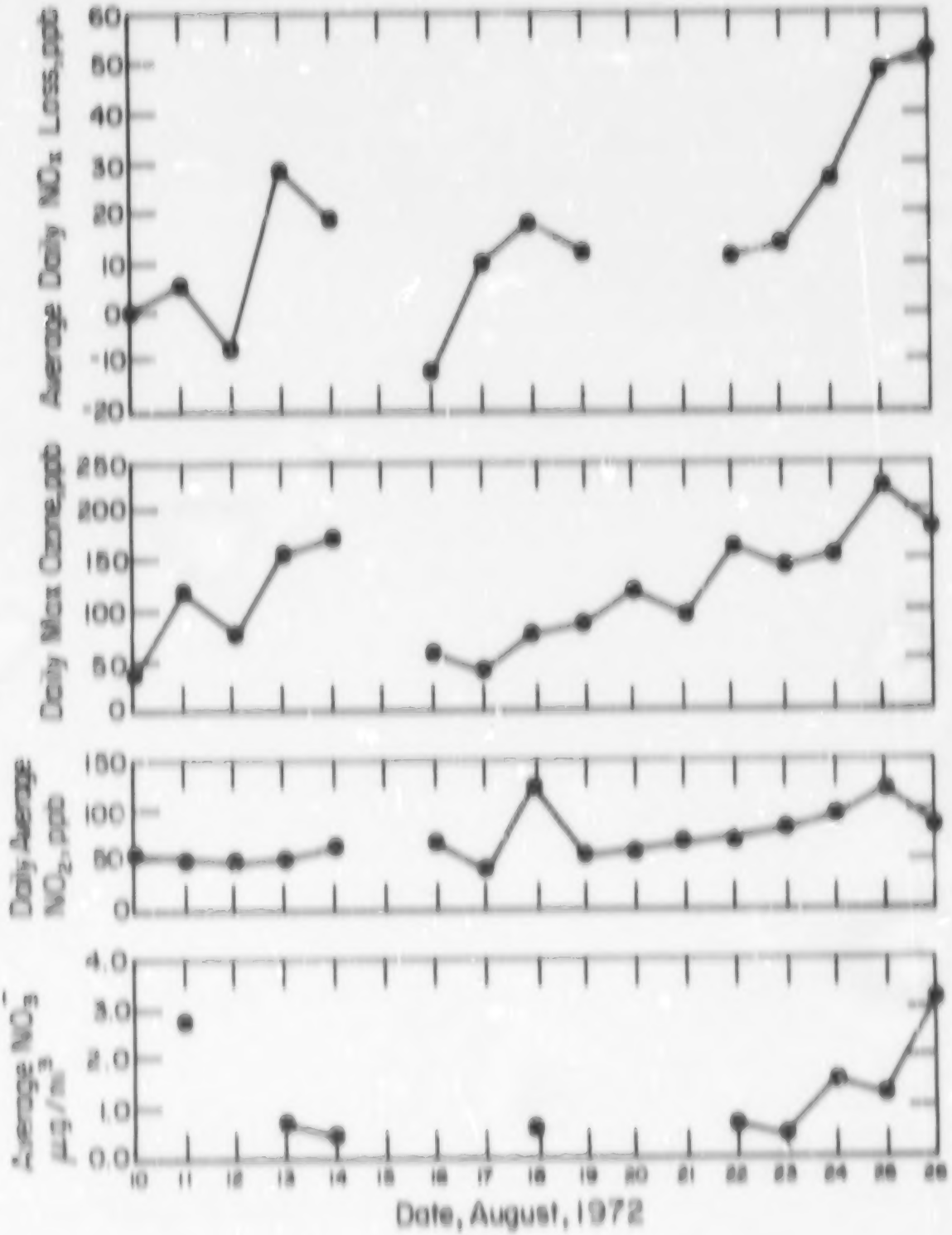

FIGURE 19. TRENDS IN NEW YORK MEASUREMENTS

chemical reactions occurring in the formation and decay of photochemical smog.

Analysis of Selected LARPP Operations for NO_x-Loss

The LARPP (Los Angeles Reactive Pollutant Program) was a jointly sponsored study by CRC and EPA whose objective was to obtain a complete data package which could be used for modeling the transport, diffusion, and chemical reactions occurring in urban photochemical smog. LARPP was conceived in 1971 by the sponsoring organizations. The study was of the Lagrangian type, in which the reacting pollutants were monitored within moving air parcels as they traversed the Los Angeles basin.

The LARPP field study was conducted between early September and mid-November, 1973. Our West Covina study was planned to overlap entirely with LARPP, however LARPP was delayed so that only the latter half of our program overlapped the early portion of LARPP. All of our West Covina data have been integrated into the LARPP data bank. Full-scale LARPP operations were conducted on 35 days. Operations were started early in the day from any one of five sites. The downtown Los Angeles and Downey sites were used most frequently.

In a typical operation, three tetroons were launched simultaneously from a single location. These tetroons were ballasted to fly below the inversion base and were tracked by radar. Once the centroid of the tetroon pattern was established a fluorescent particle tracer was released by helicopter around the centroid. At the conclusion of the tracer release the first of two Bell 212 helicopters began a series of 7-minute constant altitude rectangular flight patterns around the centroid starting near the inversion base. Four flight levels were employed, the lowest being 200 feet above ground. Normally the aircraft would descend, ascend, and descend a second time through each level before returning to base. The second helicopter began at the top level when the first craft completed its final flight pattern at the lowest level. An instrumented van on the ground was directed along the centroid path and collected data enroute and at fixed locations along the path.

Our objective in analyzing data from selected LARPP operations is to attempt to determine the NO_x deficit and more importantly the rate of NO_x removal from the moving air parcels. The NO_x-loss from the LARPP operations can then be compared to the NO_x reaction product concentrations measured at West Covina. The comparison would be especially meaningful on days when our study and LARPP were operating simultaneously and the trajectory of the air parcel approached West Covina. However, even on days after our study was concluded but while LARPP was still running, the calculation of the rate of NO_x removal from the air mass can be compared to our measured rate of reaction product accumulation on days when the meteorology and reaction conditions were similar.

The LARPP data should be well suited for the determination of NO_x deficit, since data on the concentrations of NO_x and the relatively inert species CO, C_2H_2, CH_4, and fluorescent particles are available. As in the past, we will use the inert species as tracers to account for dilution and other physical processes occurring within the air parcel. The tracer/NO_x ratio of an air parcel can be calculated throughout a given operation, and the NO_x deficit calculated by relating changes in the ratio during air parcel transport to the starting ratio. This eliminates the use of emissions inventory estimates in calculating NO_x-loss, and should result in improved accuracy.

The data obtained for investigation of selected LARPP operations were in the form of computer printouts of pattern averages; that is, the concentrations of the various species (CO, NO, NO_2, and O_3 being the most important for our purposes) were averaged over each rectangular helicopter pattern flown at a constant altitude around the centroid of the tetroons. The hydrocarbon data were provided separately and consist of tables listing the analyses of bag samples collected during the constant altitude rectangular helicopter patterns. Following receipt of these data, the hydrocarbon results from the bag collections were matched with the continuous data from the appropriate helicopter pattern and stored on magnetic tape.

Initially we planned to investigate LARPP operations 1,3,22,25, and 27. However, for a variety of reasons only 25 and 27 were suitable for our purposes, and even operation 27 is lacking CO data. Therefore data from five additional operations (5,8,10,16, and 33) were obtained. The air parcel trajectories for these operations are shown in Figure 20.

In order to study the possibility of loss of NO_x in the moving air parcels of the various LARPP operations, a number of graphical displays were generated. The graphs generated were visually examined for empirical evidence of NO_x-loss. For this purpose the ratios CO/NO_x, C_2H_2/NO_x, and CH_4/NO_x are of interest and the behavior of these ratios by time and altitude will be discussed.

The two operations with the greatest amount of data are 25 and 33. These two will be discussed first and in the most detail.

Operation 25

Operation 25 was conducted on October 26, 1973, from 10:00 a.m. to 6:25 p.m. The tetroons were launched from a site near downtown Los Angeles. The air parcel followed a curving trajectory to the southeast, east, and then northeast, as shown in Figure 20. At the conclusion of the experiment the air parcel was just southwest of West Covina. The ozone concentrations in the Los Angeles basin on this day approached 0.20 ppm.

The concentrations of a number of species monitored during the helicopter flights are plotted in Figure 21. The figure shows the variation in the concentrations of the various species within the air parcel at a constant altitude of 246 meters. The higher altitude data were used to partially uncouple the concentrations from strong ground-level emissions. The figure shows the buildup of O_3 within the air parcel to about 0.24 ppm. The CO and NO_x concentrations decrease during the first 2 - 2-1/2 hours and then remain fairly constant.

The CO/NO_x ratio can be used as an indicator of NO_x removal from the air mass, if certain assumptions are valid. The main assumption we must make is that the air parcel accumulates a large burden of pollutants during the early morning and that during its subsequent transport through

FIGURE 20. TRAJECTORIES TRACKED DURING LARPP OPERATIONS

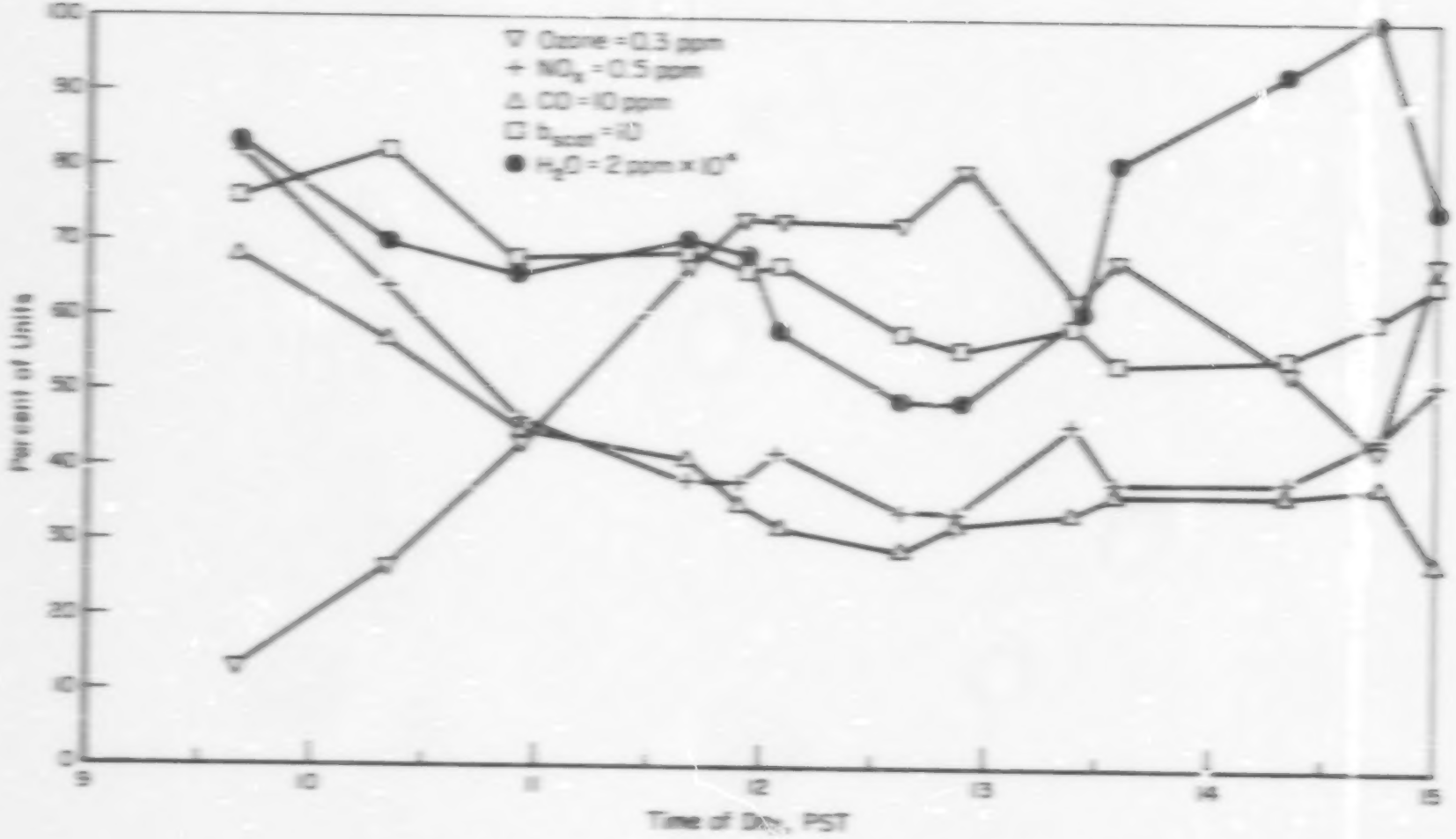

FIGURE 21. CONSTANT ALTITUDE PLOT FOR LARPP OPERATION 25 (~246 Meters)

the basin, the injection of fresh emissions only has a minor impact on the pollutant concentrations. Under these conditions we are effectively following the reactions occurring in a moving, leaky smog chamber. The dilution caused by leakage is accounted for by using an inert tracer such as CO or C_2H_2.

A plot of the profile average CO/NO_x ratio with time for Operation 25 is shown in Figure 22. The profile average incorporates the data from all altitudes. Loss of NO_x relative to the inert CO should manifest itself as an increase in the CO/NO_x ratio with time*. It is clear from Figure 22 that after 11:00 there is a steady declining in the ratio. A decrease in the ratio could be caused by a loss of CO relative to NO_x, which is very unlikely, or injection of fresh, NO_x-rich emissions into the air parcel. We expect the air parcel to be diluted from the sides by air with similar pollutant concentrations. However, if high concentrations of fresh emissions are injected into the air parcel from ground-level sources they will obviously have an impact on the pollutant concentrations within the parcel. If the fresh emissions have a tracer/NO_x ratio significantly different from the initial air parcel ratio, the calculation of NO_x removal using tracer/NO_x ratios becomes intractable. This appears to be the case for Operation 25.

To determine whether the CO/NO_x ratio behaves similarly at all altitudes, a plot of the ratio by altitude was constructed and is shown in Figure 23. The identification of the helicopter (Smog 2, Smog 3) used at different times during the operation is also shown. Visual examination of the figure suggests that the CO/NO_x ratio is either constant or declining after 11:00 at all altitudes.

Since the CO/NO_x ratio does not appear to be amenable to determination of NO_x removal, we have calculated and plotted the C_2H_2/NO_x ratio for Operation 25 in Figure 24. This ratio follows the same pattern as CO/NO_x. A least squares line for these points is shown in the figure. It is clear that, except for the brief period between 10:00-11:00, there is no evidence of loss of NO_x relative to either CO or acetylene.

*Note that if the chemiluminescence instrument employed during the LARPP program responds to PAN and HNO_3, and if PAN and HNO_3 are the major NO_x reaction products as our smog chamber and West Covina results indicate, then the tracer/NO_x ratios should remain constant in a reacting air parcel.

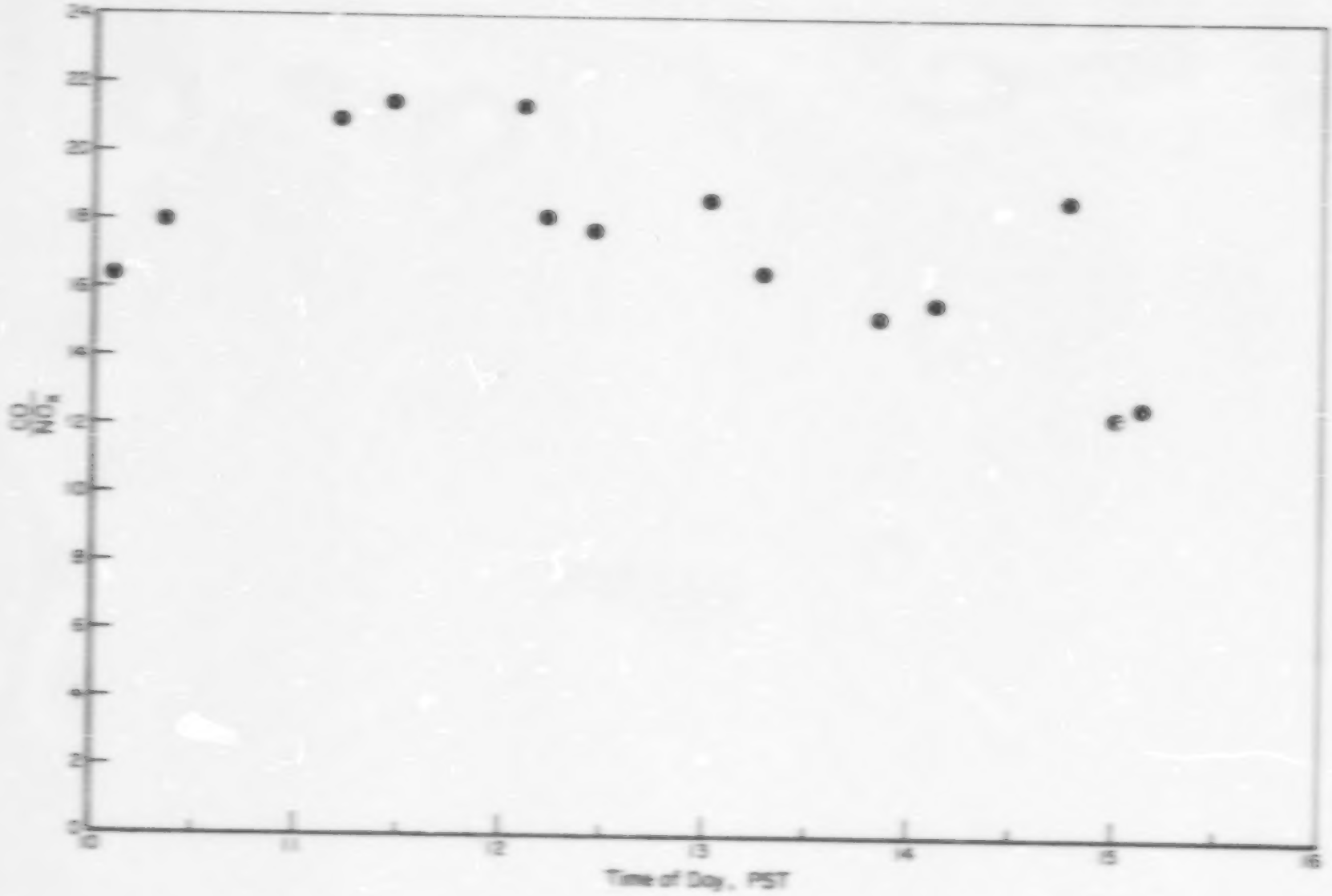

FIGURE 22. PLOT OF CO/NO_x (PROFILE AVERAGE) FOR LABPP OPERATION 25

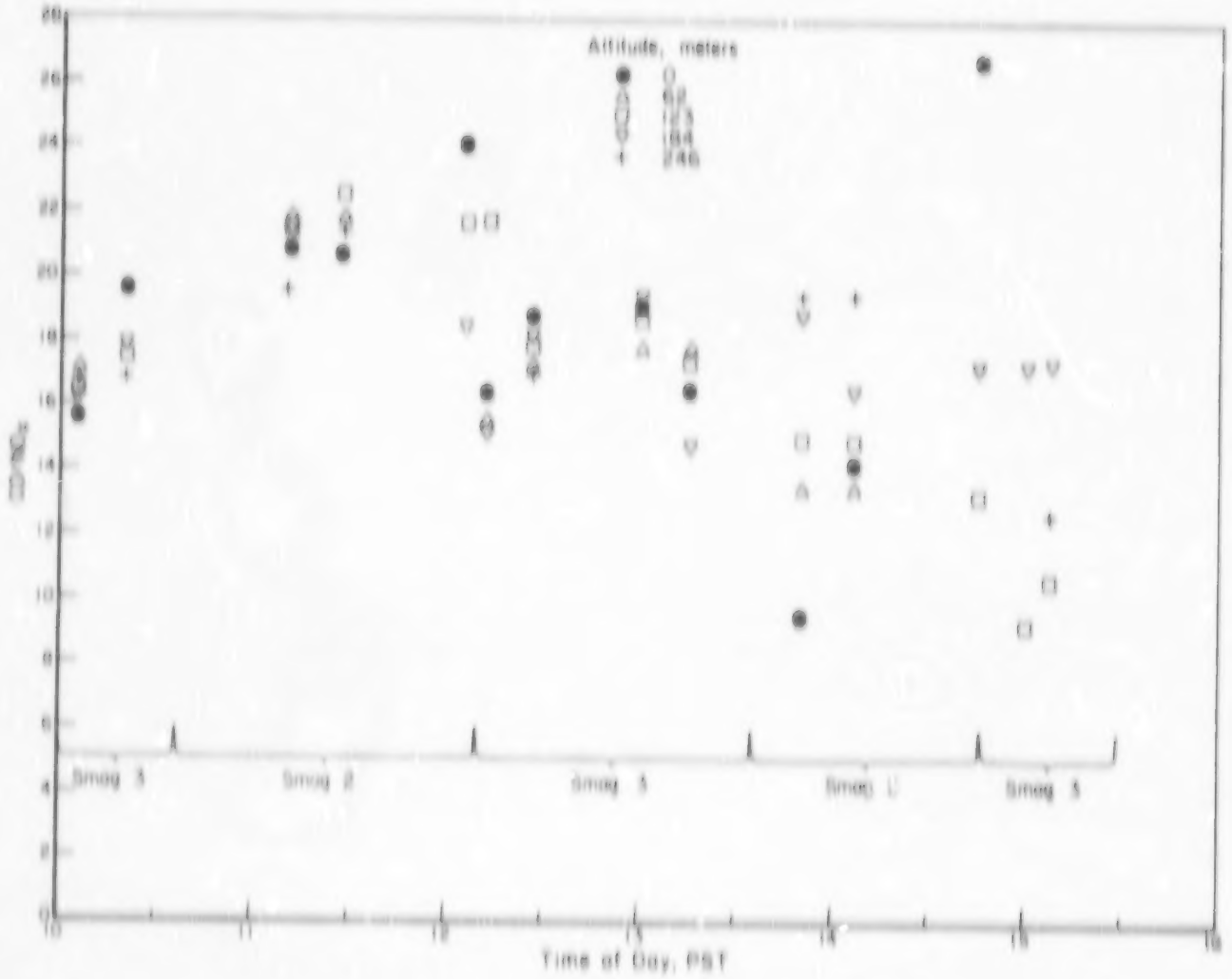

FIGURE 23. PLOT OF CO/NO_x BY ALTITUDE FOR LARPP OPERATION 25

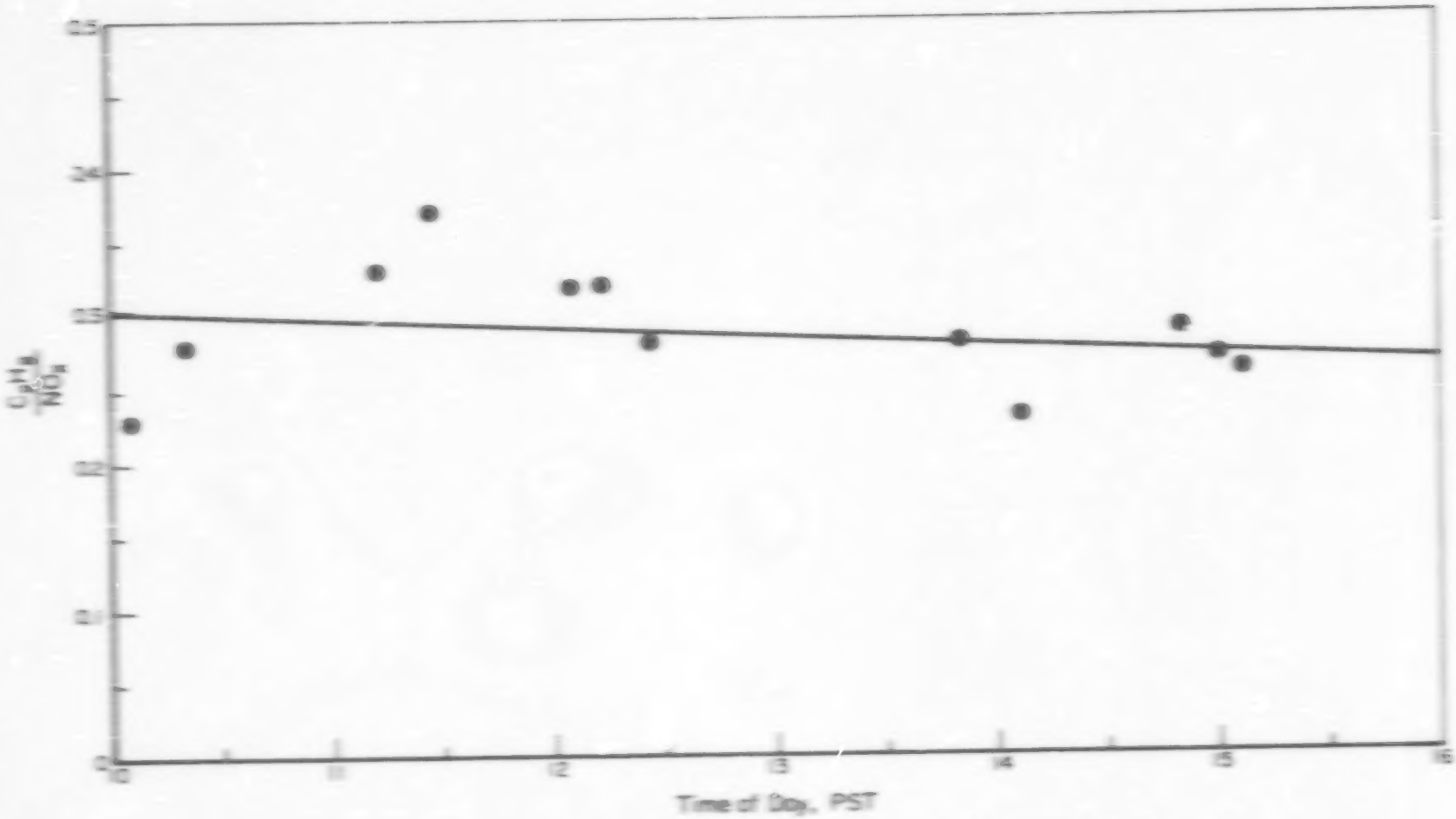

FIGURE 24. PLOT OF $C_{2}H_{2}/NO_{x}$ (PROFILE AVERAGE) FOR LABPP OPERATION 25

A plot of the C_2H_4/C_2H_2 ratio for this operation is included in Figure 25. The least squares line for these points is almost horizontal. The slight slope of this line indicates that the concentration of C_2H_4 decreases at less than 1% per hour relative to C_2H_2. Such a slow decay of the moderately reactive ethylene suggests either (1) very little photochemical activity on this day or (2) injection of fresh emissions into the air parcel which maintain the C_2H_4/C_2H_2 ratio constant. The former explanation can be disregarded, since high levels of ozone were observed within the air parcel. Thus all indicators point to injection of fresh emissions as a major contributor to the concentrations of the measured pollutants within the air mass. Under such circumstances the determination of NO_x removal within the moving air mass is impossible.

Operation 33

Operation 33 was conducted on November 5, 1973, between 7:15 a.m. and 7:20 p.m. The tetroons were launched from the Downey launch site and followed a curving trajectory to the south, southeast, east, and finally northeast. At the conclusion of the experiment the air parcel was several miles south of West Covina, as noted in Figure 20. The peak ozone concentration in the Los Angeles basin on this day varied between 0.1-0.2 ppm. Calvert[41] has reviewed the results of this operation for one elevation using methane and acetylene as tracers. He reports a rate of NO_x removal of $3.0 \pm 2.6 \times 10^{-4}$ ppm min^{-1}, or about 18 ppb per hour. This is not too different from the rates of NO_x reaction product accumulation we observed in West Covina (on peak days over 70 ppb of products accumulated between 10:00-15:00). However, over half of the product yield was PAN, which is known to respond to the chemiluminescent technique used to measure NO_x in the LARPP study. Thus a large fraction of the removal rate reported by Calvert cannot be accounted for in terms of known products.

We have reinvestigated NO_x removal in Operation 33, using CO, C_2H_2, and CH_4 as tracers. Even though methane is quite inert, we are dubious about its use as a tracer due to the fact that natural background methane comprises the major fraction of the measured CH_4 concentration.

Time of Day, EST

Since dilution of the air parcel with clean air does not affect the CH_4 concentration nearly as drastically as the NO_x concentration, the CH_4/NO_x ratio tends to increase by dilution alone. Any additional increase due to chemical removal of NO_x from the air is very difficult to separate from this dilution effect.

Graphics showing the variation in tracer/NO_x ratio with altitude and time may be found in Figures 26-28 for CO/NO_x, CH_4/NO_x and C_2H_2/NO_x, respectively. The ratios at each altitude and time are shown in the figures. This type of data presentation is advantageous in that it allows us to visually examine the variation in ratios both vertically and horizontally (with time).

Examination of the CO/NO_x ratios in Figure 26 along any altitude stratification given no evidence of the steadily increasing ratios which would be expected if NO_x were being removed from the air parcel faster than CO. This is verified by the plots in Figure 29, where the ratios are plotted against time for each altitude stratum. Once again, within the scatter of the data the ratio remains virtually constant.

The CH_4/NO_x data shown in Figure 27 are not as extensive and seem more widely scattered than the CO/NO_x results. These ratios are plotted against time in Figure 30. Except for the ground-level results, the ratios increase if we neglect the earliest data point in the three upper level plots. However, even these increases must be viewed with suspicion due to the dilution effect discussed earlier. Because of our doubts regarding the validity of NO_x-loss determination from the CH_4/NO_x ratios, these data will not be discussed further.

Plots of the C_2H_2/NO_x ratios are shown in Figure 28 and 31. The ground level data are limited but show a decrease with time. The ratios from the other elevations, plotted in Figure 31, generally trend upward. Visually fitted lines have been drawn through the data points for each altitude. The earliest ratio in the 225-275 meter elevation plot has been neglected. The slopes of these lines suggest an average rate of loss of about 9% per hour, as reported by Calvert[41]. This rate of loss is in addition to any loss due to formation of PAN (and probably some fraction of HNO_3) since any specie which is measured by the chemiluminescent instrument

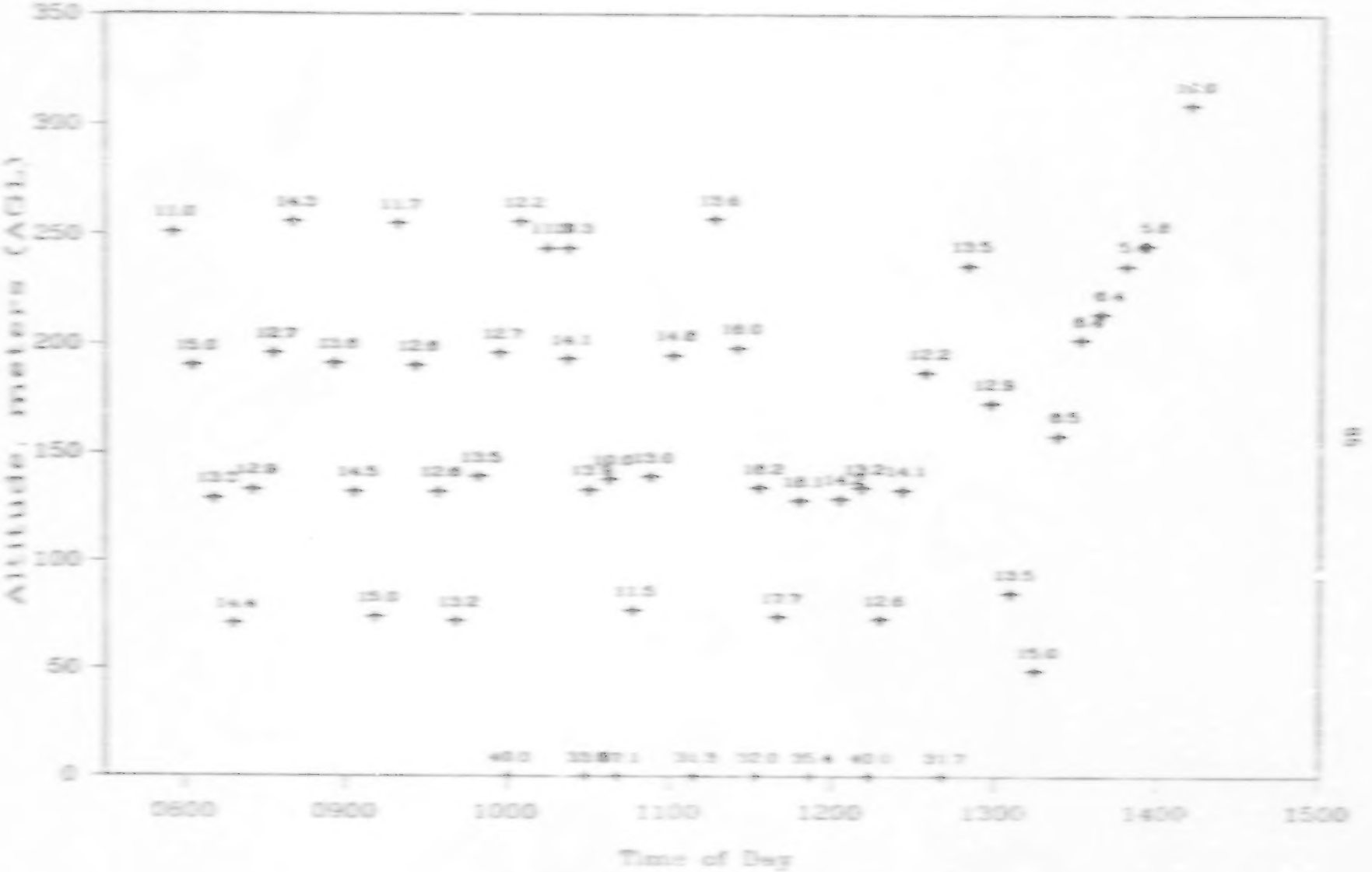
350
300
250
200
150
100
50
0
0600
0900
1000
1100
1200
1300
1400
1500
Time of Day

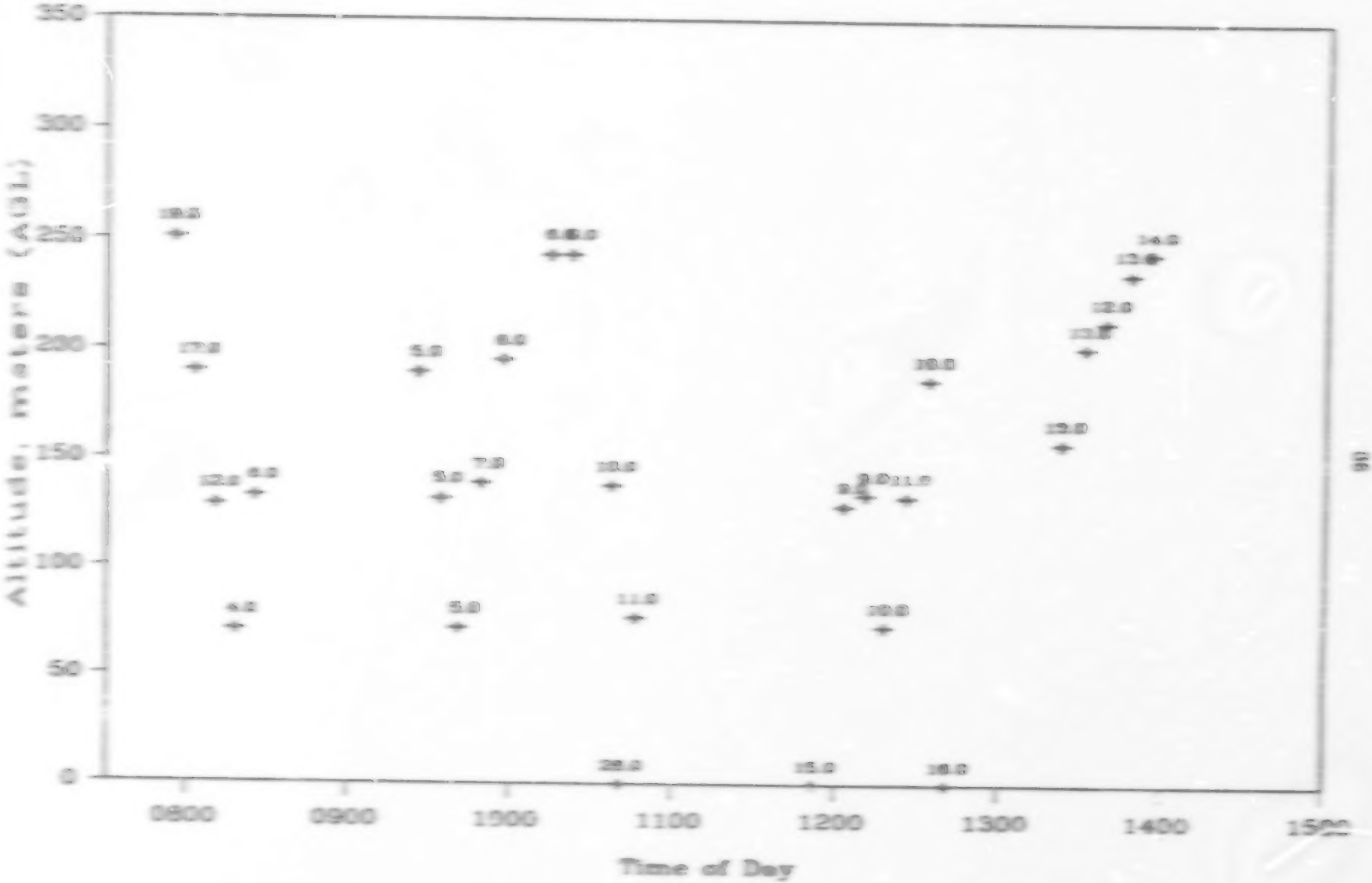

FIGURE 27. CH_4/NO_x RATIO (OPERATION II)

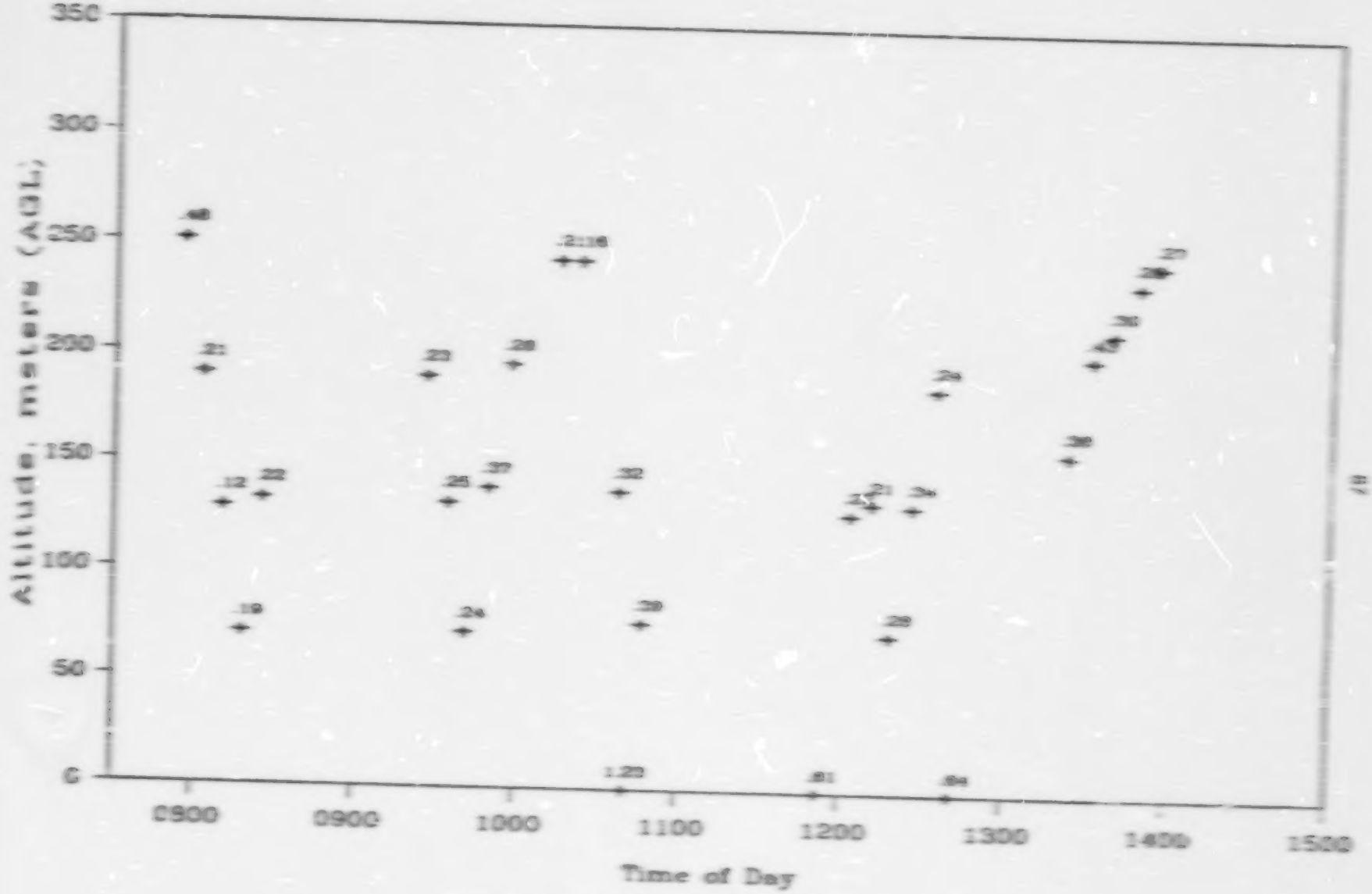

FIGURE 28. C_2H_2/NO_x RATIO (OPERATION II)

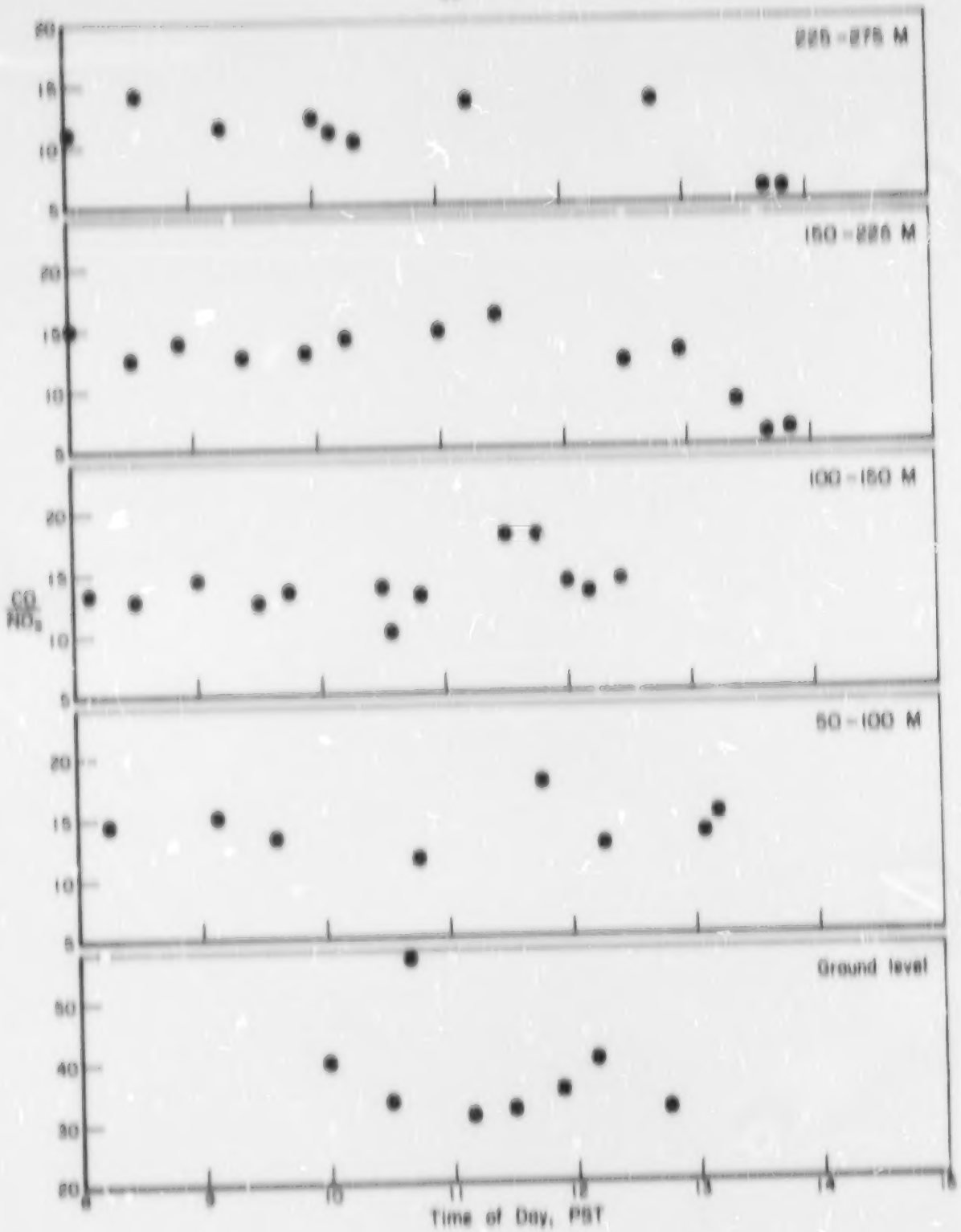

FIGURE 29. CO/NO_x RATIOS BY ALTITUDE FOR LARPP OPERATION 33

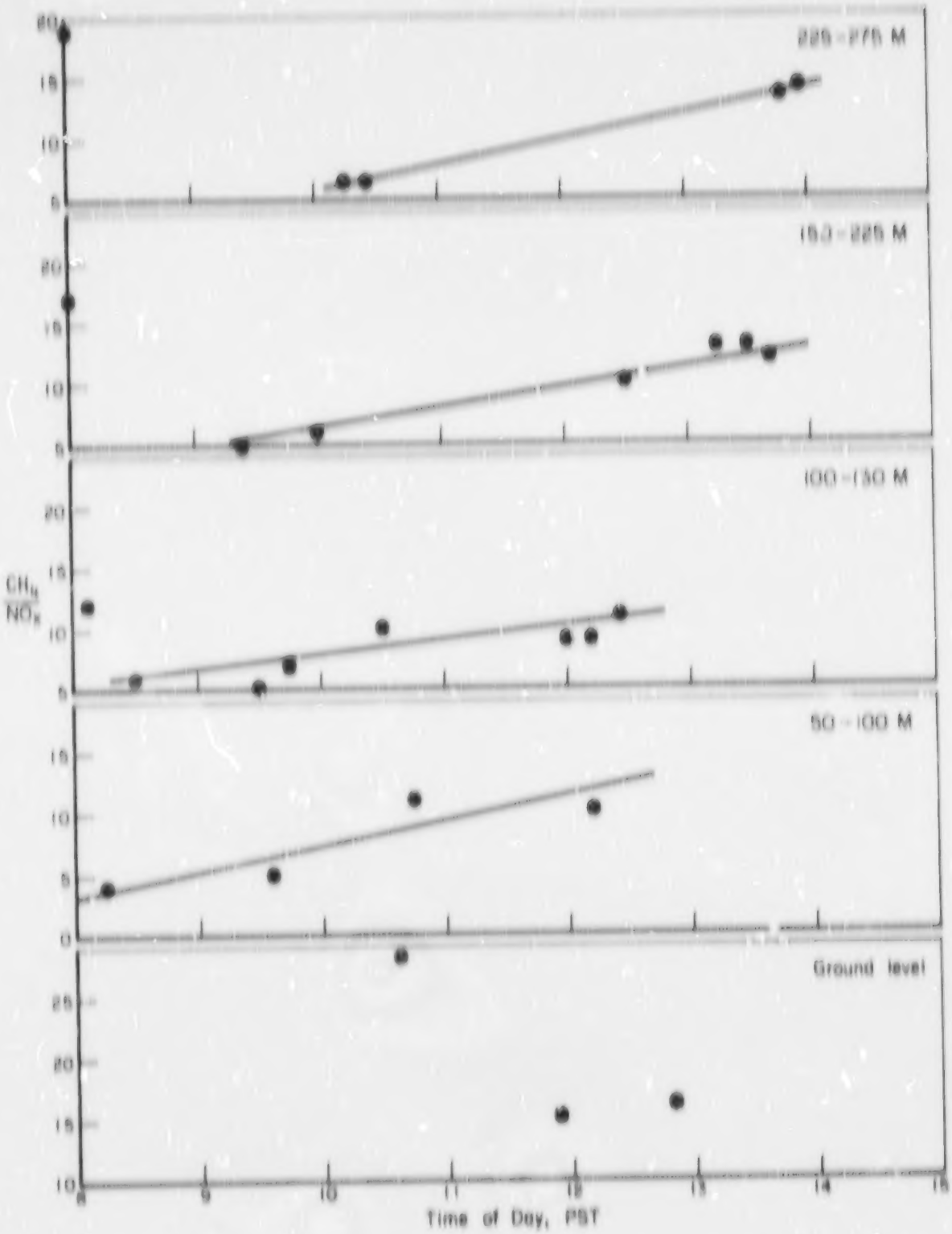

FIGURE 30. CH_4/NO_x RATIOS BY ALTITUDE FOR LARPP OPERATION 33

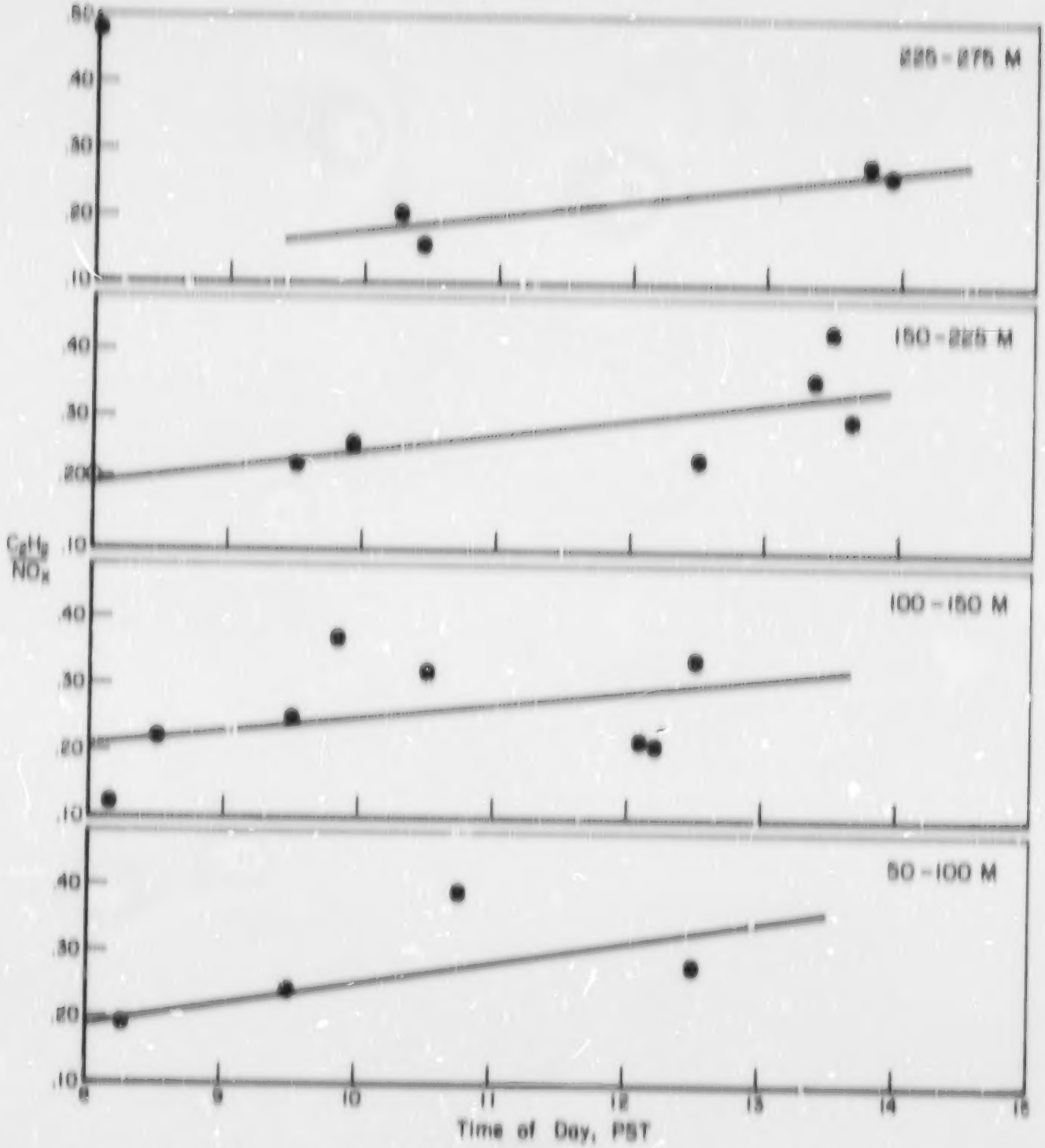

FIGURE 31. C_2H_2/NO_x RATIOS BY ALTITUDE FOR LARPP OPERATION 33

will not appear as a loss. A 9% per hour loss is greater than expected from our West Covina results. The fact that the West Covina study and this LARPP operation were run on different days under different conditions may partly explain the difference. However, the results from smog chamber and field studies gives no indication of any process removing NO_x to a non-measured product at such a rapid rate. The fact that no such process appeared during Operation 25 (a stronger smog day), combined with the fact that the CO/NO_x ratio for this operation gave no indication of rapid removal, makes us suspicious of this result. At the very least, it is difficult to explain why the C_2H_2/NO_x ratio increases while the CO/NO_x ratio remains constant; both CO and C_2H_2 are assumed to be inert over these short time periods, and both come primarily from the same source (vehicular exhaust). Since the source of these gases is the same and both are inert, we expect to find a constant ratio of CO to C_2H_2 in the Los Angeles air. If the CO/C_2H_2 ratio does not remain constant, then either our assumptions are wrong or a measurement problem exists. The CO/C_2H_2 ratio for Operation 33 is plotted versus time in Figure 3i. Contrary to expectations, the ratio decreases with time, and at about the same rate as the C_2H_2/NO_x ratio. Apparently the C_2H_2 concentration increases relative to CO during the operation. This relative increase in C_2H_2 explains the increase observed in the C_2H_2/NO_x ratio. These results suggest that CO and NO_x (including the NO_x products measured by chemiluminescence) disperse at about the same rate and that, for some unknown reason, C_2H_2 increases relative to the rate of dilution. Whether this relative increase is actual or is an artifact of the measurements is unknown. In either case, it explains the increase in the C_2H_2/NO_x ratio and casts doubt on the high apparent rate of NO_x conversion to unknown products.

The remaining operations generally contain less data than 25 and 33 and will only be described briefly in the remainder of this section.

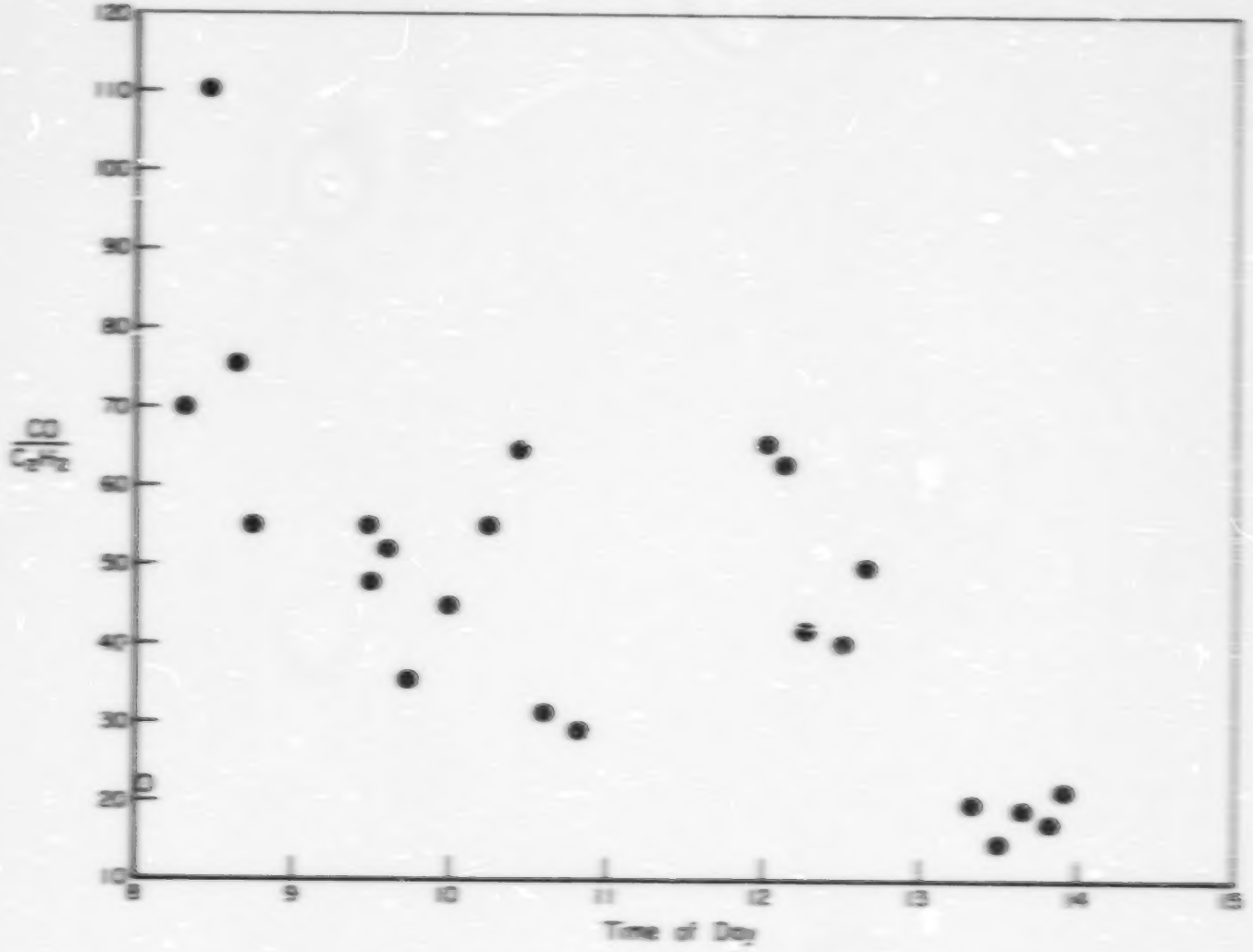

FIGURE 32. CO/C_2H_2 RATIO FOR LAMPF OPERATION 33

Operation 6

Operation 6 was run on September 18, 1973, from 10:30 a.m. to 2:20 p.m. The air parcel trajectory was shown earlier in Figure 20. Figures 33 to 35 show the behavior of the ratios CO/NO_x, C_2H_2/NO_x, and CH_4/NO_x, respectively for Operation 6. Unfortunately, there are limited data for Operation 6, especially for Figures 34 and 35. What data there are in Figure 33 suggests the possibility of an increase in the level of CO/NO_x ratio; however, the data are too sparse to draw any firm conclusions regarding possible NO_x-loss.

Operation 8

Operation 8 was conducted on September 24, 1973, from 8:45 a.m. to 3:20 p.m. The trajectory followed by the air parcel is shown in Figure 20. The ratios of CO/NO_x, C_2H_2/NO_x, and CH_4/NO_x are presented in Figures 36-38. Only the CO/NO_x data are extensive enough for comment, and they seem to show a decrease in the ratio with time. The implications and possible causes of a decrease in the ratio were discussed earlier in conjuction with Operation 25.

Operation 10

LARPP Operation 10 was launched from the Los Angeles site at 8:50 a.m. on September 27, 1973. The operation lasted until 3:20 p.m. The trajectory of the air parcel is shown in Figure 20. The tracer/NO_x ratios for this operation are presented in Figures 39-41. The data available to us for this operation are sparse and widely scattered. No clear trends emerge from the ratio plots for this operation.

Operation 16

Operation 16 was conducted on October 10, 1973. The tetroons were launched from Downey and followed the trajectory indicated in Figure 20. The operation lasted from 8:30 a.m. to 4:45 p.m.

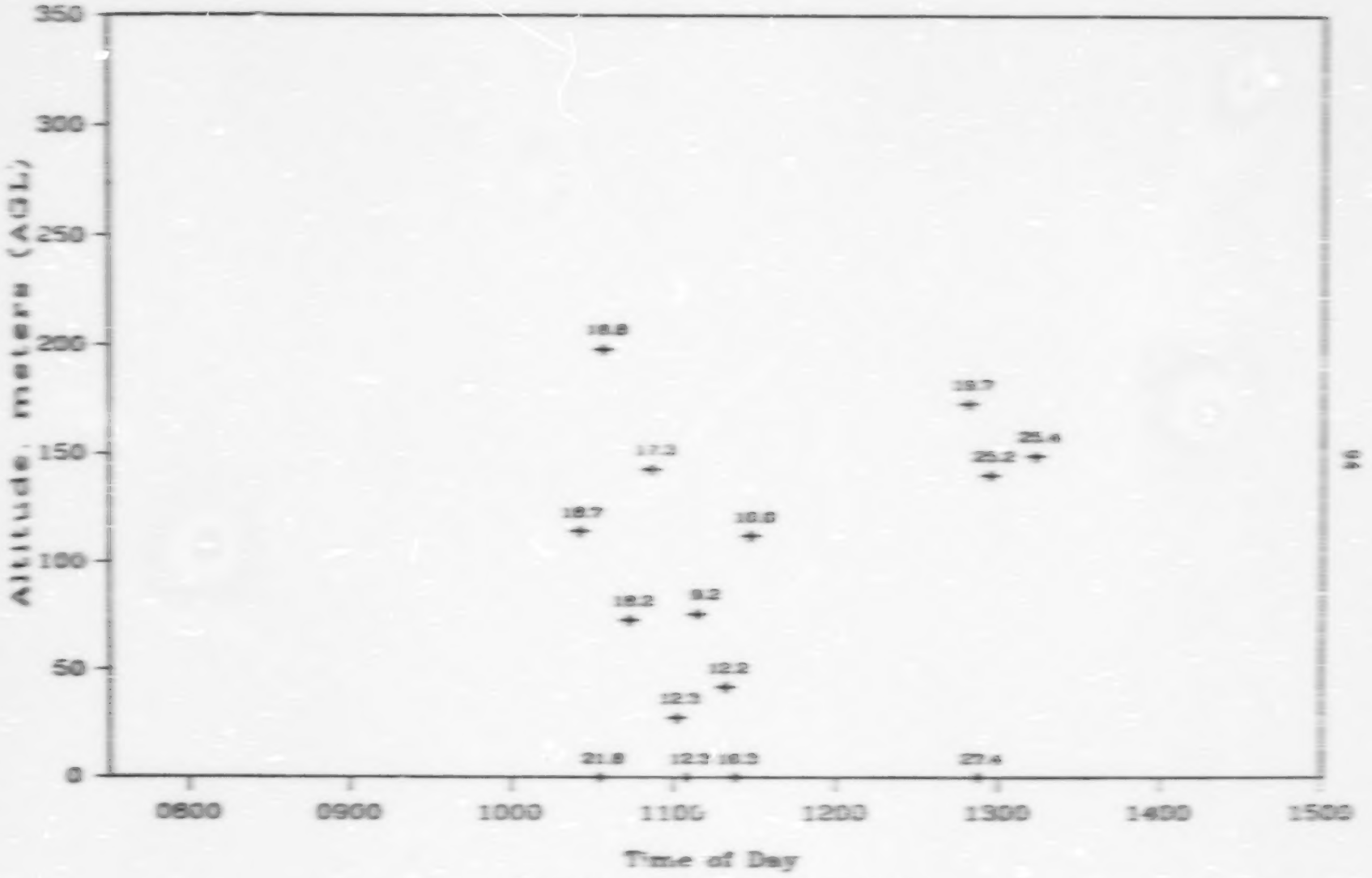

FIGURE 33. CO/NO_x RATIO (OPERATION 5)

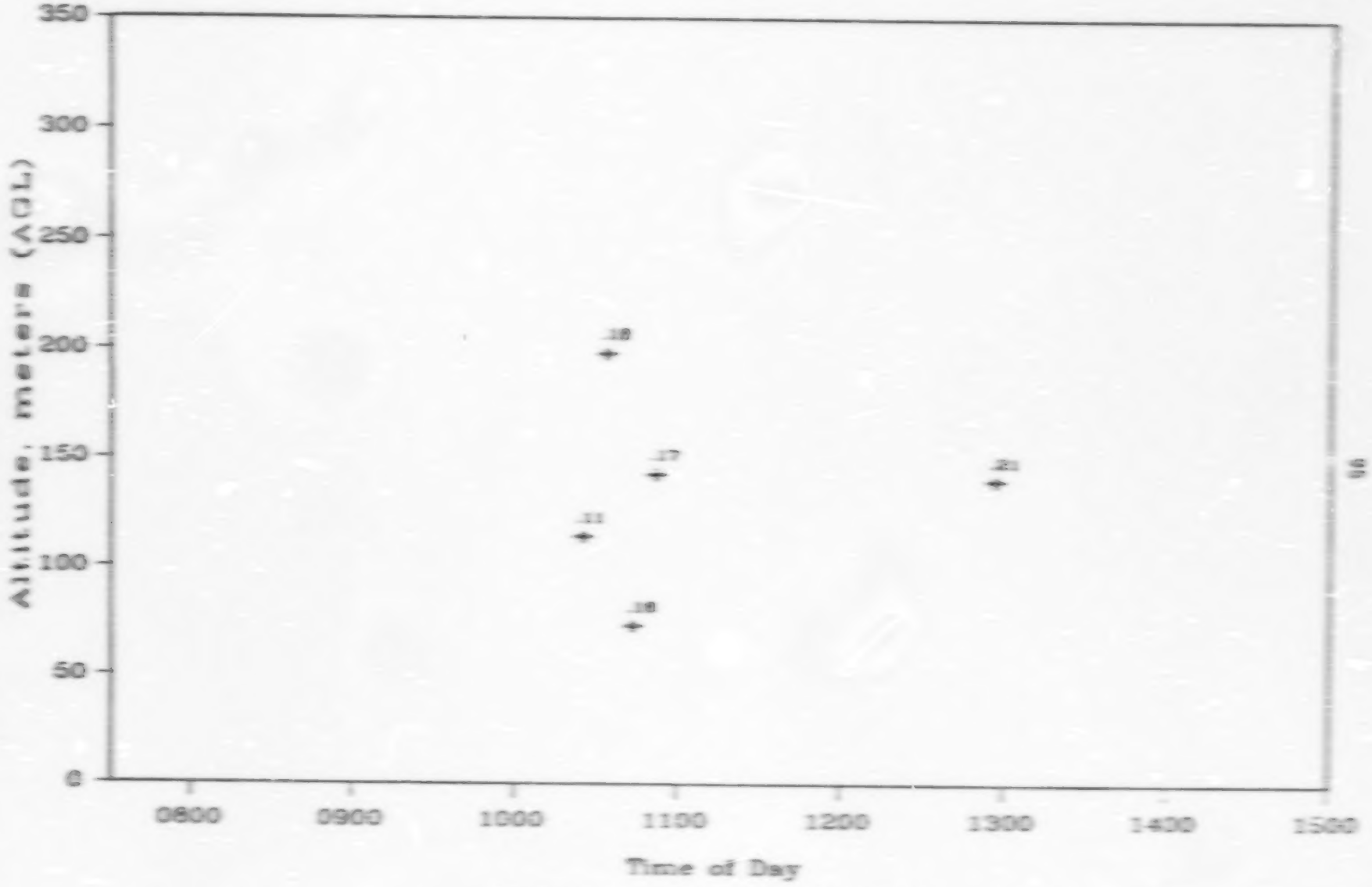

FIGURE 34. C_2H_2/NO_x RATIO (OPERATION 5)

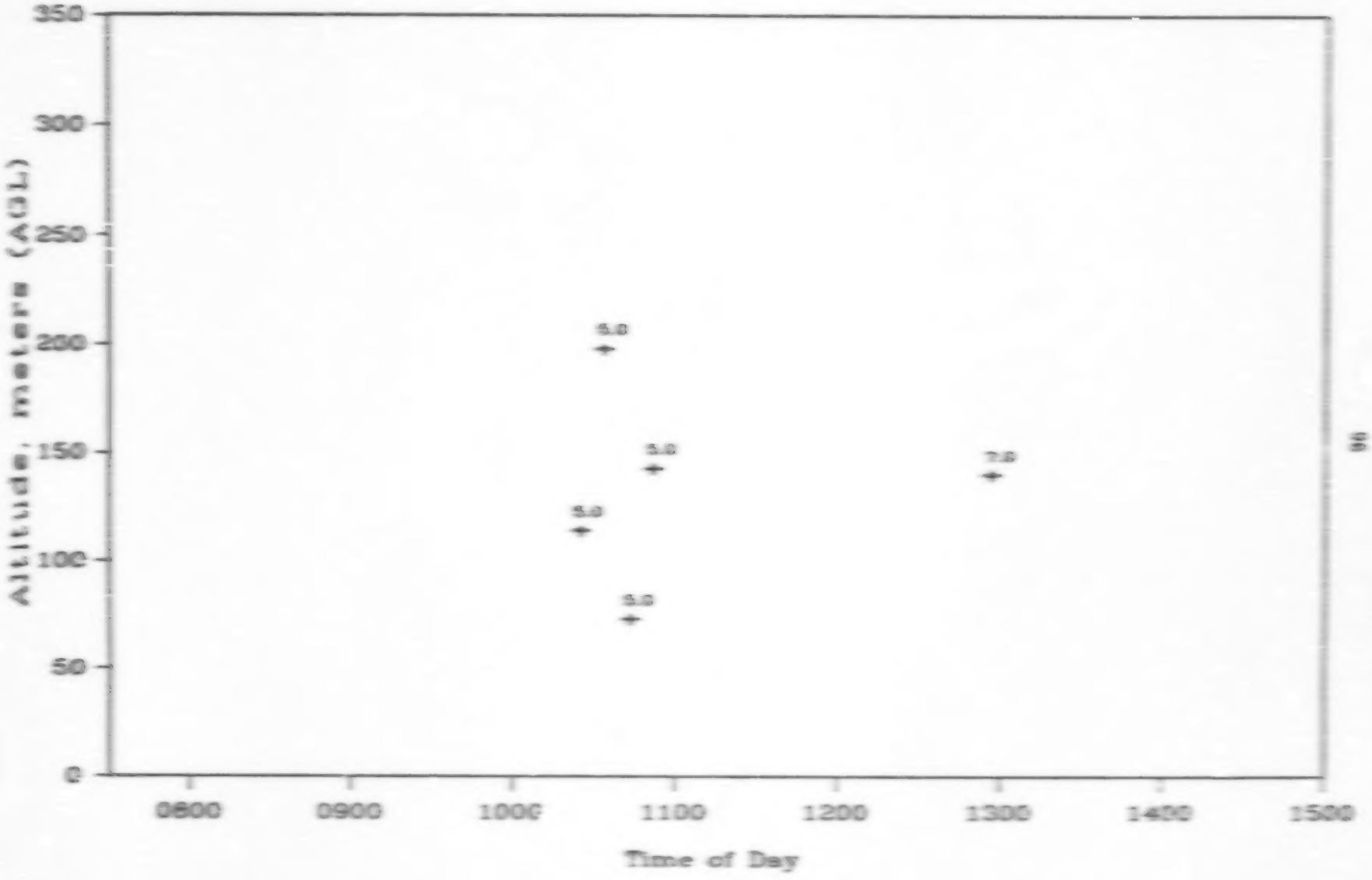

FIGURE 35. CH_4-NO_x RATIO (OPERATION 5)

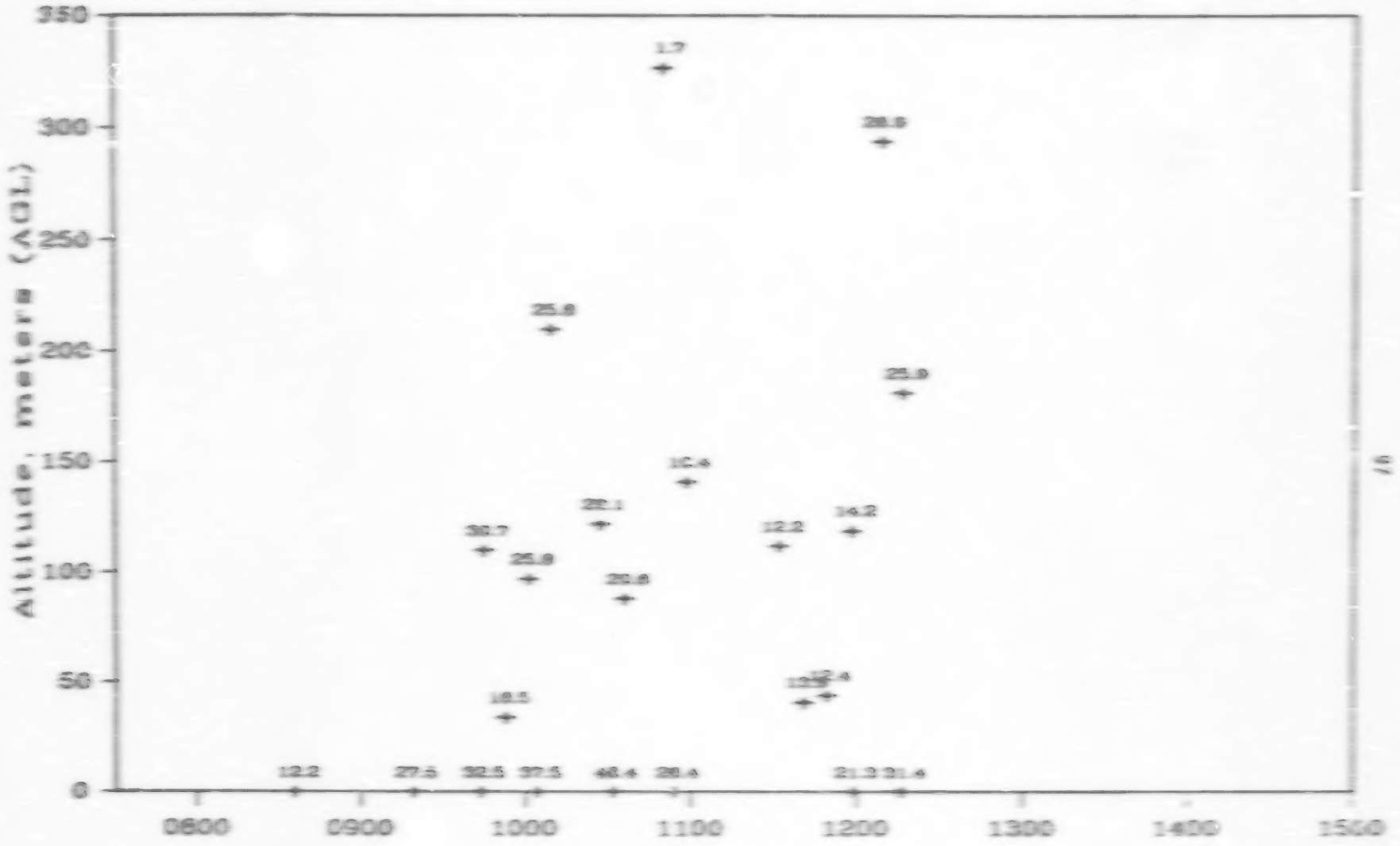

FIGURE 36. CO/NO_x RATIO (OPERATION 8)

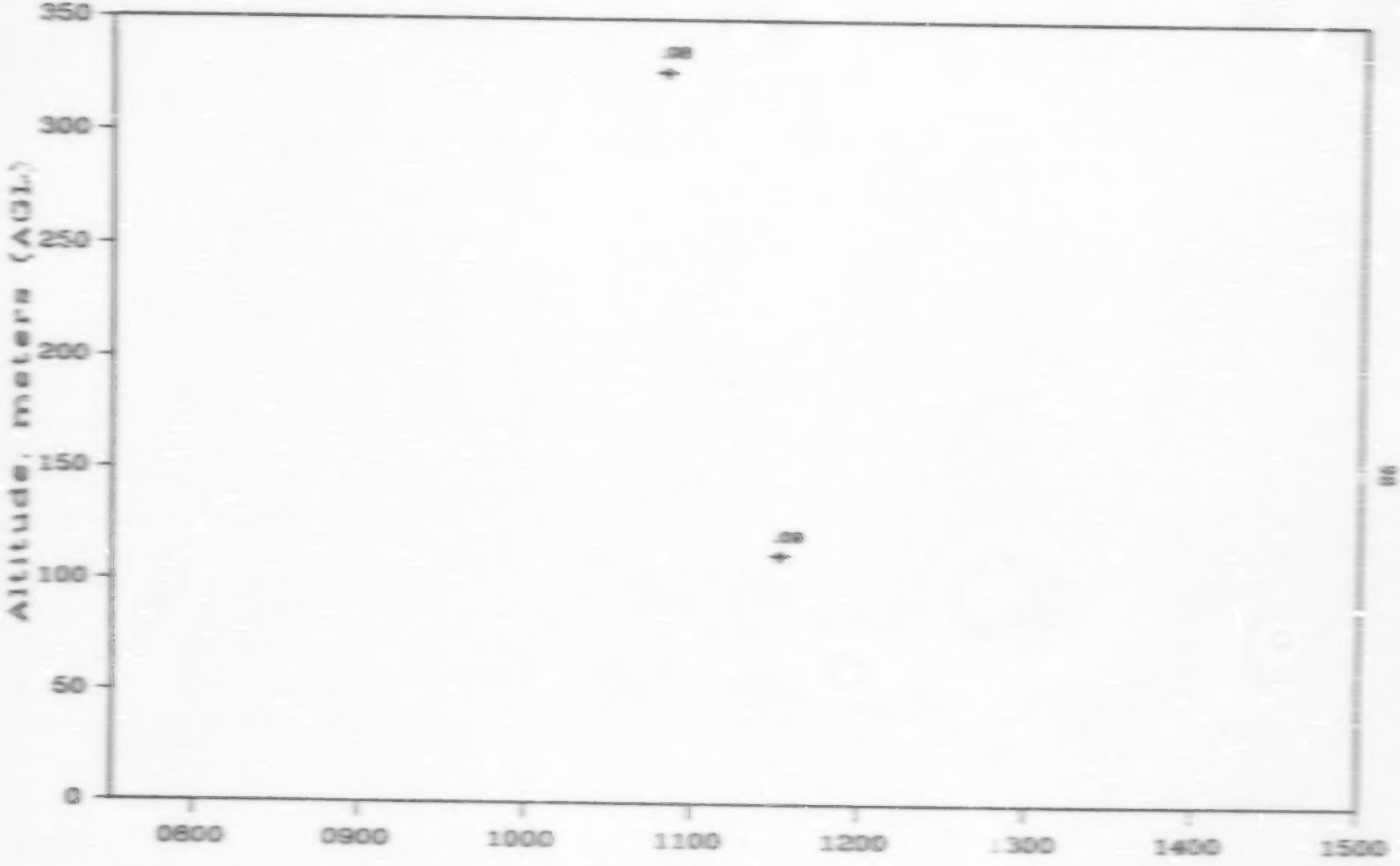

FIGURE 37. C_2A_2/NO_x RATIO (OPERATION 5)

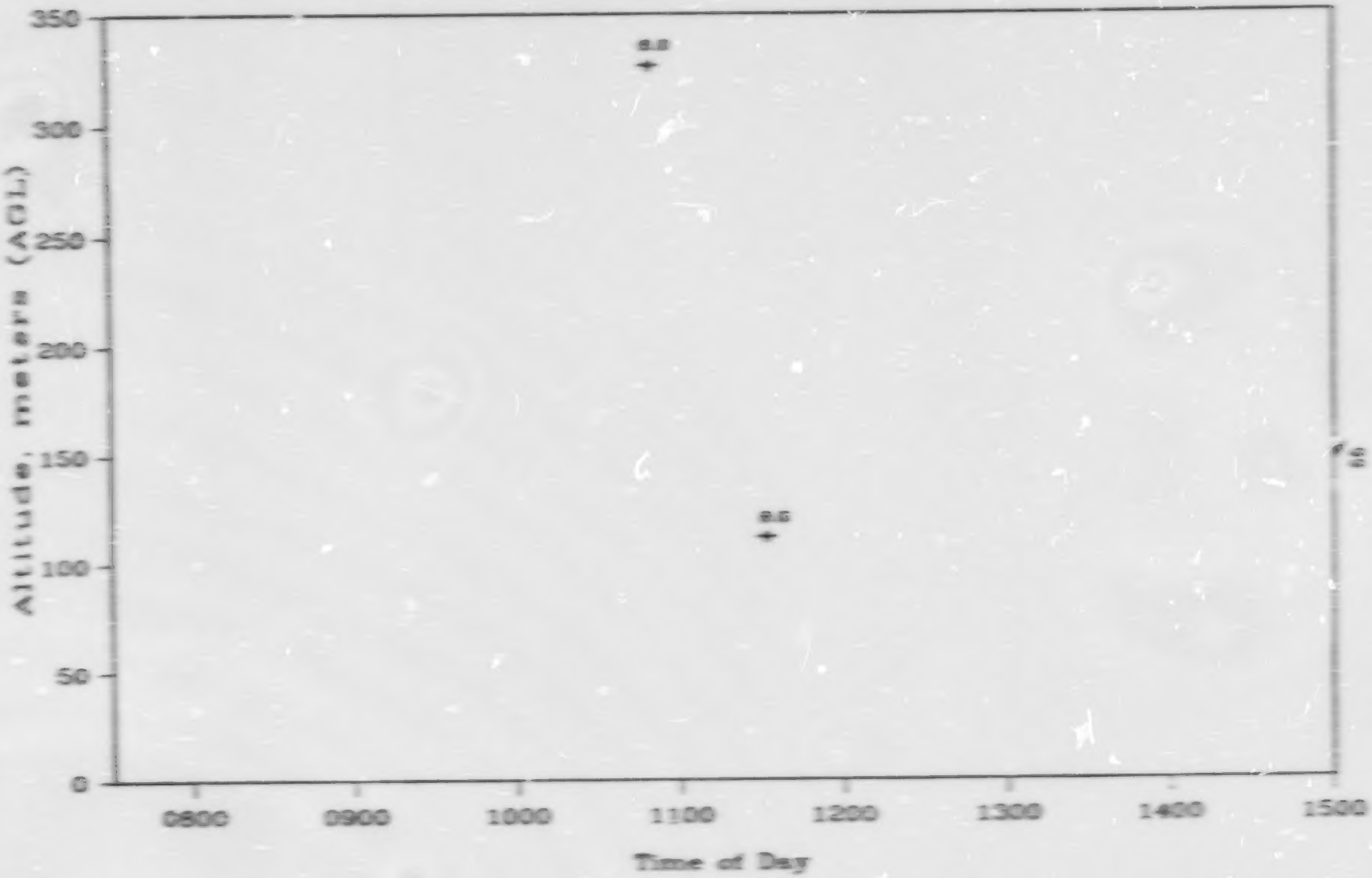

FIGURE 38. CH_4/NO_x RATIO [OPERATION E]

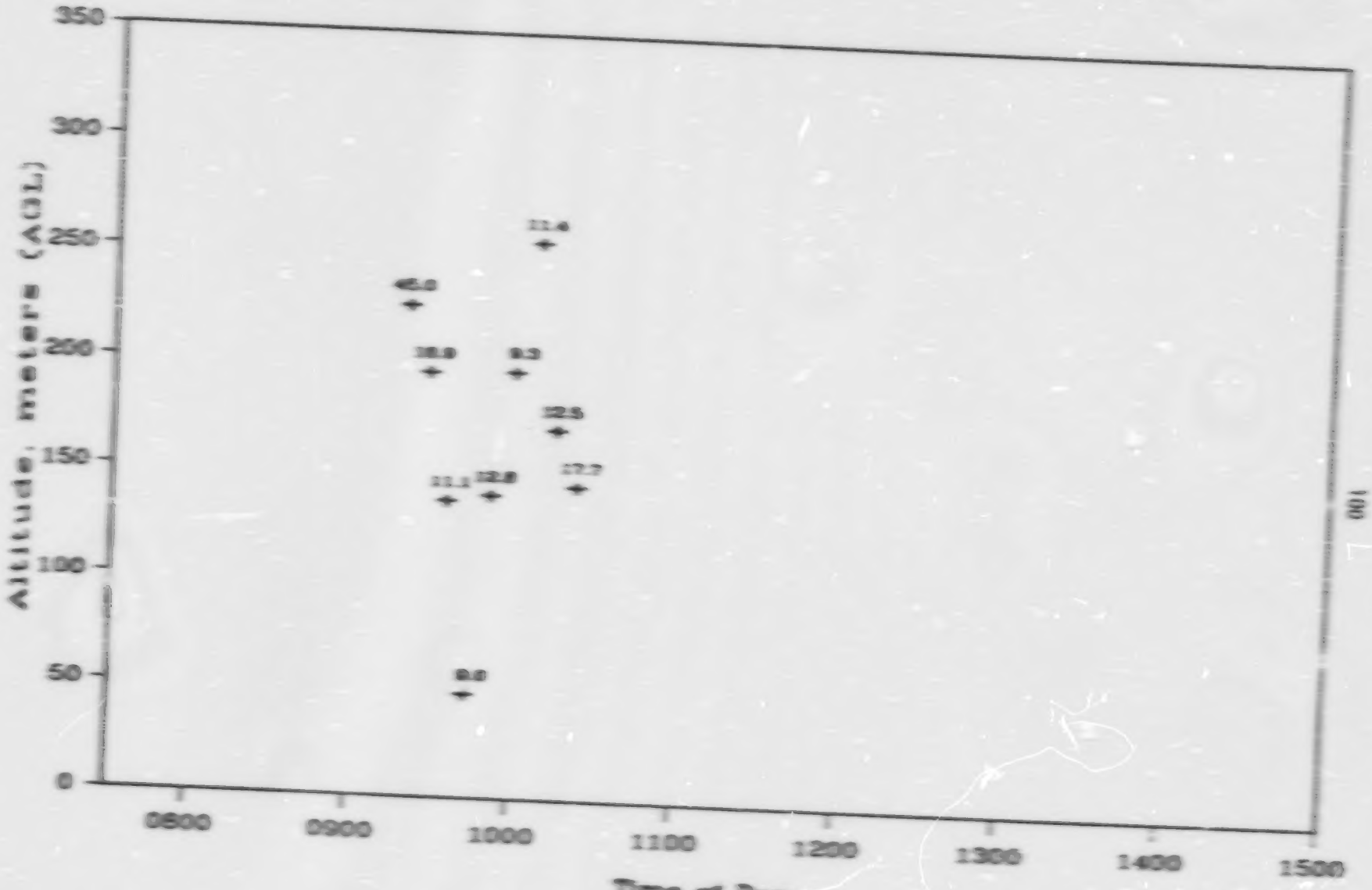
350
300
250
200
150
100
50
0
Altitude, meters (AGL)
11.4
45.0
38.9
9.3
32.5
11.1
32.8
27.7
8.0
0600
0900
1000
1100
1200
1300
1400
1500
Time of Day

FIGURE 35. [illegible]

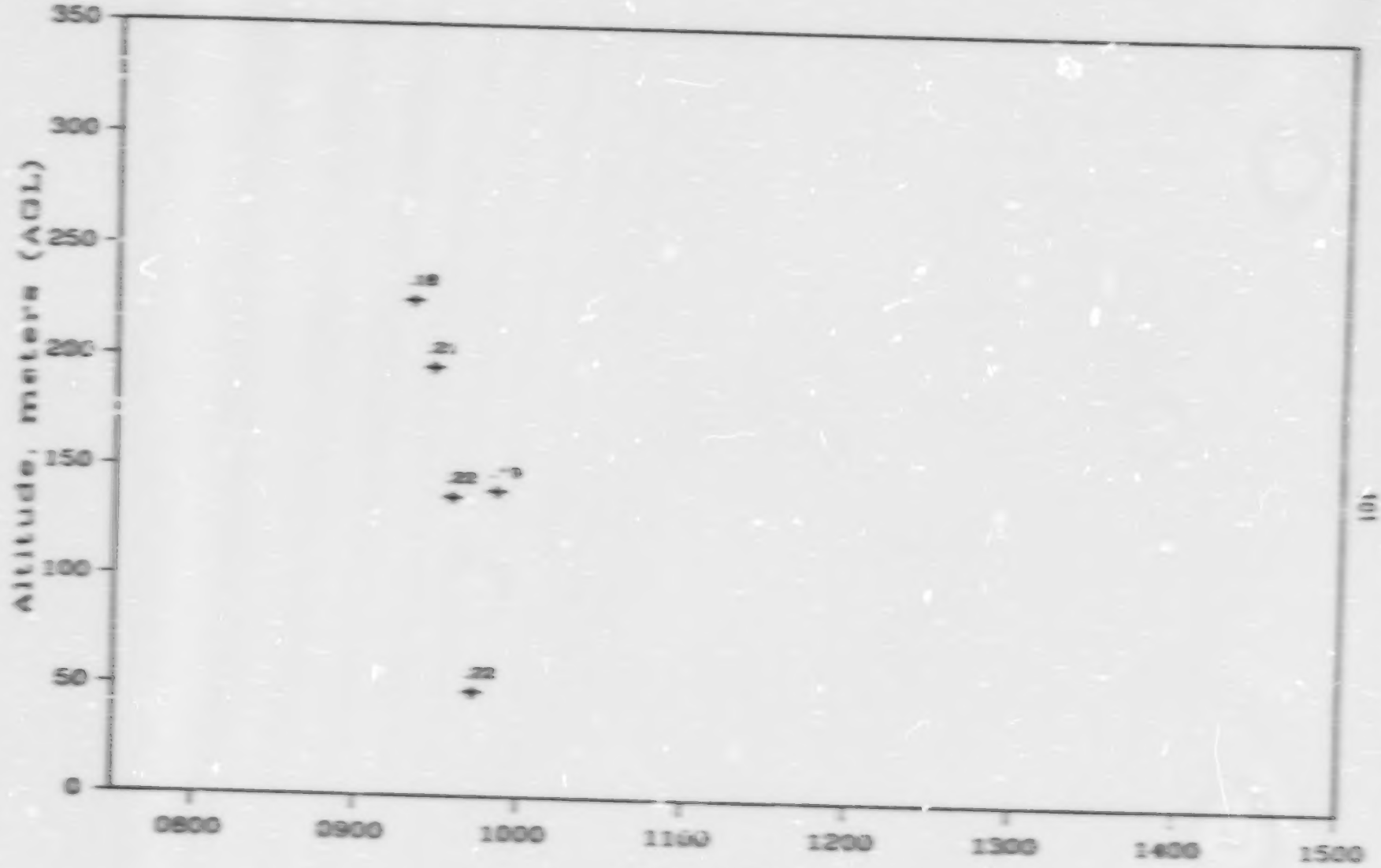

FIGURE 41. C_2H_2/NO_x RATIO (OPERATION 10)

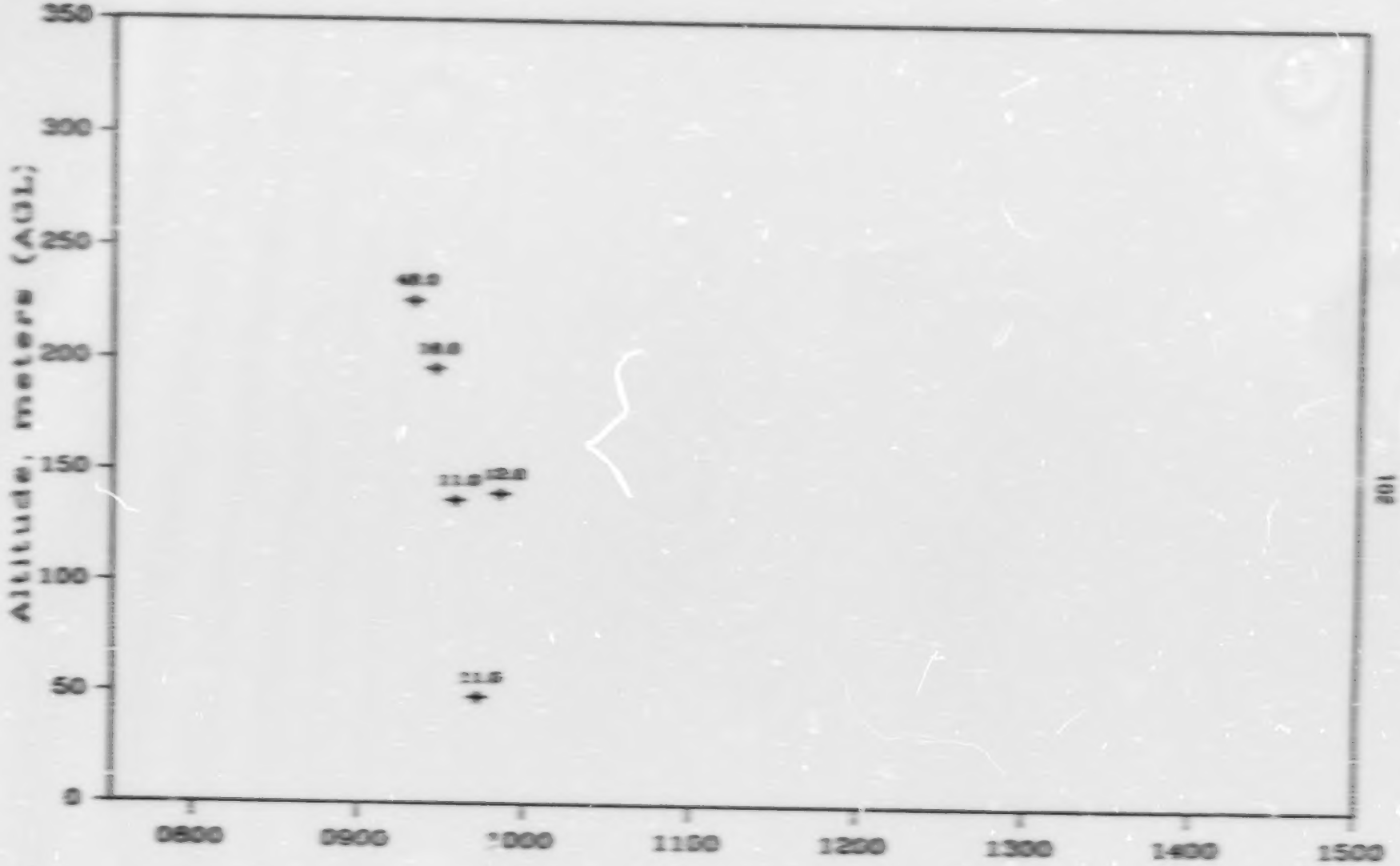

FIGURE 41. O_3/NO_x RATIO [OPERATION 1G]

The ratio plots for Operation 16 are given in Figures 42-44. The CO/NO_x ratio from Figure 42 shows evidence of a gradual increase with time, possibly indicating some removal of NO_x from the air parcel. These data have been plotted in a slightly different manner in Figure 45 to display this upward trend. The data prior to 10:30 show no definite trend, nor do the points after 10:30; rather, there seems to be a step change in the value of the ratio at about 10:30. The may be partly explained by variation in the analytical calibration of the instruments in the two different helicopters, but this is uncertain. The C_2H_2/NO_x and CH_4/NO_x ratios for this operation, shown in Figures 43 and 44, are quite scattered and cannot substantiate the upward trend. If the trend is real, a loss of NO_x of about 12% per hour is indicated. This loss is in addition to PAN and HNO_3 formation, since these species are measured as NO_x by the chemiluminescent instrument used in the helicopters. Particulate nitrate and other unknown products which do not respond to the instrument would have to be postulated to account for the loss. Such a loss rate to products other than PAN and HNO_3 is considerably higher than observed in the West Covina study.

Operation 27

Data from Operation 27 are insufficient to warrant discussion.

One of the difficulties faced in studying the preceding LARPP operations is the inconsistency observed in the tracer/NO_x ratios. This is not unexpected for the CH_4/NO_x ratio for reasons discussed earlier. It is the inconsistency in the CO/NO_x and C_2H_2/NO_x trends that is most troublesome. For some operations we attempted to verify the trends using the fluorescent particle tracer results. Our attempts were unsuccessful, probably because of the infusion of fresh pollutants into the air parcel during dilution of the fluorescent particle tracer.

In an effort to understand the discrepancies, the ratio of CO to C_2H_2 has been plotted versus time of day in Figure 46 for Operations 5,8,10, 16, and 33. In theory this ratio should remain constant during the day due

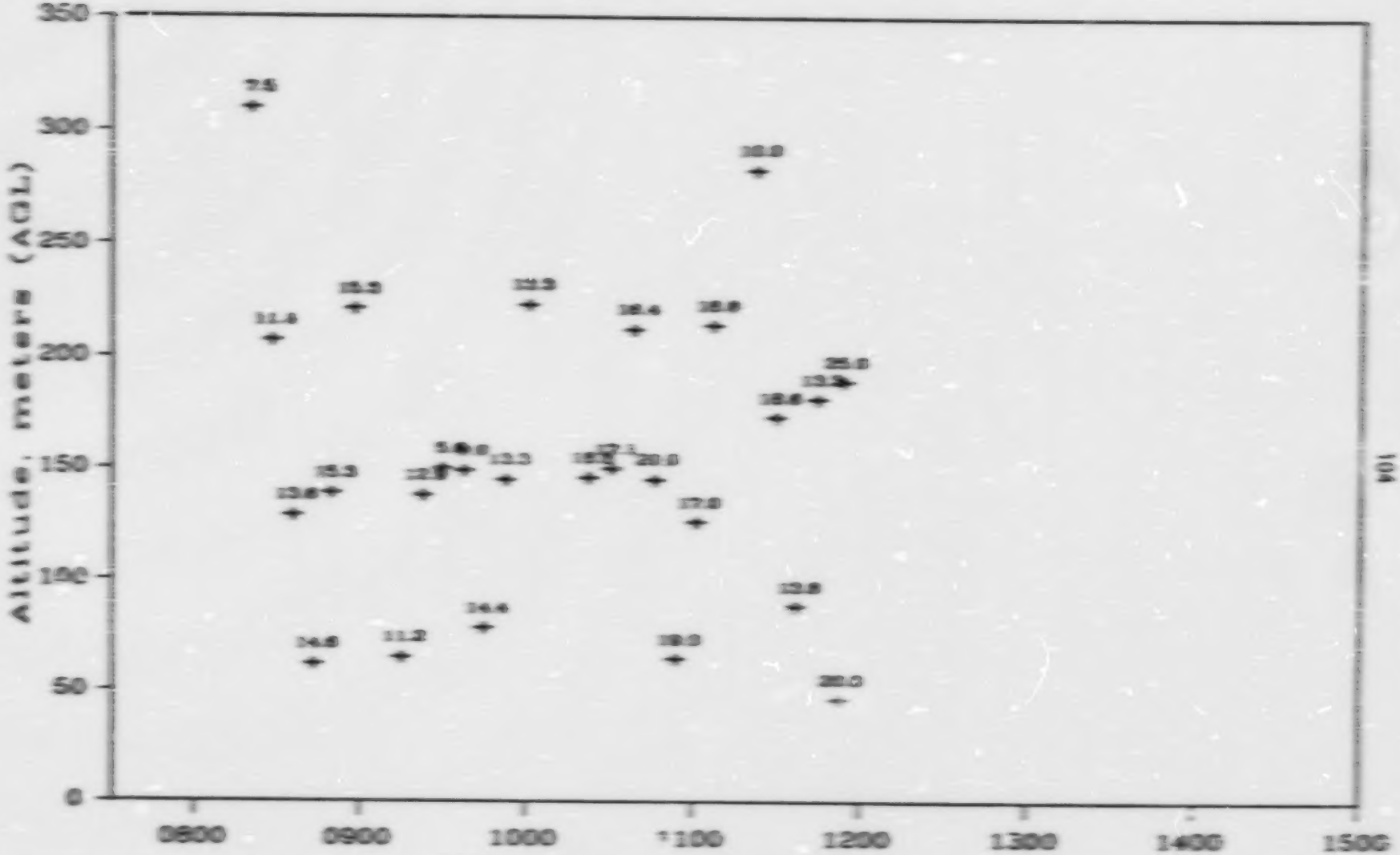
Altitude, meters (AGL)
350
300
250
200
150
100
50
0
0800
0900
1000
1100
1200
1300
1400
1500
Time of Day

FIGURE 42. [illegible]

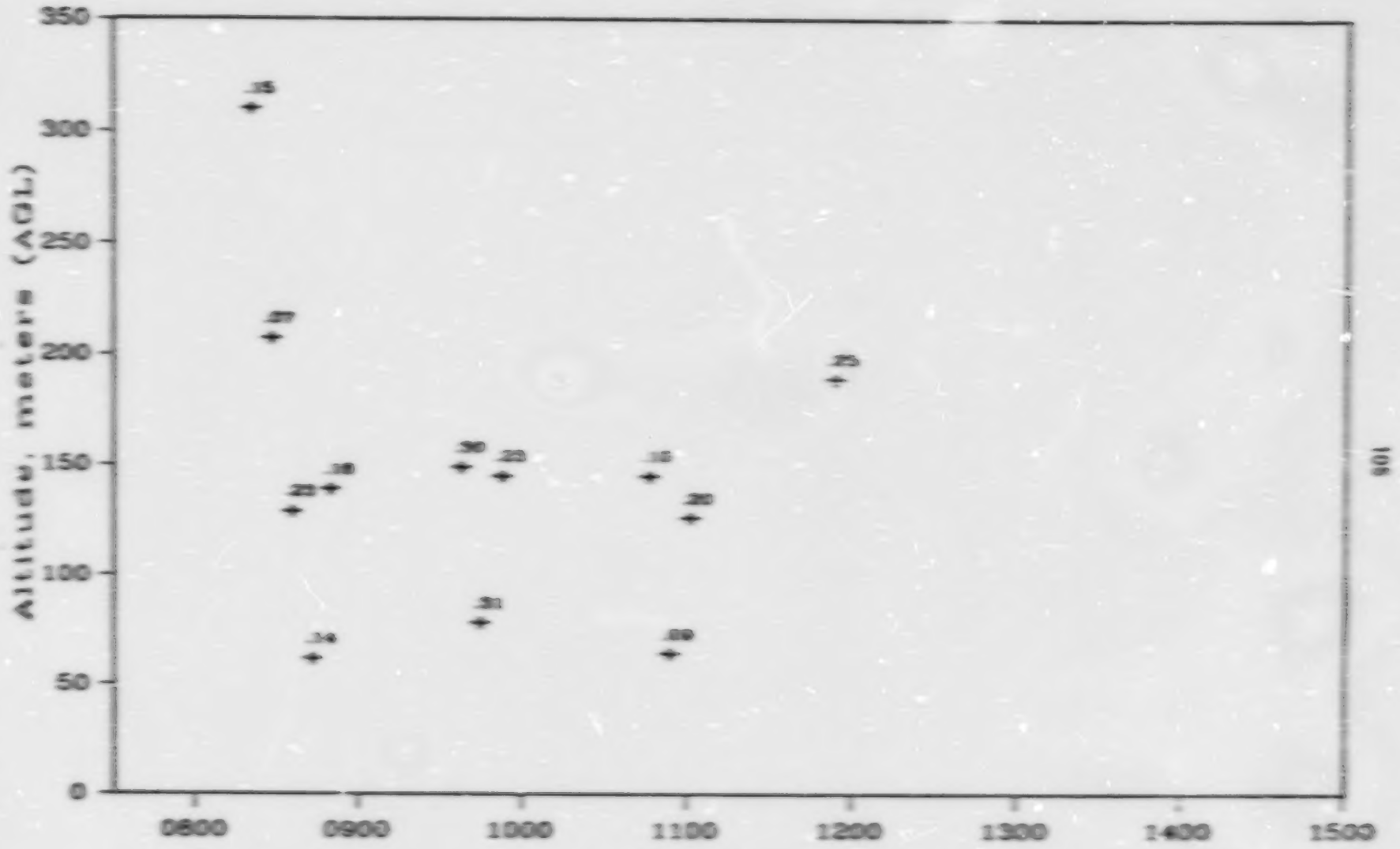

FIGURE 43. $C_2H_2Br_2$ WATER (SPECIMEN 16)

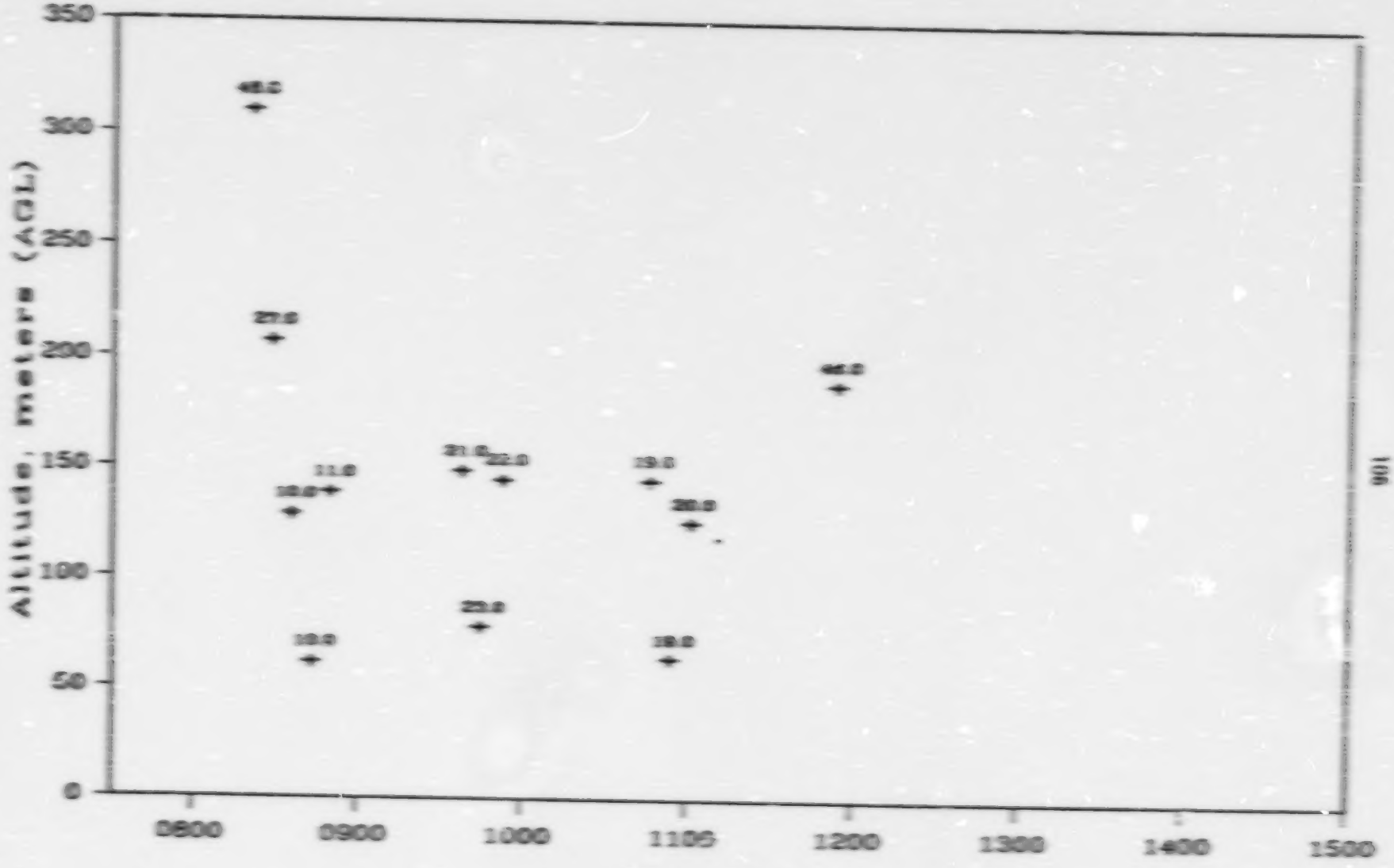

FIGURE 44. O_3-NO_x RATIO (OPERATION 16)

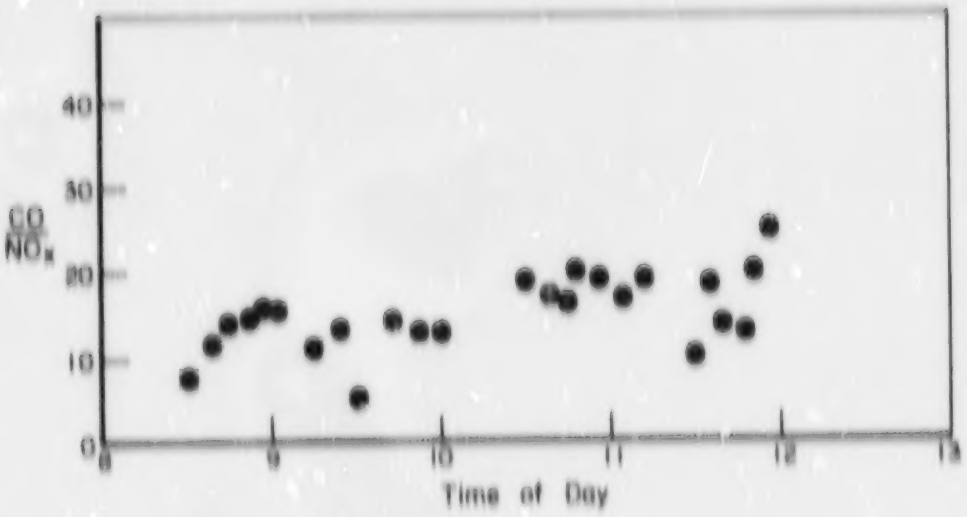

FIGURE 41. CO/NO_x RATIO FOR LARPP OPERATION 16

to the inertness of these gases and their similar sources. It is clear from Figure 46 that the ratio varied considerably, both within a given operation and between the different operations. It is very likely this variation which has caused the uncertainty in the tracer/NO_x ratio trends. Analytical imprecision must be considered as a possible explanation of the CO/C_2H_2 ratio variation, especially for C_2H_2 which is determined by gas chromatographic analysis of bag samples collected aboard the helicopters. Normally the imprecision in the determination of the CO and C_2H_2 concentrations increases at lower concentrations. If so, a plot of the CO/C_2H_2 ratio versus C_2H_2 (or CO) should show the greatest scatter at low C_2H_2. This is confirmed by Figure 47. Since the concentrations of the reactant and tracer gases usually decrease with time during an operation, the scatter in the data will normally increase with time. This effect may partly explain our difficulty in obtaining consistent trends in the LARPP operations.

It should be noted that the calculation of NO_x-loss in the manner we have attempted here is extremely sensitive to imprecision in the data and is an exceedingly severe test for any data. The imprecision observed in the LARPP data is of the magnitude expected from careful operation of state-of-the-art instrumentation; in other words, this is the best anyone can do under field conditions. Overall, the LARPP data seem reliable and should serve as a valuable resource for atmospheric scientists for years to come.

The results of our CAPA-9 studies and our brief investigation of portions of the LARPP data suggest two different strategies for studying NO_x chemistry in the field. One field study design involves measurements in large urban areas where the concentrations of NO_x and NO_x reaction products are conveniently measurable, but where injection of fresh emissions into moving air masses makes it difficult to follow NO_x reactions in particular air masses (as in a Lagrangian study). A great deal has been learned about NO_x reaction product distribution and <u>average</u> NO_x accountability through such studies, and much more must still be learned about average NO_x accountability, NO_x reaction product distribution, residence time and fate of reaction products, and the effect of seasonal changes on the fate of nitrogen oxides. All these topics can be investigated in nonisolated urban areas such as Los Angeles.

The second type of field study would be conducted in a Lagrangian manner in an isolated source area to minimize the impact of fresh emissions to the air parcel. As discussed earlier, the injection of fresh pollutants into a reacting air mass is one factor which has frequently confused the interpretation of field study data. The input of fresh emissions makes it very difficult to follow the rate of chemical and physical removal of NO_x from moving air masses over short times (hours). For this reason a study with this objective should be conducted within and downwind of an isolated urban area. Under appropriate conditions the polluted air mass could be followed and studied as it moves downwind of the isolated source, with only minimal addition of fresh pollutants to the air mass. Ideally, the city chosen for such a study should

(1) Be isolated and compact—only minimal emissions sources more than a few miles downwind of the urban center
(2) Be a strong source of emissions
(3) Be dominated by one type of NO_x emissions source (e.g., auto exhaust)
(4) Be subject to periods of strong solar irradiation and frequent inversion conditions
(5) Have a stable and predictable prevailing wind direction
(6) Have an existing monitoring network.

Obviously for such a study to succeed, the pollutant concentrations must be measurable downwind of the city after dilution. We are currently investigating the feasibility of such a study downwind of an isolated urban source.

REFERENCES

1. (a) Spicer, C.W., "The Fate of Nitrogen Oxides in the Atmosphere", Battelle-Columbus report to CRC (CAPA-9-71) and EPA (EPA-600/3-76-030), September, 1974.

   (b) Spicer, C.W., "The Fate of Nitrogen Oxides in the Atmosphere", in Advances in Environmental Sciences", Pitts and Metcalf, Eds., Wiley, New York (in press).

2. Miller, D.F. and Spicer, C.W., J. Air Poll. Control Assoc., 25, 940 (1975).

3. Miller, D.F., Wilson, W.E., Jr., and Kiing, R.G., J. Air Poll. Control Assoc., 21, 414 (1971).

4. Gantner, B.A., Masters Thesis, Department of Environmental Science, University of North Carolina, Chapel Hill, NC 1975.

5. Hanst, P.L., Wilson, W.E., Jr., Patterson, R.K., Gay, B.W., Chaney, L.W., and Burton, C.S., "A Spectroscopic Study of Pasadena Smog", paper presented at 167th ACS Meeting, Los Angeles, April, 1974.

6. Hanst, P.L., Letohn, A.S., and Gay, B.W., App. Spectro., 27, 188 (1973).

7. Spicer, C.W. and Miller, D.F., J. Air Poll. Control Assoc., 26, 46 (1976).

8. Hodgeson, J.A., Rehme, K.A., Martin, B.E., and Stevens, R.K., "Measurements for Atmospheric Oxides of Nitrogen and Ammonia by Chemiluminescence", paper presented at 65th Annual Meeting of the Air Pollution Control Association, June, 1972.

9. Winer, A.M., Peters, J.W., Smith, J.P., and Pitts, J.N., Jr., Environ. Sci. and Tech., 8, 1118 (1974).

10. Breitenbach, L.P. and Shelef, M., J. Air Poll. Control Assoc., 23, 128 (1973).

11. Stedman, D., personal communication, 1976.

12. Bufalini, J.J., personal communication, 1976.

13. Air Quality Data for 1967 from the National Air Surveillance Networks, Revised 1971. Environmental Protection Agency, Research Triangle Park, NC, Publ. No. APTD 0741 (1971).

14. Gordon, R.J. and Bryan, R.J., Environ. Sci. and Tech., 7, (7), 645 (1973).

15. Air Quality Report No. 79, "Airborne Particulate Matter in Los Angeles County", Los Angeles Air Pollution Control District, 1973.

16. Spicer, C.W., "Studies of the Effect of Environmental Variables on the Collection of Atmospheric Nitrate", paper presented at EPA Symposium on Recent Developments in the Sampling and Analysis of Atmospheric Sulfate and Nitrate, Research Triangle Park, NC, March, 1976.

17. Charlson, R.J., Vanderpol, A.H., Covert, D.S., Waggoner, A.P., and Ahlquist, N.C., Atm. Environ., 8, (7) 125 (1974).

18. Spicer, C.W., Gemma, J.L., Joseph, J.W., Sticksel, P.R., and Ward, G.F., "The Transport of Oxidant Beyond Urban Areas", EPA-600/3-76-018, February, 1976.

19. Hidy, G.M. and Burton, C.S., "Atmospheric Aerosol Formation by Chemical Reactions", in Proceedings of the Symposium on Chemical Kinetics Data for the Upper & Lower Atmosphere, Benson, S.W., Ed., Wiley, New York (1975).

20. Navskov, T., Mueller, P.K., Alcocer A.E., and Otvos, J.W., J. Colloid and Interface Sci., 39 (1) 225 (1972).

21. "Profile of Air Pollution Control", Air Pollution Control District, County of Los Angeles (1971).

22. "1974 Profile of Air Pollution Control", Air Pollution Control District, County of Los Angeles (1974).

23. "Los Angeles County Emissions - 1974", Air Pollution Control District, County of Los Angeles (1975).

24. Roberts, P.J.W., Roth, P.M., and Nelson, C.L., Appendix A of "Development of a Simulation Model for Estimating Ground Level Concentrations of Photochemical Pollutants", PB 206-409, 1971.

25. 1972 National Emissions Report, Environmental Protection Agency, Research Triangle Park, NC, EPA-450/2-74-012, June, 1974.

26. Swinnerton, J.W. and Lamontagne, R.A., Tellus, 26, 136 (1974).

27. Seiler, W., Tellus, 26, 116 (1974).

28. Junge, C.E., Tellus, 26, 477 (1974).

29. Blumenthal, D.L. and White, W.H., "The Stability and Long Range Transport of Ozone or Ozone Precursors", Paper No. 75-07.4, presented at 68th Air Pollution Control Association Meeting, Boston, Mass, June, 1975.

30. Spicer, C.W., Joseph, J.W., and Ward, G.F., "The Transport of Oxidant Beyond Urban Areas - Compilation of Data", Battelle-Columbus report to EPA, January, 1976.

31. "Proceedings: Ozone/Oxidants Interactions with the Total Environment Specialty Conference", Air Poll. Control Assoc., Ed., APCA, Pittsburgh, Pa., 1976.

32. Spicer, C.W., unpublished results, 1976.

33. Jefferies, H., personal communication to D.F. Miller, 1976.

34. Hecht, T.A., Seinfeld, J.H., and Dodge, M.C., Environ. Sci. and Tech., 8, 327 (1974).

35. Leighton, P.A., "Photochemistry of Air Pollution", Academic Press, New York, 1961.

36. Dufalini, J.J., Gay, B.W., Jr., and Brubaker, K.L., Environ. Sci. and Tech., 6, 816 (1972).

37. Rodhe, H. and Grandell, J., Tellus, 24, 422 (1972).

38. Bolin, B., Aspling, G., and Persson, C., Tellus, 26, 185 (1974)

39. Tingley, D.T., "Foliar Absorption of Nitrogen Dioxide", Department of Botany, University of Utah, M.A. Thesis (1968).

40. Miller, D.F., Schwartz, W.E., Jones, P.E., Joseph, D.W., Spicer, C.W., Riggle, C.J., and Levy, A., "Haze Formation: Its Nature and Origin-1973", Battelle-Columbus report to EPA and CRC, June, 1973.

41. Calvert, J.G., Environ. Sci. and Tech., 10, 256 (1976).